

N73-16561
NASA CR-120876

WANL-M-FR-72-007

DECEMBER 1972



CASE FILE
COPY

FINAL REPORT

WELDABILITY, STRENGTH, AND HIGH TEMPERATURE
STABILITY OF CHEMICALLY VAPOR DEPOSITED TUNGSTEN

BY

W. A. BRYANT

PREPARED FOR

NATIONAL AERONAUTICS AND SPACE ADMINISTRATION

NASA LEWIS RESEARCH CENTER
CLEVELAND, OHIO 44135

CONTRACT NAS 3-13222



Astronuclear Laboratory
Westinghouse Electric Corporation

NOTICE

This report was prepared as an account of Government-sponsored work. Neither the United States, nor the National Aeronautics and Space Administration (NASA), nor any person acting on behalf of NASA:

- A.) Makes any warranty or representation, expressed or implied, with respect to the accuracy, completeness, or usefulness of the information contained in this report, or that the use of any information, apparatus, method, or process disclosed in this report may not infringe privately-owned rights; or
- B.) Assumes any liabilities with respect to the use of, or for damages resulting from the use of, any information, apparatus, method or process disclosed in this report.

As used above, "person acting on behalf of NASA" includes any employee or contractor of NASA, or employee of such contractor, to the extent that such employee or contractor of NASA or employee of such contractor prepares, disseminates, or provides access to any information pursuant to his employment or contract with NASA, or his employment with such contractor.

Request for copies of this report should be referred to

National Aeronautics and Space Administration
Scientific and Technical Information Facility
P. O. Box 33
College Park, Maryland 20740

1. Report No. NASA CR-120876	2. Government Accession No.	3. Recipient's Catalog No.	
4. Title and Subtitle WELDABILITY, STRENGTH AND HIGH TEMPERATURE STABILITY OF CHEMICALLY VAPOR DEPOSITED TUNGSTEN (U)		5. Report Date December, 1972	6. Performing Organization Code
		8. Performing Organization Report No. WANL-M-FR-72-007	10. Work Unit No.
7. Author(s) W. A. Bryant	9. Performing Organization Name and Address Westinghouse Astronuclear Laboratory P. O. Box 10864 Pittsburgh, Pennsylvania 15236		11. Contract or Grant No. NAS 3-13222
12. Sponsoring Agency Name and Address National Aeronautics and Space Administration Washington, D. C. 20546			13. Type of Report and Period Covered Contractor Report
		14. Sponsoring Agency Code	
15. Supplementary Notes Project Manager, R. A. Lindberg NASA Lewis Research Center, Cleveland, Ohio			
16. Abstract <p>Three types of CVD tungsten (fluoride-produced, chloride-produced and the combination of the two which is termed duplex) were evaluated to determine their weldability, high temperature strength and structural stability during 5000 hour exposure to temperatures of 1540°C and 1700°C.</p> <p>Each type of CVD tungsten could be successfully electron beam welded but the results for the chloride product were not as satisfactory as those of the other two materials. The high temperature strength behavior of the three materials did not differ greatly. However a large difference was noted for the grain growth behavior of the two basic CVD tungsten materials. Fluoride tungsten was found to be relatively stable while for the most part the grain size of chloride tungsten increased appreciably.</p> <p>The examination of freshly fractured surfaces with a scanning electron microscope revealed numerous bubbles in the fluoride material following its exposure to 1700°C for 5000 hours. Less severe thermal treatments produced relatively few bubbles in this material. Only at certain locations within the chloride material associated with the interruption of tungsten deposition were bubbles noted.</p> <p>For the chloride material the degree of microstructural stability (as indicated both by grain growth and bubble formation) varied greatly from one layer to another within a single specimen. This behavior, coupled with the presence of a layered structure, is indicative of a deposition process in need of improved control.</p>			
17. Key Words (Suggested by Author(s)) Tungsten Tungsten Chloride Tungsten Fluoride Tungsten Welding Chemical Vapor Deposition		18. Distribution Statement	
19. Security Classif. (of this report) Unclassified	20. Security Classif. (of this page) Unclassified	21. No. of Pages	22. Price*

* For sale by the National Technical Information Service, Springfield, Virginia 22151

FOREWORD

The work described herein was done at the Astronuclear Laboratory, Westinghouse Electric Corporation, under NASA Contract NAS 3-13222 with Mr. R. A. Lindberg, Materials and Structures Division, NASA Lewis Research Center, as Project Manager. This work was done during the period June 30, 1969 to April 30, 1972.

TABLE OF CONTENTS

<u>Section</u>		<u>Page</u>
1.0	SUMMARY	1
2.0	INTRODUCTION	3
3.0	MATERIALS CHARACTERIZATION	4
4.0	TEST PROGRAM PROCEDURE	11
	4.1 Welding	11
	4.2 Bend and Tensile Testing	13
	4.3 Stability Determination	15
5.0	RESULTS	16
	5.1 Weldability	16
	5.2 Bend and Tensile Strength Properties	39
	5.3 Microstructural Stability	52
6.0	DISCUSSION	75
	6.1 Ductile-Brittle Behavior	75
	6.2 Strength and Elongation	76
7.0	CONCLUSIONS	86
8.0	RECOMMENDATIONS	87
9.0	REFERENCES	88

LIST OF TABLES

<u>Table No.</u>	<u>Title</u>	<u>Page</u>
I	Estimated Deposition Parameters for Program Material	5
II	Impurity Content of CVD Materials Determined by Spectrographic Analysis	9
III	Relative Diffraction Intensity	10
IV	List of Weld Parameters	16
V	Ductile Brittle Transition Temperature (longitudinal/transverse) for CVD Tungsten	20
VI	Bend Ductile Brittle Transition Temperatures for Welded Fluoride CVD Tungsten	23
VII	Bend Ductile Brittle Transition Temperatures for Welded Chloride CVD Tungsten	33
VIII	Bend Ductile Brittle Transition Temperatures for Welded Duplex CVD Tungsten	37
IX	DBTT of CVD Tungsten for Various Thermal Treatments	39
X	Strength and Elongation Data for CVD Tungsten	58
XI	CVD Tungsten Microstructures and Grain Sizes	60
XII	Effect of Heat Treatment on Hardness and Grain Size of Fluoride- and Chloride-Produced Tungsten	63

LIST OF FIGURES

<u>Figure No.</u>		<u>Page</u>
1	Transverse Microstructure of Fluoride Tungsten Deposit	6
2	Transverse Microstructure of Chloride Tungsten Deposit	7
3	Transverse Microstructure of Duplex Tungsten Deposit	8
4	Sketch Showing Sectioning of Set of EB Weld Specimens into Bend Test Specimens	12
5	CVD Tungsten Tensile Specimen	14
6	Bend Test Results for Electron Beam Welds in Fluoride Process CVD Tungsten	17
7	Bend Test Results for Electron Beam Welds in Chloride Process CVD Tungsten	18
8	Bend Test Results for Electron Beam Welds in Duplex Process CVD Tungsten	19
9	Transverse Section Through Fluoride CVD Tungsten Following EB Welding	22
10	Transverse Section through Fluoride CVD Tungsten Following EB Welding and Outgassing.	24
11	Transverse Section Through Fluoride CVD Tungsten Following EB Welding, Outgassing, and Aging at 1540°C for 5000 hours	25
12	Transverse Section Through Fluoride CVD Tungsten Following EB Welding, Outgassing, and Aging at 1700°C for 5000 hours	25
13	DBTT Data for Welded Fluoride CVD Tungsten	26
14	Transverse Section Through Chloride CVD Tungsten Following EB Welding	28
15	Transverse Section Through Chloride CVD Tungsten Following EB Welding, Outgassing, and Aging at 1540°C for 5000 hours.	30
16	Transverse Section Through Chloride CVD Tungsten Following EB Welding, Outgassing, and Aging at 1700°C for 5000 hours.	31

LIST OF FIGURES (Cont'd.)

<u>Figure No.</u>		<u>Page</u>
17	DBTT Data for Welded Chloride CVD Tungsten	32
18	Transverse Section Through Duplex CVD Tungsten Following EB Welding	34
19	Transverse Section Through Duplex CVD Tungsten Following EB Welding and 50 Hours at 1800°C	35
20	Transverse Section Through Duplex CVD Tungsten Following EB Welding, Outgassing, and Aging at 1540°C for 5000 Hours	36
21	Transverse Section Through Duplex CVD Tungsten Following EB Welding, Outgassing, and Aging at 1700°C for 5000 Hours	36
22	DBTT Data for Welded Duplex CVD Tungsten	38
23	Bend Data for Unwelded Fluoride CVD Tungsten	40
24	Bend Data for Unwelded Chloride CVD Tungsten	41
25	Bend Data for Unwelded Duplex CVD Tungsten	42
26	Elevated Temperature Tensile Properties of Fluoride CVD Tungsten Stress Relieved (1 hour at 1200°C) and Outgassed 50 hours at 1800°C	45
27	Elevated Temperature Tensile Properties of Fluoride CVD Tungsten Stress Relieved, Outgassed, and Aged (5000 hours at 1540°C)	46
28	Elevated Temperature Tensile Properties of Fluoride CVD Tungsten Stress Relieved, Outgassed, and Aged (5000 hours at 1700°C)	47
29	Elevated Temperature Total Elongation of Fluoride CVD Tungsten	48
30	Elevated Temperature Tensile Properties of Chloride CVD Tungsten Stress Relieved (1 hour at 1200°C) and Outgassed (50 hours at 1800°C)	49
31	Elevated Temperature Tensile Properties of Chloride CVD Tungsten Stress Relieved, Outgassed, and Aged (5000 hours at 1540°C)	50
32	Elevated Temperature Tensile Properties of Chloride CVD Tungsten Stress Relieved, Outgassed, and Aged (5000 hours at 1700°C)	51

LIST OF FIGURES (Cont'd.)

<u>Figure No.</u>		<u>Page</u>
33	Elevated Temperature Total Elongation of Chloride CVD Tungsten	53
34	Elevated Temperature Tensile Properties of Duplex CVD Tungsten Stress Relieved (1 hour at 1200°C) and Outgassed (50 hours at 1800°C)	54
35	Elevated Temperature Tensile Properties of Duplex CVD Tungsten Stress Relieved, Outgassed, and Aged (5000 hours at 1540°C)	55
36	Elevated Temperature Tensile Properties of Duplex CVD Tungsten Stress Relieved, Outgassed, and Aged (5000 hours at 1700°C)	56
37	Elevated Temperature Total Elongation of Duplex CVD Tungsten	57
38	Grain Structure of Fluoride Tungsten Following Stress Relief, Outgassing, and Aging for 5000 Hours at 1700°C	64
39	Grain Structure of Chloride Tungsten Following Stress Relief, Outgassing, and Aging for 5000 Hours at 1700°C	64
40a	Scanning Electron Micrograph of Fractured Surface of Stress Relieved and Outgassed Duplex Tungsten	65
40b	Scanning Electron Micrograph of Fluoride Portion of Stress Relieved and Outgassed Duplex Tungsten Showing Near Absence of Bubbles on Grain Boundary	67
40c	Scanning Electron Micrograph of Fluoride Portion of Stress Relieved and Outgassed Duplex Tungsten Showing Bubble Formation at Several Grain Boundaries	67
40d	Scanning Electron Micrograph of Stress Relieved and Outgassed Duplex Tungsten Showing Absence of Bubbles at Fluoride-Chloride Interface	68
40e	Scanning Electron Micrograph of Stress Relieved and Outgassed Duplex Tungsten Showing Grain Boundaries in One Chloride Layer that are Heavily Populated with Bubbles	68

LIST OF FIGURES (Cont'd.)

<u>Figure No.</u>		<u>Page</u>
41a	Scanning Electron Micrograph of Fractured Surface of Duplex Tungsten (Stress Relieved, Outgassed, and Aged 5000 Hours at 1540°C)	69
41b	Fluoride-Chloride Interface of Specimen Shown in Figure 41a	70
41c	Chloride-Chloride Interface of Specimen Shown in Figure 41a	70
41d	Chloride-Chloride Interface of Specimen Shown in Figure 41a	71
41e	Interface of Figure 41d Showing Isolated Area Containing Bubbles	71
42a	Scanning Electron Micrograph of Fractured Surface of Duplex Tungsten (Stress Relieved, Outgassed, and Aged 5000 Hours at 1700°C)	72
42b	Fluoride Tungsten Portion of Specimen of Figure 42a Showing Presence of Numerous Bubbles	73
42c	Chloride Tungsten Portion of Specimen of Figure 42a Showing Absence of Bubbles	73
43	Comparison of UTS and 0.2% Yield Strength for CVD Tungsten Materials Following Stress Relief (1 hour at 1200°C) and Outgassing (50 hours at 1800°C)	77
44	Comparison of UTS and 0.2% Yield Strength for CVD Tungsten Materials Following Stress Relief, Outgassing, and Aging (5000 hours at 1540°C)	78
45	Comparison of UTS and 0.2% Yield Strength for CVD Tungsten Materials Following Stress Relief, Outgassing, and Aging (5000 hours at 1700°C)	79
46	Fluoride Tungsten (Stress Relieved and Outgassed) Following Tensile Testing at 1100°C	81
47	Fluoride Tungsten (Stress Relieved and Outgassed) Following Tensile Testing at 1540°C	81
48	Fluoride Tungsten (Stress Relieved and Outgassed) Following Tensile Testing at 1700°C	83

LIST OF FIGURES (Cont'd.)

<u>Figure No.</u>		<u>Page</u>
49	Fluoride Tungsten (Stress Relieved, Outgassed, and Aged 5000 Hours at 1700°C) Following Tensile Testing at 1100°C	83
50	Fluoride Tungsten (Stress Relieved, Outgassed, and Aged 5000 Hours at 1700°C) Following Tensile Testing at 1540°C	84
51	Fluoride Tungsten (Stress Relieved, Outgassed, and Aged 5000 Hours at 1700°C) Following Tensile Testing at 1700°C	84

1.0 SUMMARY

An investigation was made of the weldability, high temperature strength, and structural stability during 5000 hour exposure to temperatures of 1540°C and 1700°C of CVD tungsten. Comparisons were made between three forms of this material: fluoride-produced, chloride-produced, and the combination of these which is termed duplex.

Each type of material was successfully EB welded with a virtual absence of weld porosity. The ductile-brittle transition temperature for the chloride tungsten welds was generally about 160°C higher than that of either fluoride or duplex material which had nominal DBTT values (considering all orientations and thermal treatments as a simple population) of 320°C and 335°C, respectively.

In unwelded material the chloride product possesses a bend ductile-brittle transition temperature which is generally 200°C greater than that of the fluoride tungsten and about 150°C greater than that of the duplex material. These relations are, at least in part, the result of the chloride material's coarser grain structure following exposure to high temperature.

At the highest temperatures investigated (1540°C and 1700°C) the tensile strengths of the two basic material's types were essentially equal. At lower temperatures, chloride tungsten was found to have lower yield strength but higher ultimate strength than the fluoride material. The strength behavior of the duplex tungsten was generally intermediate to that of its constituents.

It was generally observed that elongation as a function of test temperature passes through a maximum at about 60-70% elongation for temperatures near 1000°C and then, depending upon prior thermal treatment, either decreased further or passes through a minimum at about 1500°C. This behavior may be explained with a model based on grain boundary cavity formation and recrystallization.

The average grain growth behavior of the two basic CVD tungsten materials was vastly different. Fluoride tungsten was found to be relatively stable. Its average grain size increased from an as-stress relieved value of 41 microns to 49 microns following 5000 hours at 1540°C and to 68 microns following 5000 hours at 1700°C. In contrast, the chloride tungsten grain size increased from 50 microns to nearly 600 microns following each of the high temperature treatments.

Freshly fractured surfaces of duplex tungsten were examined with the aid of a scanning electron microscope. Comparisons were made between the fluoride and chloride components for material given a number of thermal treatments. Numerous bubbles were noted in the fluoride material following its exposure to 1700°C for 5000 hours. The material contained only 2 ppm fluorine but is known to also contain approximately this much or more chlorine. Following lower temperature exposures, very few bubbles were found in this material but could be noted in the chloride material in regions associated with the interruption of tungsten deposition.

2.0 INTRODUCTION

The projected use of CVD tungsten thermionic emitters under increasingly more severe conditions of temperature and time of operation required that additional data on the properties of this class of material be determined. It was thus the purpose of this program to study the weldability, high temperature strength, and structural stability during 5000 hour exposure to temperatures of 1540°C and 1700°C of CVD fluoride, chloride, and duplex tungsten. The latter material is a layered combination of the other two in which chloride tungsten is deposited onto a fluoride tungsten substrate. The duplex material thus has an emitting surface of chloride tungsten (possessed of greater electron work function) backed by fluoride tungsten which is known to have greater high temperature stability.

3.0 MATERIALS CHARACTERIZATION

Material from each of the three CVD tungsten types in the form of 1.52 mm (60 mil) thick sheet was purchased from the San Fernando Laboratories of Fansteel Corporation. Parameters for the deposition of these materials onto molybdenum substrates were not obtainable from the vendor, however they can be approximated from their values reported in the literature. These estimated parameters are shown in Table 1.

The as-deposited sheets were ground to 6-32 rms finish on the surfaces perpendicular to the growth direction. At least 0.1 mm (4 mils) was removed from the surface adjacent to the deposition mandrel by this operation to assure removal of the randomly oriented grain structure. Following cutting and grinding to test specimen blank size, all material was stress relieved at 1200°C for 1 hour in a vacuum of 1.33×10^{-4} N/m² (1×10^{-6} torr) or better.

The materials microstructures, taken parallel to the growth direction in each case, are shown in Figures 1 through 3. The fluoride tungsten (Figure 1) possesses the characteristic columnar microstructure associated with a preferred growth orientation. Several layers corresponding to interruptions in the deposition process are visible in the microstructure. The associated transitions between tungsten deposition cycles were effected without introducing contamination to the surface of the tungsten. This is evident from the microstructure which shows a high degree of epitaxial growth.

The microstructure of the chloride tungsten is shown in Figure 2. At least five layers are visible. Unlike the fluoride tungsten there is little epitaxial growth apparent in the chloride tungsten. In this particular sample of duplex tungsten (Figure 3), neither the chloride nor the fluoride portions are layered, and the transition between the two has been accomplished with a minimum appearance of randomly oriented grains. [Generally, however, the chloride portion of the duplex material did contain several layers.] However, this interface can still be expected to be one of high energy since a rather large dislocation density would be required to accommodate the approximately 13% disregistry found with an

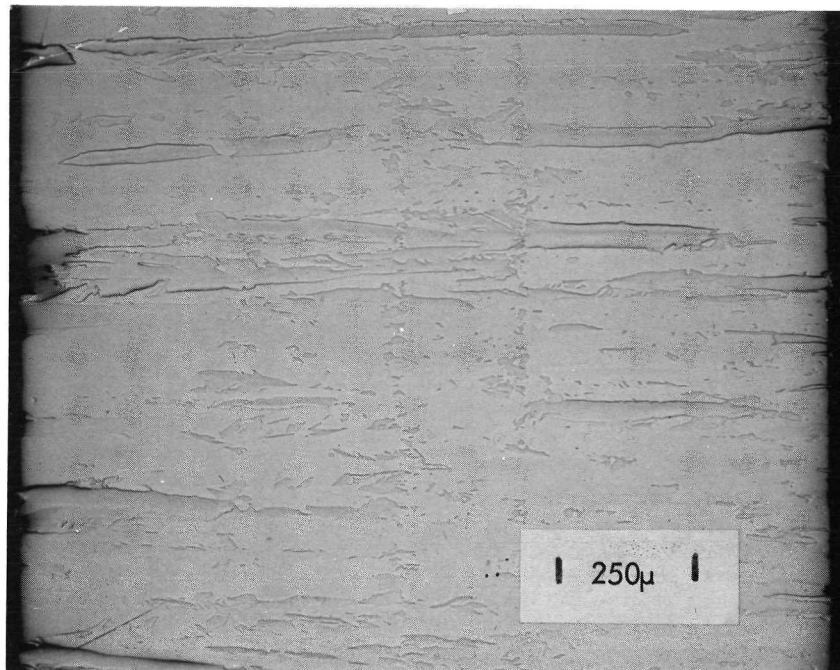
Table I. Estimated Deposition Parameters for Program Material

Material	H ₂ /Halide Vol. Ratio	Pressure (N/m ²)	Pressure (torr)	Temp. (°K)	Temp. (°C)	Oxygen Addition (vol. %)*	Deposition Rate (mm/min.)	Deposition Rate (mil/hr)	Ref.
Fluoride Tungsten	0.53	61.1 x 10 ³	458	923	650	0.34	1.13 x 10 ⁻²	26.7	1
Chloride Tungsten	1.0	1.3 x 10 ³	10	1323	1050	0	N. R.	N. R.	2

*Standard volume as percentage of standard volume WF₆

N. R. - not reported

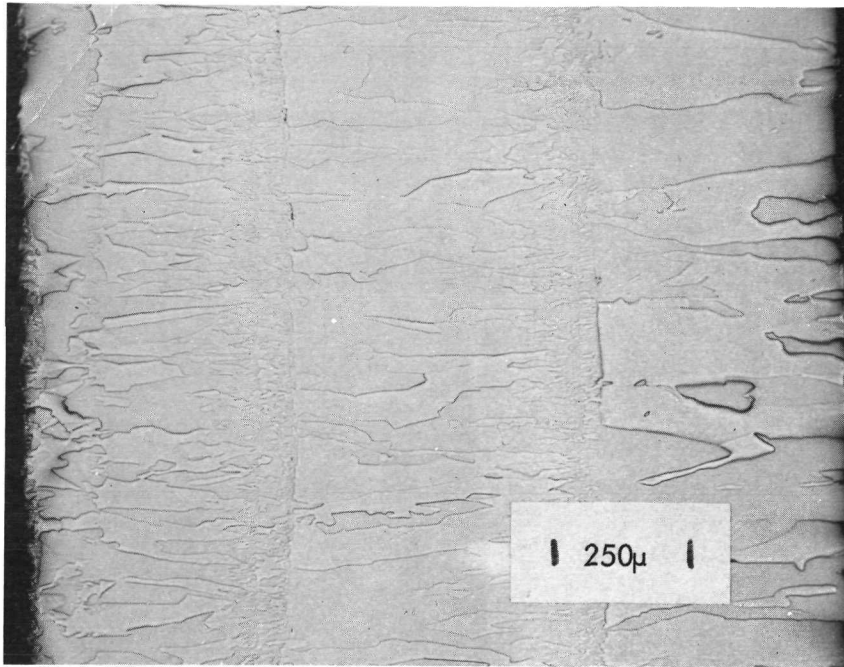
Growth Direction →



70X

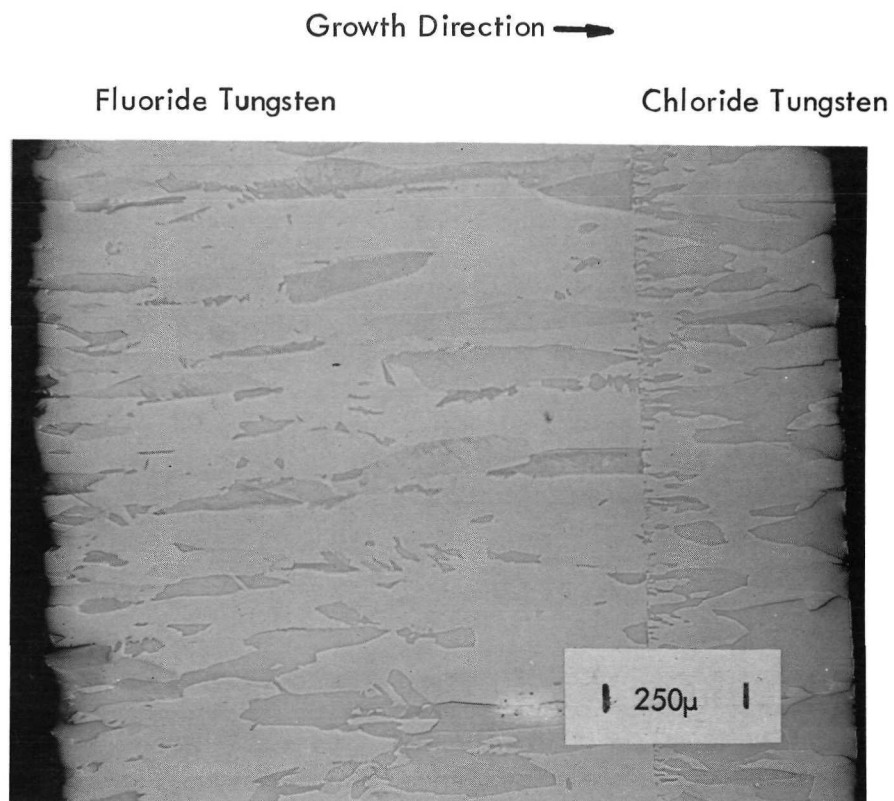
Figure 1. Transverse Microstructure of Fluoride Tungsten Deposit
(as acid polished-chromic acid/jeweler's rouge)

Growth Direction →



70X

Figure 2. Transverse Microstructure of Chloride Tungsten Deposit
(as acid polished—chromic acid/jeweler's rouge)



70X

Figure 3. Transverse Microstructure of Duplex Tungsten Deposit (as acid polished-chromic acid/jeweler's rouge)

overlay of a $\{110\}$ type plane onto a $\{100\}$ type plane. Chemical analyses of each type of CVD material are presented in Table II.

Table II.
Impurity Content of CVD Materials Determined by Spectrographic Analysis
Amount of Impurity (ppm)*

<u>Impurity</u>	<u>Duplex Tungsten</u>	<u>Chloride Tungsten</u>	<u>Fluoride Tungsten</u>
Oxygen	20	20	5
Nitrogen	8	8	10
Carbon	23	27	32
Fluorine	27	48	35
Fluorine**	1.8	1.1	1.5
Chlorine	30	25	30
Silicon	9	10	10
Iron	2	1	6
Aluminum	4	7	2
Copper	1	1	2
Molybdenum	300	40	20

* Analyzed by Crobaugh Laboratory, Cleveland, Ohio. Values based on average of determinations wherein < 1 was taken as $= 1$.

** Results of Oak Ridge National Laboratory using pyrohydrolysis technique.

The fluorine contents determined by ORNL are preferred over the spectrographically determined ones because of the considerable experience associated with the former.

The chlorine contents for the three materials are essentially equal and, because of the method of analysis, may be much greater than actual.

The degree of preferred orientation of both the fluoride and chloride tungsten was determined using data obtained with a Siemens diffractometer. These data, normalized using the values for randomly oriented tungsten, are presented in Table III.

Table III. Relative Diffraction Intensity

	<u>(110)</u>	<u>(200)</u>	<u>(211)</u>	<u>(220)</u>	<u>(310)</u>
Fluoride Tungsten	0	6.7	.04	0	0
Chloride Tungsten	1.0	0	.26	2.1	0.9

It is apparent that the fluoride material is much more highly oriented than the chloride material. Other characteristics of the starting materials such as grain size and hardness are presented in the Results section of this report.

Diamond pyramid hardnesses for 30 kg load were obtained on all thermally treated material except those given the cycling treatment.

Scanning electron microscopy was performed on fresh fractures of duplex material. This material was chosen for study because of its importance to thermionic diode fabrication. Also, this choice provided a convenient means of comparing fluoride and chloride tungsten given identical treatments and permitted examination of the interface existing between the CVD tungsten types.

4.0 TEST PROGRAM PROCEDURE

The following procedures were instituted to supply specimens for the determination of weldability, ductile brittle transition behavior, and elevated temperature strength of the subject materials and to study the effect on these same strength properties of a number of heat treatments.

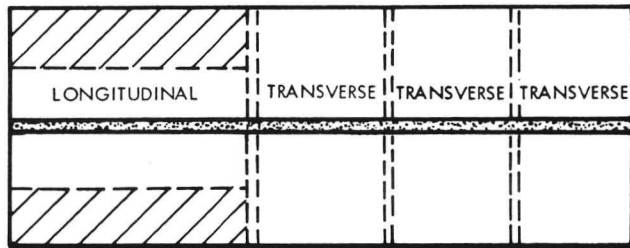
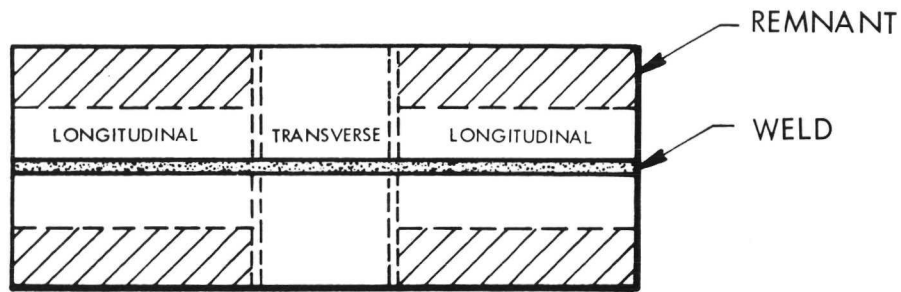
4.1 WELDING

Prior to EB welding, test sheets (Fig. 4) 8.26 cm long by 3.17 cm wide by 1.52 mm thick*(3-1/4 in.) x 1-1/4 in. x 0.060 in.) were degreased with M-6 solvent, etched in a 30 lactic-3HNO₃-1HF solution (ratio by volume) and consecutively rinsed with flowing hot tap water, boiling distilled water, and ethyl alcohol prior to being hot air dried. All handling during cleaning was done using pre-scrubbed and rinsed latex gloves. The cleaned specimens were then degassed at 1095°C for 1 hour at 10⁻⁵ torr.

Full penetration welds were then made with the first deposited surface facing upward (which is fluoride for the duplex material). During welding, the sheet was fully restrained within a fixture (described in Reference 3). All welding was performed in vacuum with pressures of 2 x 10⁻⁵ torr or lower using the 30 KW Sciaky weld facility.

All welds were visually, dye penetrant, and radiographically inspected. Each of the two test sheets of a given set was sectioned with an abrasive cut-off wheel according to Figure 4 to provide three longitudinal and four transverse EB weld specimens. Each specimen had the dimensions 3.17 cm long by 1.59 cm wide by 1.52 mm thick (1-1/4 in. x 5/8 in. x 0.060 in.).

* In the case of duplex material, this total thickness is comprised of 1.14 mm of fluoride tungsten and 0.38 mm of chloride tungsten.



613642-19B

Figure 4. Sketch Showing Sectioning of Set of EB Weld Specimens into Bend Test Specimens

4.2 BEND AND TENSILE TESTING

Bend specimens having the dimensions 3.17 cm long by 1.59 cm wide by 1.52 mm thick (1-1/4 in. x 5/8 in. x 0.060 in.) were received from the vendor cut to size.

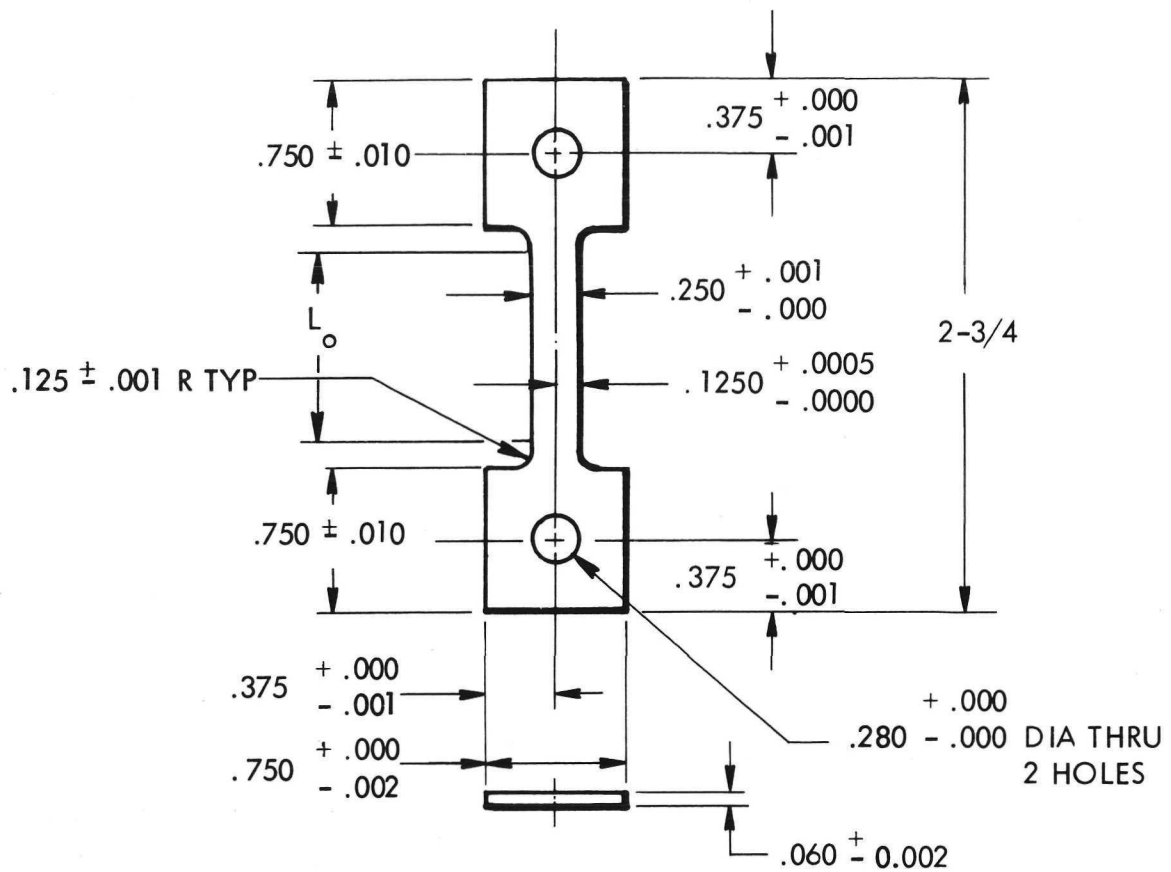
Tensile specimens having a 2.54 cm (1.00 in.) gage length (Figure 5) were obtained from sheet stock by electric discharge machining in oil. Carbon pickup resulting from this operation did not exceed 1.0×10^{-3} mm (1.0 micron) as determined by microprobe analysis. This contamination was removed by hand polishing the specimens.

Prior to any thermal treatment, the specimens were cleaned using the procedure described previously. Fixturing for thermal treatment consisted of spacing the specimens with corrugated, 0.002 in. thick tungsten foil and binding with 0.016 in. diameter tungsten wire.

Bend testing was used to determine the effect of several heat treatments on the ductile brittle transition temperature of each CVD tungsten type. This testing was done under inert atmosphere and utilized a punch radius of 5.36 mm (0.211 in.) to give a bend factor of 3.4t. This produced an outer fiber strain of approximately 13%. The crosshead speed was 2.54 cm/min (1.0 in/min) with a span of 2.54 cm (1.0 in.). The heat treatments used were meant to simulate the thermal exposure that would be experienced by a thermionic diode in actual startup practice and included:

- Outgassing for 50 hours at 1800°C
- Outgassing for 50 hours at 1800°C followed by ten thermal cycles within a 500 hour period between near room temperature and 1540°C
- Outgassing for 50 hours at 1800°C followed by ten thermal cycles within a 500 hour period between near room temperature and 1700°C.

Heating to temperature was generally accomplished within 1/2 to 1 hour while cooling to ambient required about 3 to 4 hours.



$$L_o = 1.00$$

$$A_o = .015 \text{ in}^2$$

Figure 5. CVD Tungsten Tensile Specimen
(dimensions given in inches)

These results were compared with those determined on material in the stress relieved condition.

The strength of the CVD tungsten materials following long time exposure to expected operating temperature was determined using tensile specimens given the following thermal treatments:

- o outgassing for 50 hours at 1800°C
- o outgassing for 50 hours at 1800°C followed by aging for 5000 hours at 1540°C
- o outgassing for 50 hours at 1800°C followed by aging for 5000 hours at 1700°C.

Tensile testing was performed at room temperature and a number of elevated temperatures using a strain rate of 0.02 min⁻¹. Elevated temperature testing was performed in a vacuum of 1 x 10⁻⁵ torr or better.

4.3 STABILITY DETERMINATION

Grain size changes produced by exposure to high temperature were studied for each type of material. The heat treatments included:

1. stress relief (1 hour at 1200°C)
2. stress relief plus outgassing (50 hours at 1800°C)
3. stress relief, outgassing and cycling 10 times between room temperature and 1540°C in a period of 500 hours
4. stress relief, outgassing and cycling 10 times between room temperature and 1700°C in a period of 500 hours
5. stress relief, outgassing and aging (5000 hours at 1540°C)
6. stress relief, outgassing and aging (5000 hours at 1700°C).

Grain size was determined at a magnification of 100X by using the Jeffries planimetric method.

5.0 RESULTS

5.1 WELDABILITY

Initially three sets of weld parameters were used on each material type. These parameters are presented in Table IV.

Table IV

Test Set	Type CVD W	Weld Speed (ipm)	Preheat (°C)	Voltage (KV)	Current (ma)
C1-F1	Fluoride	15	None	30	63
-C1	Chloride	15	None	30	68
-D1	Duplex	15	None	30	68
C1-F2	Fluoride	15	705	30	68
-C2	Chloride	15	705	30	60
-D2	Duplex	15	705	30	55
C1-F3	Fluoride	15	428	30	55
-C3	Chloride	15	428	30	55
-D3	Duplex	15	428	30	55

Visual inspection revealed all welds to be crack-free with the exception of a small transverse crack in one piece of test set C1-D3. This degree of cracking was confirmed by dye penetrant and radiographic inspection.

Bend testing of specimens cut from the welded sheet was used to determine the bend ductile-brittle transition temperature for each CVD tungsten type as a function of welding parameters (essentially limited to preheat temperature).

The results of these tests are presented in Figures 6 through 8 where the symbols used have the following meaning:

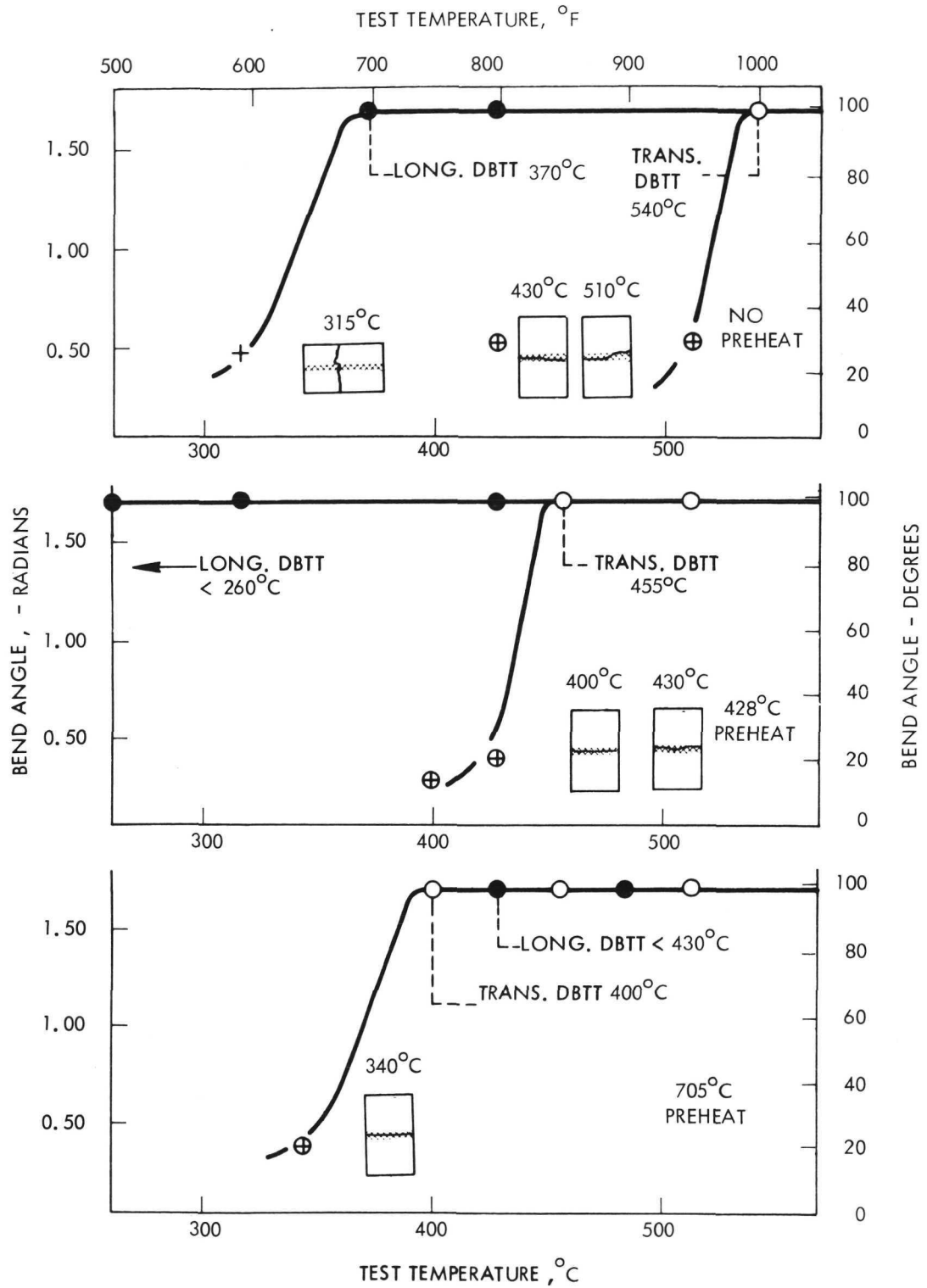


Figure 6. Bend Test Results for Electron Beam Welds in Fluoride Process CVD Tungsten

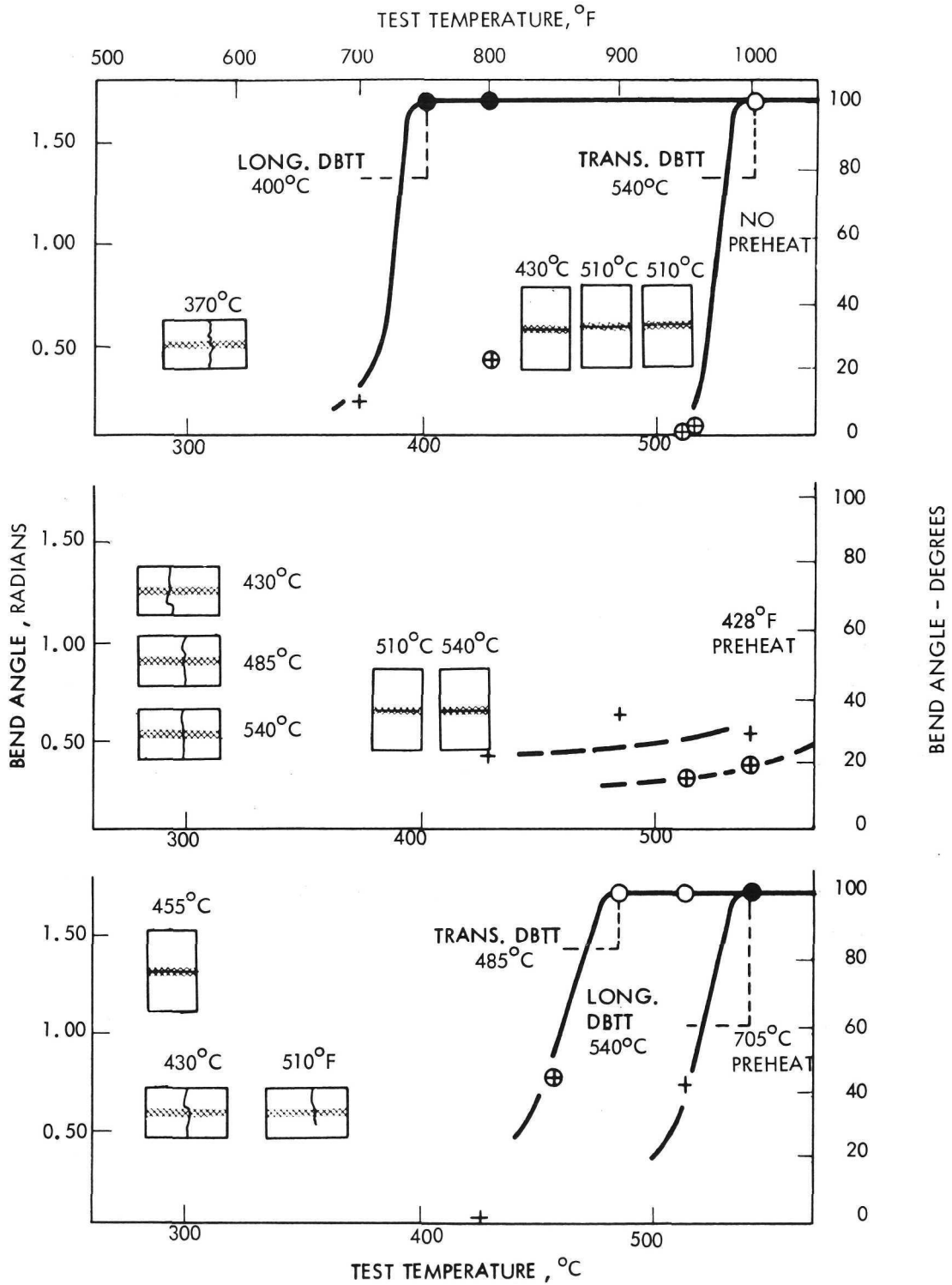


Figure 7. Bend Test Results for Electron Beam Welds in Chloride Process CVD Tungsten

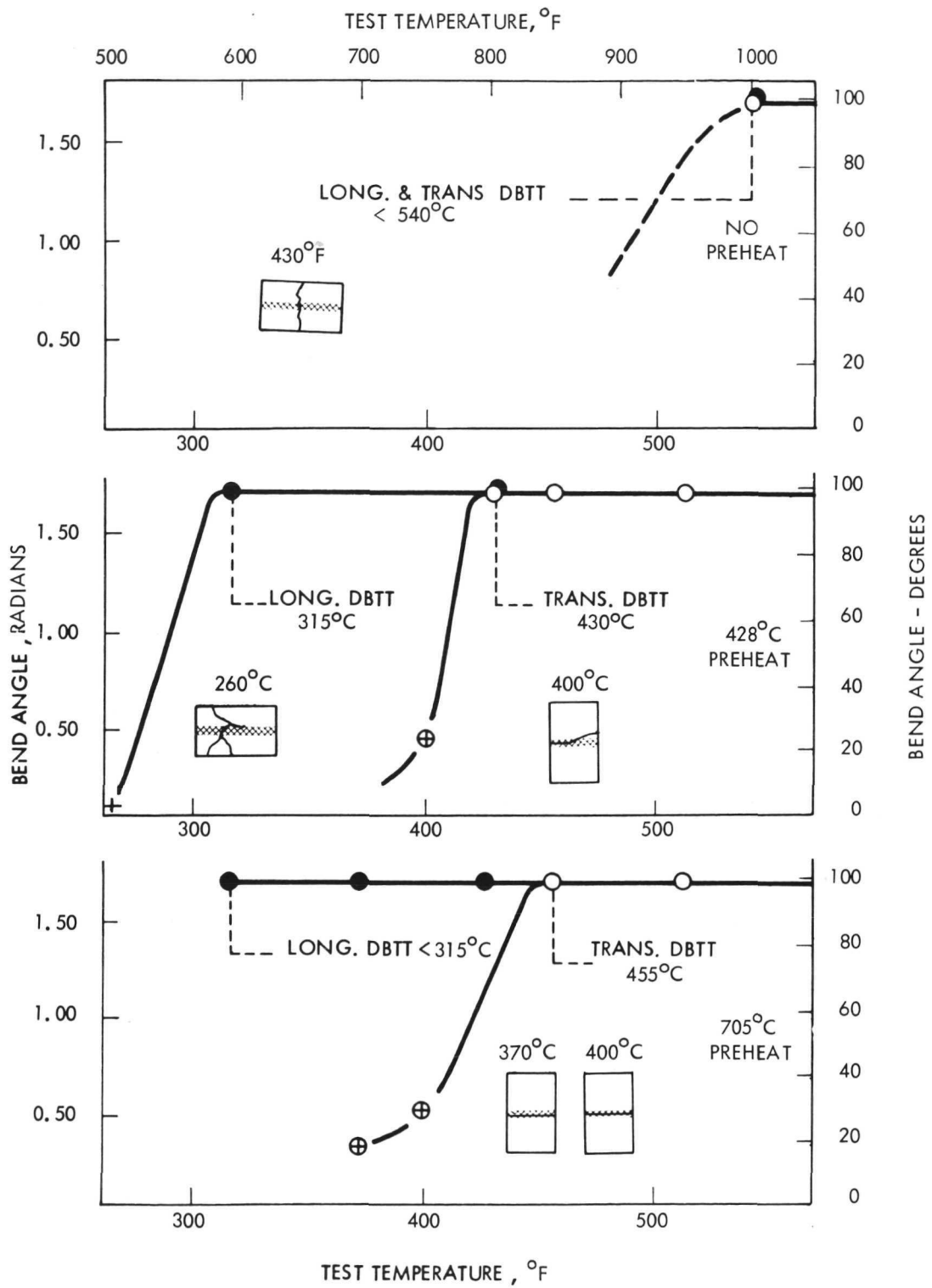


Figure 8. Bend Test Results for Electron Beam Welds in Duplex Process CVD Tungsten

- transverse bend
- ⊕ transverse break
- longitudinal bend
- + longitudinal break

From the illustrations of the crack location on the individual fractured specimens, the preference for weld centerline failures in the transverse specimens is obvious. This is typical of EB welded tungsten and tungsten-base alloys where failure has been observed to occur preferentially along the vertical array of grain boundaries. This pattern is produced by solidification in which columnar grain growth follows the direction of greatest rate of heat removal.

The results from Figures 6 through 8 are summarized in the following table.

Table V.
Ductile Brittle Transition Temperature (longitudinal/transverse)
for CVD Tungsten

Preheat Condition	Temperature (°C)		
	Fluoride CVD	Chloride CVD	Duplex CVD
No Preheat	370/540	400/540	540/540
428°C Preheat	< 260/455	> 540/> 540	315/430
705°C Preheat	< 430/400	540/480	315/455

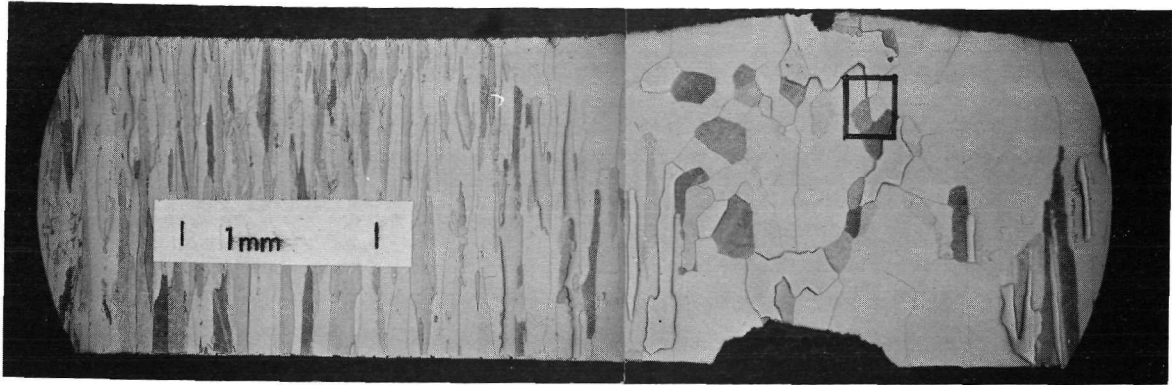
To simulate actual joint behavior, full section weldments were bend tested (i. e., no post weld conditioning of the weld bead), with the top of the weld bead, the tension face in bending. As a consequence, some variability in the results may have been introduced from the rough weld surface which is intrinsic to high energy density electron beam welding. Root defects were not considered critical since they were on the compression side of the bend specimen.

Thus, to properly analyze and interpret these data we must integrate into the analysis such factors as the general weld condition, the number of specimens available for bend testing, and the relative ease of welding using any given set of welding conditions. All of these factors can influence and alter the observed DBTT behavior if not properly controlled.

Based on these preliminary results, the welding of specimens for further evaluation utilized a preheat temperature of 428°C for the fluoride and duplex materials and no preheat for the chloride material. In each case the other parameters attendant with the chosen preheat (Table IV) were used. The desired number of bend specimens (3 longitudinal and 4 transverse) were not obtained from each weld set (Figure 4) due to weld cracking. One duplex and 11 chloride (out of a possible total of 21) bend specimens were lost in this manner. The chloride material was apparently not as weldable as the fluoride material. In all cases failure was intergranular.

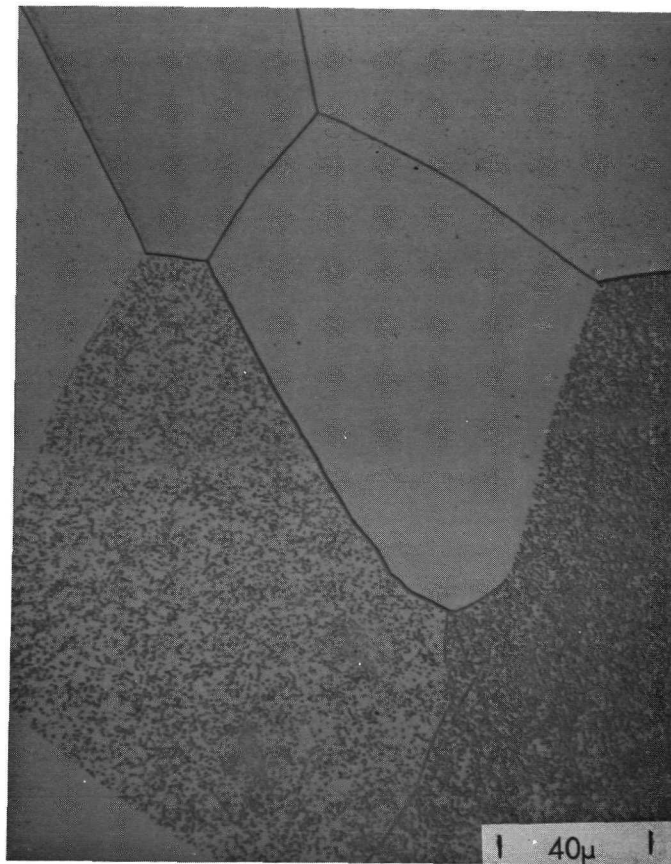
Following outgassing for 50 hours at 1800°C bend specimens were given one of the treatments consisting of aging 5000 hours at 1540°C or aging 5000 hours at 1700°C. Bend testing was conducted as previously described. The fractures were examined and the welds metallographically examined to ascertain changes in structure resulting from the heat treatments.

The microstructure of the welded fluoride-produced material is shown in Figure 9-a, which indicates the extent of the fusion and heat affected zones. Also seen are top of weld and root defects which were generally typical of the bead-on-plate electron beam welds. The entire cross section of the metallographic specimen was checked at 500X magnification for the presence of porosity. Very few pores were noted. Those present were mostly to be found at grain boundaries lying in the heat affected zone. This inspection was complicated by the presence of etch pits which for particular grain orientations (Figure 9-b) occurred in great number. Repolishing and etching with 50 H₂O₂-50 NH₄OH (parts by volume) instead of 30 lactic-3HNO₃-1HF (parts by volume) did not eliminate this pitting to any appreciable degree.



a)

25X



b)

500X

Figure 9. Transverse section through fluoride CVD tungsten following EB welding.
(50 H₂O₂ - 50 NH₄OH etch)

Outgassing (50 hours at 1800°C) produced no perceptible change in this material (Figure 10-a). Where porosity was noted it was found to occur at grain boundaries as shown in Figure 10-b (taken at the fusion line) and Figure 10-c (taken in the region lying just outside of the heat affected zone).

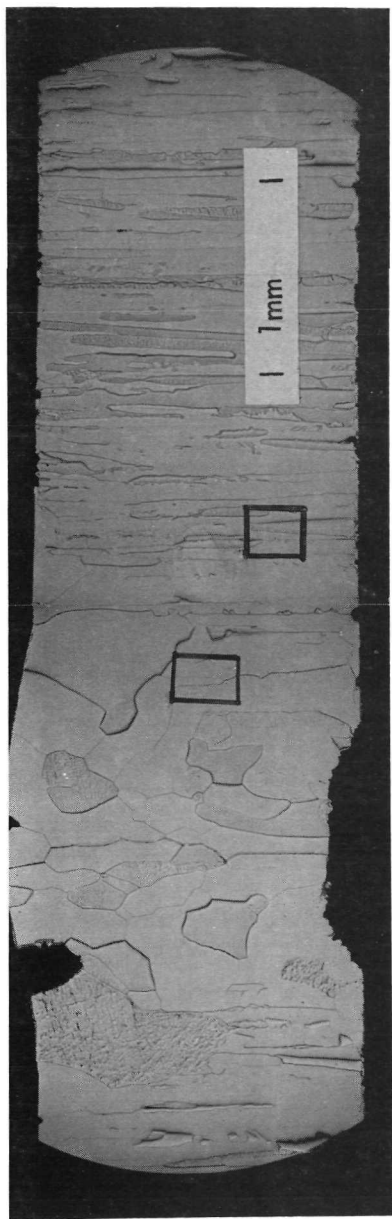
Aging the welded material for 5000 hours at 1540°C did not alter the microstructure (as evidenced by Figure 11) nor increase the incidence of porosity.

Figure 12 shows that aging for 5000 hours at 1700°C resulted in minimal grain coarsening outside of the fusion zone. However, the distribution and frequency of porosity was not changed from the as-welded condition. As evidenced by this figure, full weld penetration was not achieved.

The bend ductile-brittle transition temperatures were determined for the welded material in each state of heat treatment. These data are given in Table VI and were determined from the plots of Figure 6 (800°F preheat) and Figure 13. As in the as-welded material, there is a preference in the heat treated materials for weld centerline fractures to occur in the bending of transverse weld specimens.

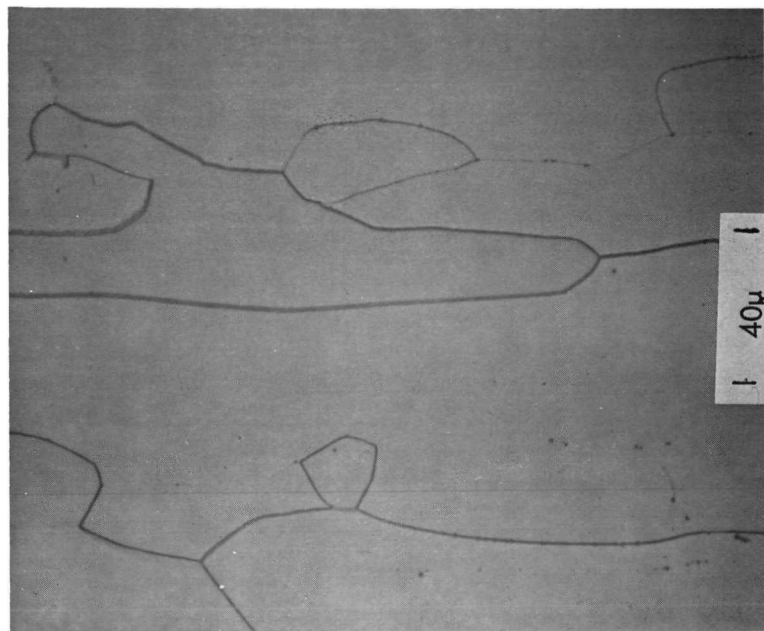
Table VI. Bend Ductile-Brittle Transition Temperatures for Welded Fluoride CVD Tungsten

Heat Treat Condition	DBTT (°C)	
	Longitudinal	Transverse
As-welded	< 260	455
Outgassed 50 hours at 1800°C	305	360
Outgassed + aged 5000 hours at 1540°C	290	340
Outgassed + aged 5000 hours at 1700°C	305	305



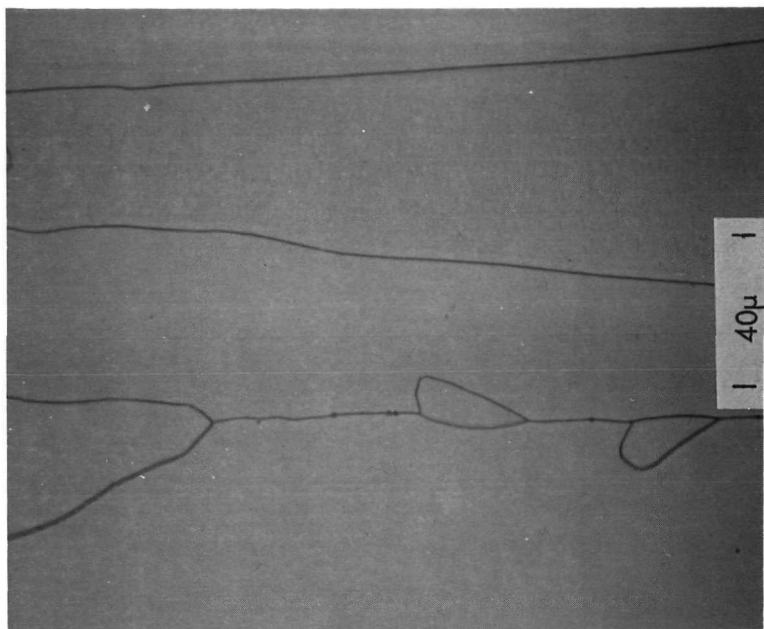
25X

a)



500X

b)



500X

c)

Figure 10. Transverse section through fluoride CVD tungsten following EB welding and outgassing. (50 H₂O₂ - 50 NH₄OH etch)

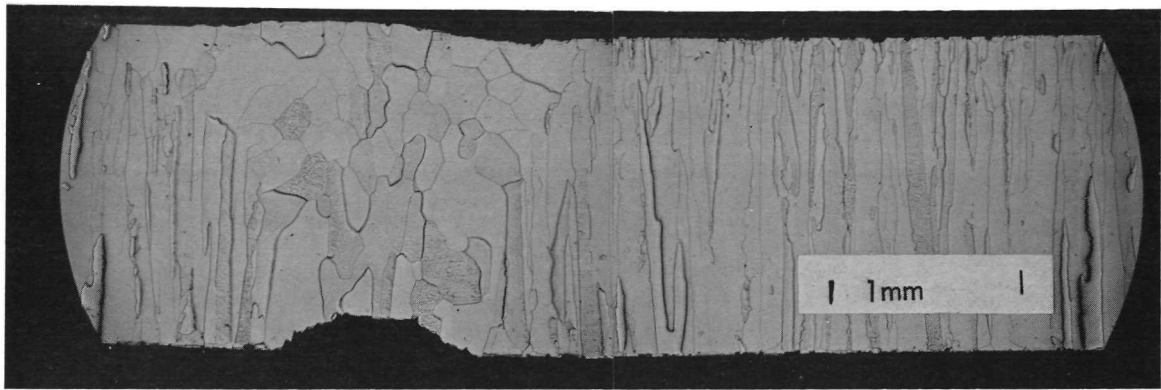


Figure 11. Transverse section through fluoride CVD tungsten following EB welding, outgassing and aging at 1540°C for 5000 hours. ($50\ \text{H}_2\text{O}_2 - 50\ \text{NH}_4\text{OH}$ etch)

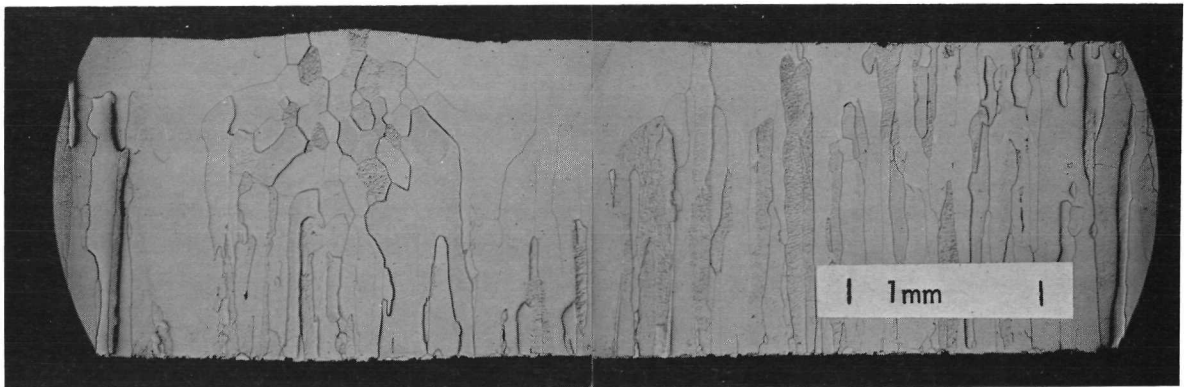


Figure 12. Transverse section through fluoride CVD tungsten following EB welding, outgassing and aging at 1700°C for 5000 hours. ($50\ \text{H}_2\text{O}_2 - 50\ \text{NH}_4\text{OH}$ etch)

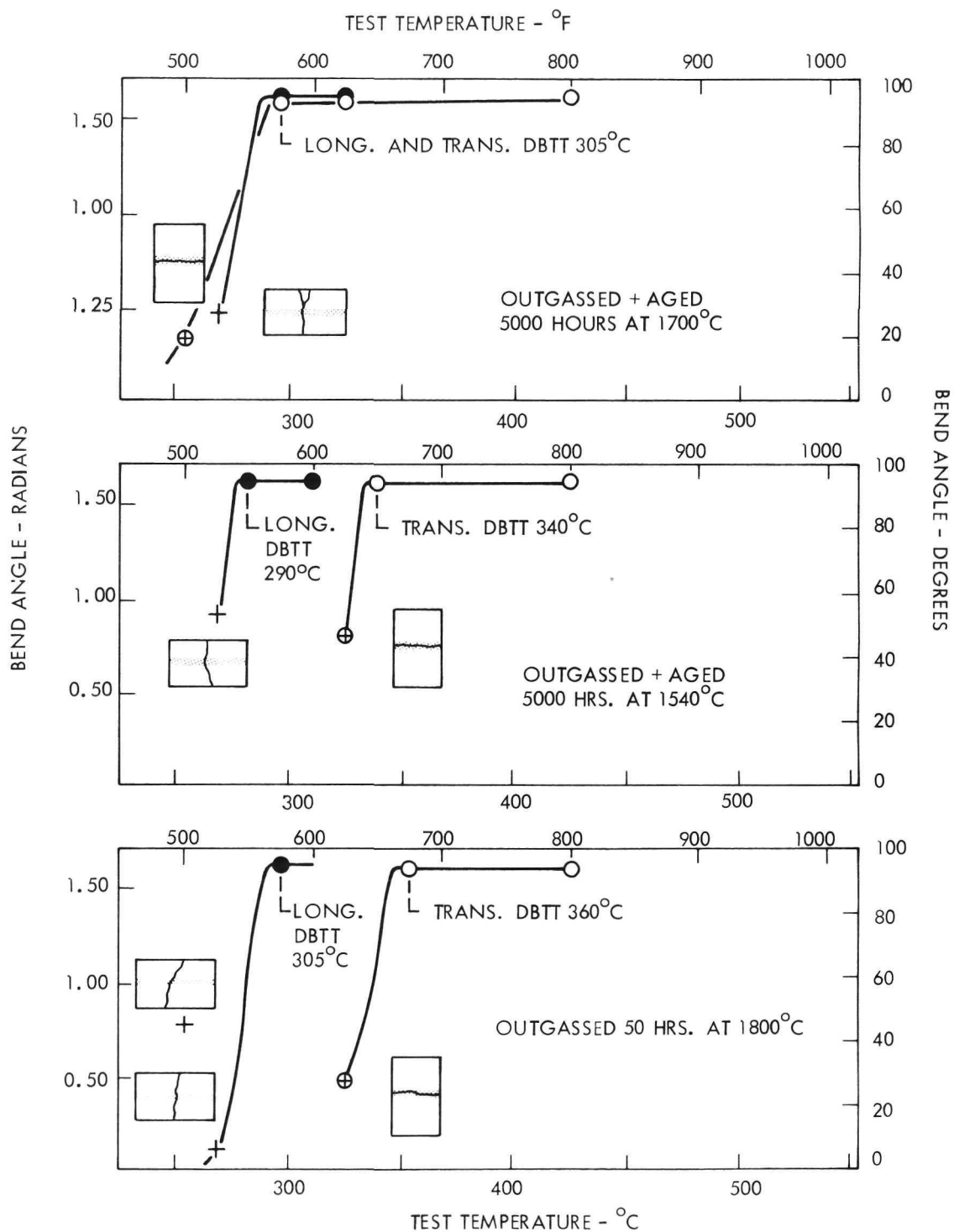


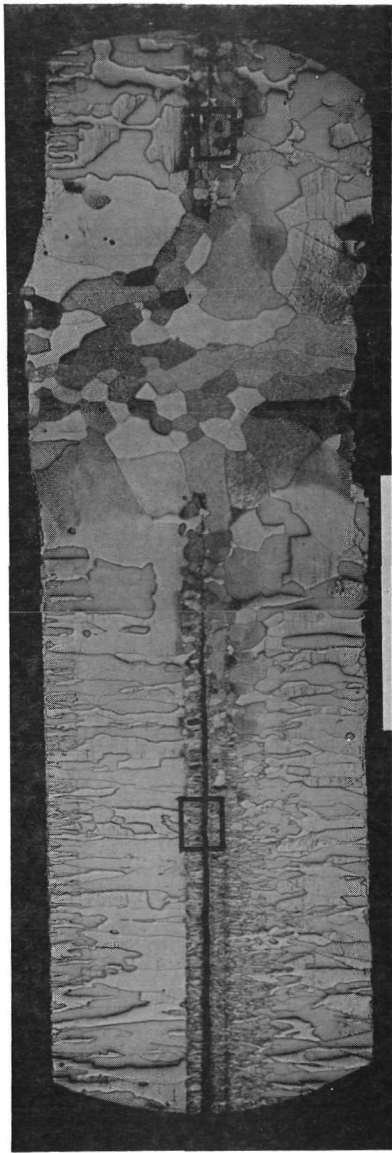
Figure 13. DBTT Data for Welded Fluoride CVD Tungsten

The DBTT for the transverse welds is lowered by the outgassing treatments. This reduction can likely be attributed to relief of residual stresses which attend solidification. No further significant reduction is affected by the aging treatments.

From a consideration of the weld specimen geometry (Figure 4), it is reasonable to expect that for longitudinal weld specimens ductile-brittle behavior would be much less affected by the properties of the weld and more affected by the structure of the unwelded portion of the specimen than would be the case for transverse weld specimens. This observation is borne out by the data of Table VI. The increased DBTT value found in the outgassed longitudinally welded material as compared to the as-welded material cannot be accounted for by any marked increase in grain size as the result of the outgassing treatment (Figure 10-a). If this value for the DBTT is taken as 260°C , it would not be judged to be significantly different from those associated with the heat treated specimens. No further increase in the transition temperature (within the limits of experimental determinations) accompanied either of the aging treatments. The corresponding change in grain size was minimal judging from Figures 11 and 12.

The microstructure of the welded chloride-produced tungsten is shown in Figure 14a. Within the heat-affected zone, porosity was noted at one of the interlayer interfaces (Figure 14b). The dark band passing through the portion of the specimen unaffected by welding is not a crack but, as shown by Figure 14c, is a layer of extremely fine grain size.

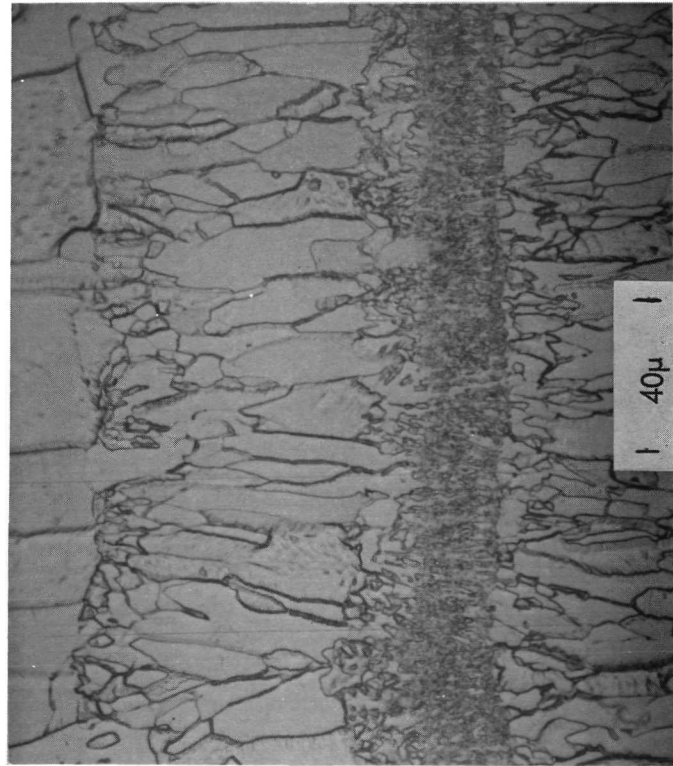
The remainder of the material is essentially pore free except for the very fine porosity occasionally noted throughout the length of the one layer.



25X

| 1mm |

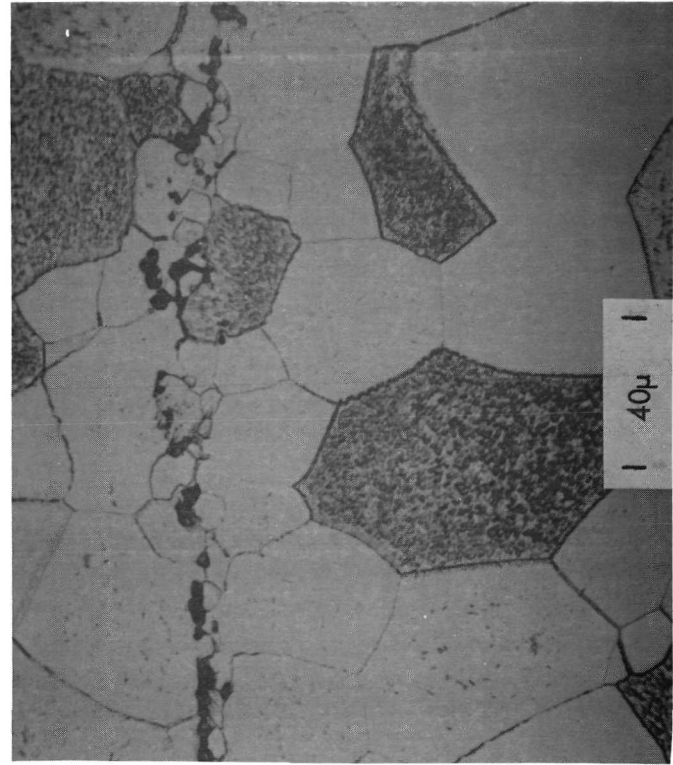
a)



500X

| 40μ |

c)



500X

| 40μ |

b)

Figure 14. Transverse Section Through Chloride CVD Tungsten Following EB Welding
(30 lactic - 3 HNO₃ - 1 HF etch)

No specimens were available with which the effect of outgassing on welded material could be determined. However, it was noted from unwelded material that this heat treatment produced considerable grain growth. (This is described more fully in the section on Bend and Tensile Strength Properties.)

Aging at 1540°C produced the microstructure of Figure 15a. Grain growth occurred beyond the size (135 μ) found in outgassed material. Within the heat affected zone several very large pores can be seen at locations once occupied by interlayer interfaces. Fine porosity was noted at these interfaces in regions lying outside the weld-affected region (see Figure 15b) and occurred to a greater extent than it did in as-welded material indicating a coalescence of vacancies.

This interlayer interface porosity was accentuated by the 1700°C aging treatment (Figure 16a). Large pores are now evident throughout the specimen rather than just within or near the heat affected zone as occurred during the lower temperature aging treatment. Examination at 500X revealed some fine porosity as typified by the photomicrograph of Figure 16b. The grain size is equivalent to that produced by the 1540°C age.

The ductile-brittle transition temperatures as a function of heat treatment were determined. These results are contained in Table VII and were obtained from the data of Figures 7 and 17. A general preference for weld centerline failures for transverse welds was noted. It would appear that the DBTT of both the longitudinal and transverse weldments are essentially identical. The variability noted is believed to result from the variation in top of weld surface topography as discussed earlier. The increase in DBTT for the longitudinal specimens can be attributed to the grain size increase during the post weld thermal treatments. The DBTT values for each heat treatment condition are significantly higher than for their fluoride tungsten counterparts.

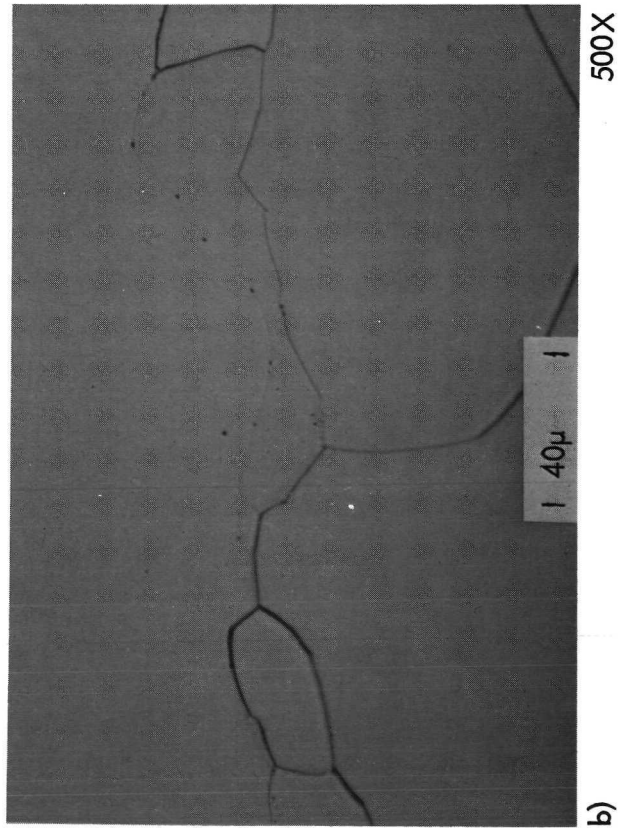
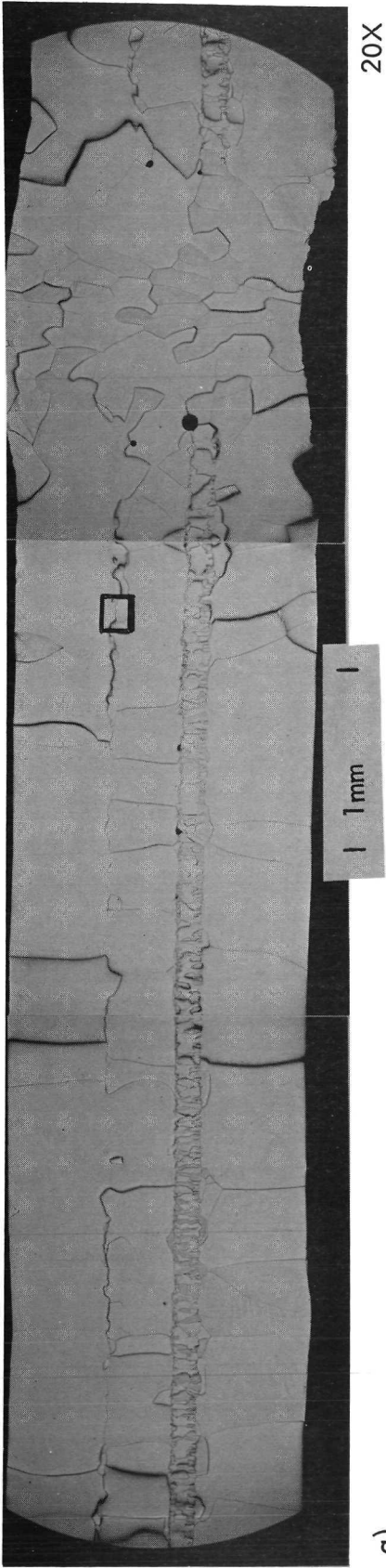
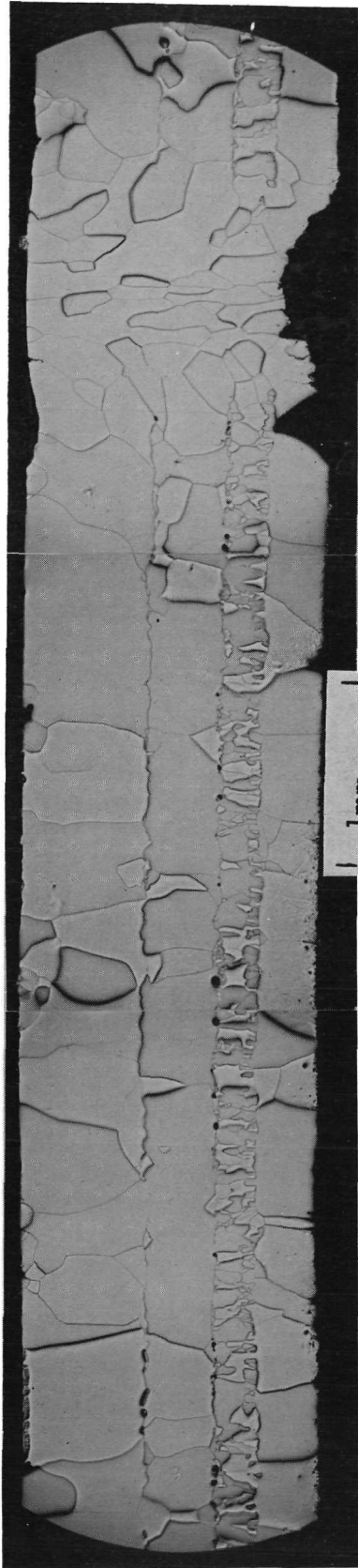
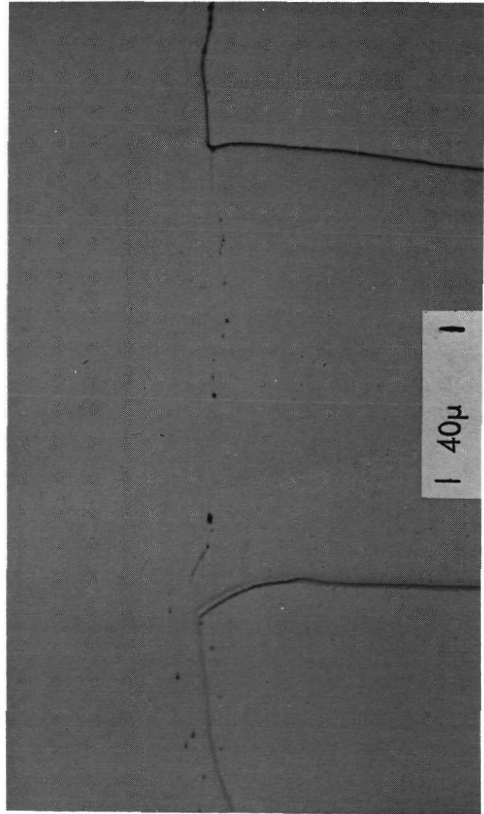


Figure 15. Transverse Section Through Chloride CVD Tungsten Following EB Welding, Outgassing and Aging at 1540°C for 5000 Hours. (30 lactic - 3 HNO₃ - 1 HF etch)



25X

a)



500X

b)

Figure 16. Transverse Section Through Chloride CVD Tungsten Following EB Welding, Outgassing and Aging at 1700°C for 5000 Hours. (30 lactic - 3 HNO₃ - 1 HF etch)

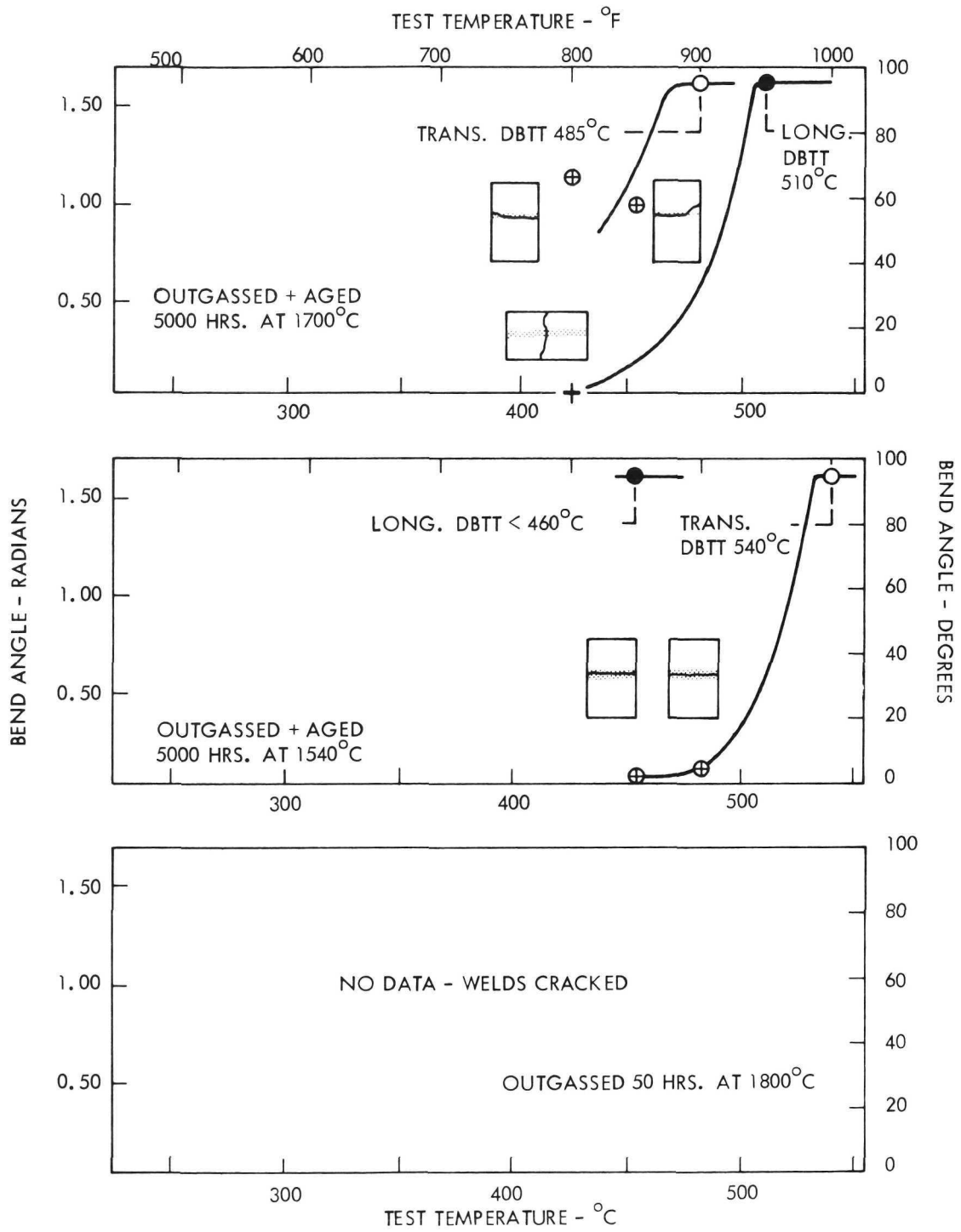


Figure 17. DBTT Data for Welded Chloride CVD Tungsten

Table VII

Bend Ductile-Brittle Transition Temperatures for Welded Chloride CVD Tungsten

<u>Heat Treat Condition</u>	<u>DBTT (°C)</u>	
	<u>Longitudinal</u>	<u>Transverse</u>
As welded (no preheat)	400	540
Outgassed 50 hours at 1800°C	No Data -Welds Cracked Prior to Testing	
Outgassed + aged 5000 hours at 1540°C	<460	540
Outgassed + aged 5000 hours at 1700°C	510	485

Figure 18a is a transverse view of a weld made in the duplex material prior to any post-weld heat treatment. Very little porosity was noted in either the weld zone or outside of it. That which was noted was very fine and generally was found in the heat-affected zone at a location of an interlayer interface (Figure 18b).

Outgassing the welded material produced considerable grain coarsening of the chloride-produced portion (Figure 19a) but did not appreciably increase the amount of porosity. That porosity which was noted was again found in the heat-affected zone lying along grain boundaries (Figure 19b).

Aging at either 1540°C or 1700°C had no effect on the extent of porosity but did produce grain coarsening in the chloride portion (Figures 20 and 21). Weld centerline cracking was noted in the latter specimen.

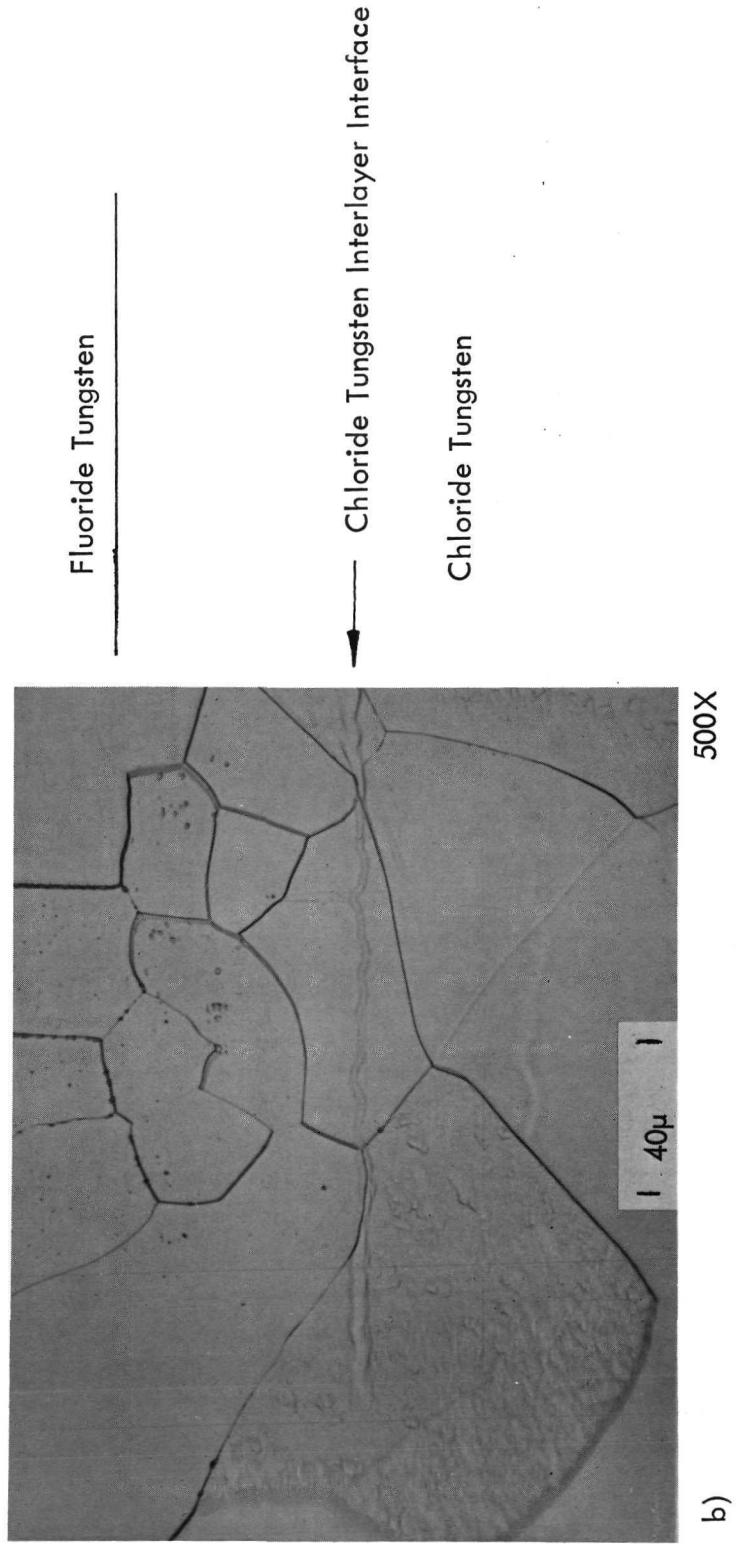
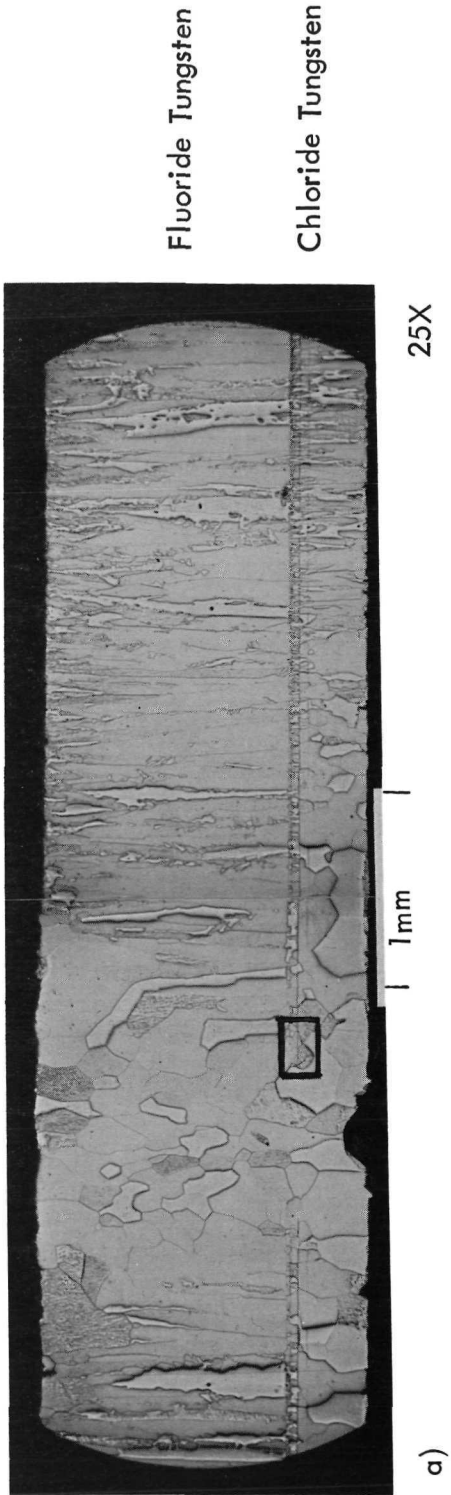


Figure 18. Transverse Section Through Duplex CVD Tungsten Following EB Welding
(30 lactic - 3 HNO₃ - 1 HF etch)

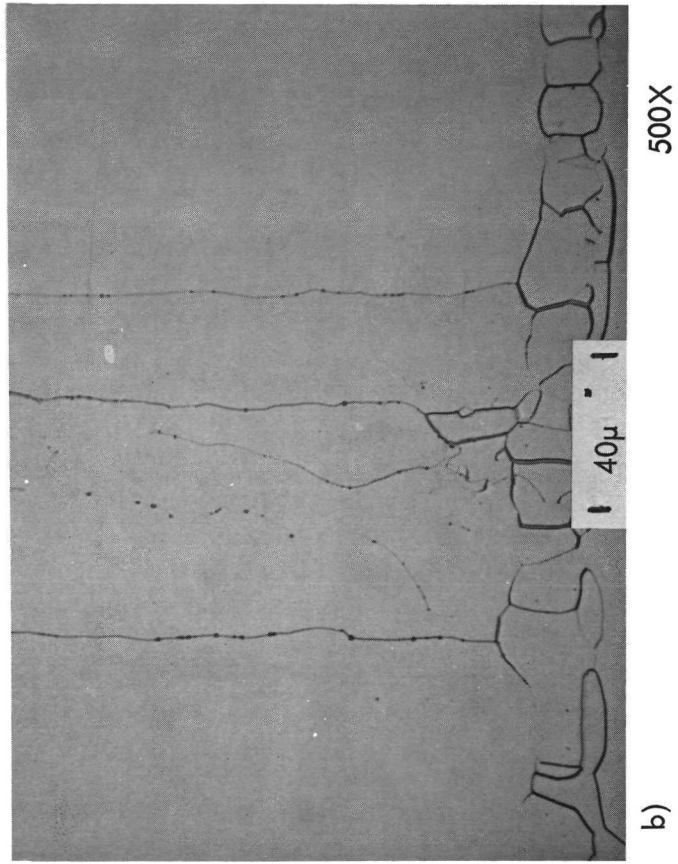
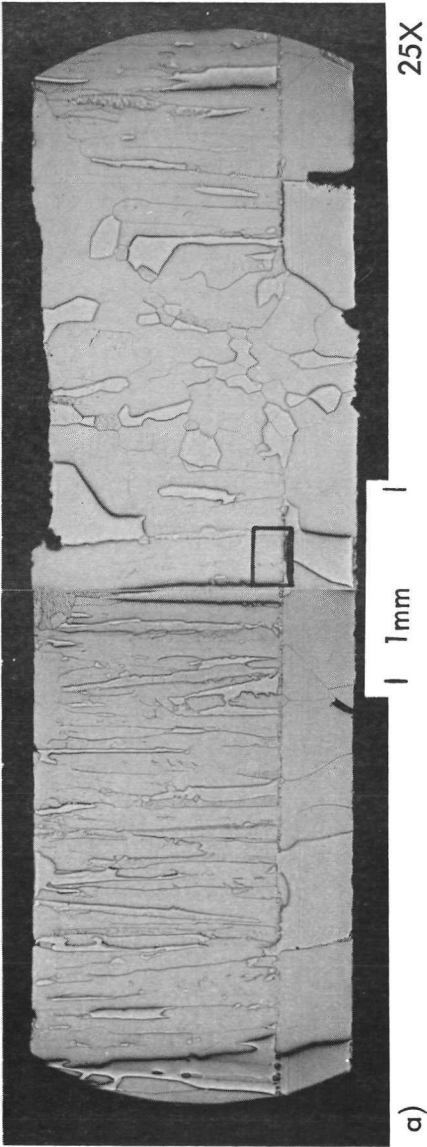


Figure 19. Transverse Section Through Duplex CVD Tungsten Following EB Welding and 50 Hours at 1800°C. (30 lactic - 3 HNO₃ - 1 HF etch)

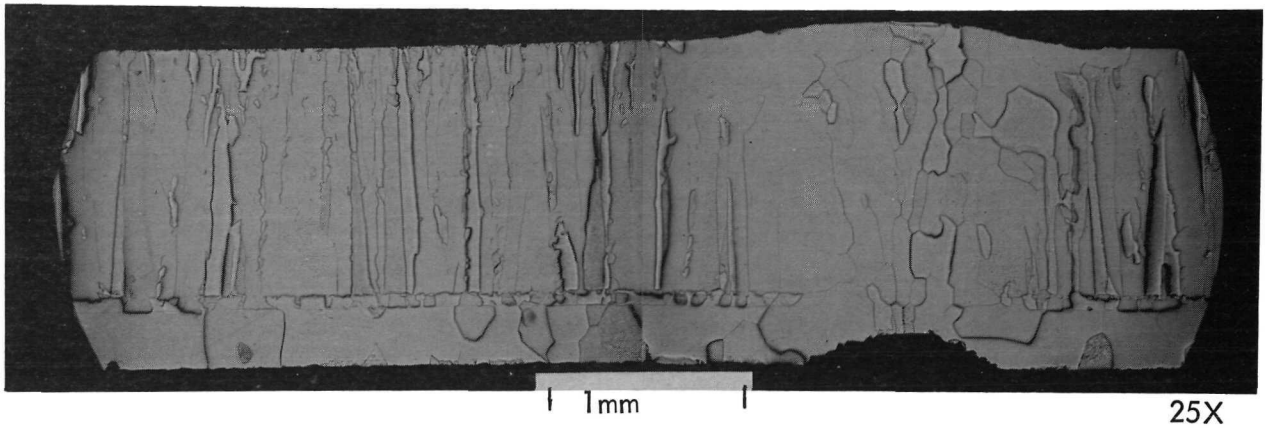


Figure 20. Transverse Section Through Duplex CVD Tungsten Following EB Welding, Outgassing and Aging at 1540°C for 5000 Hours
(30 lactic - 3 HNO₃ - 1 HF etch)

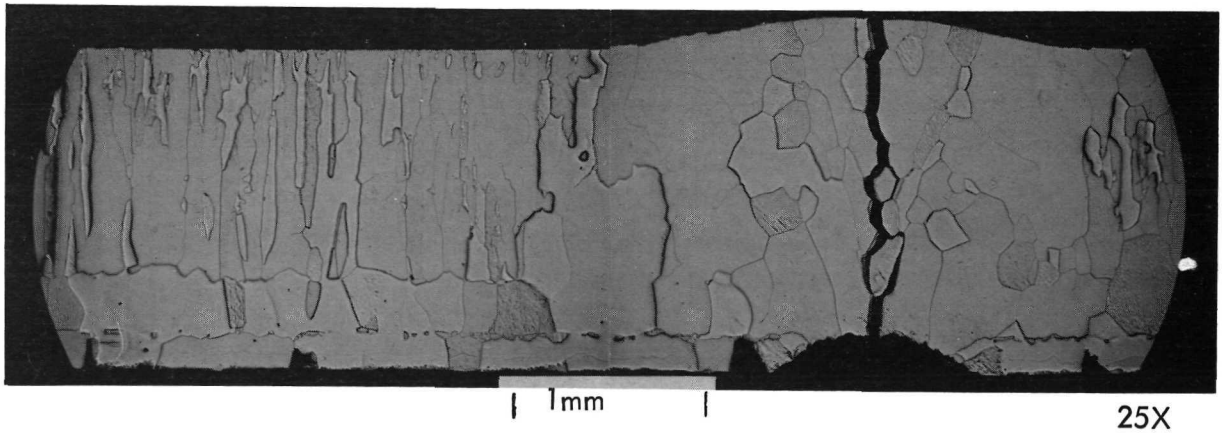


Figure 21. Transverse Section Through Duplex CVD Tungsten Following EB Welding, Outgassing, and Aging at 1700°C for 5000 Hours.
(30 lactic - 3 HNO₃ - 1 HF etch)

Since the welds were bend tested with the fluoride component being placed in tension, the results on the DBTT determinations (Table VIII obtained from data of Figures 8 and 22) would be expected to be similar to those obtained on the fluoride-produced tungsten (Table VI). The data for transverse welds are very similar, the only significant difference being in the DBTT following outgassing, which is considerably higher for the duplex material. As in the other two materials weld centerline failures were found in the fracture transverse specimens.

The DBTT data for the longitudinally welded duplex tungsten (Table VIII) is, on the whole, approximately equivalent to the corresponding data for fluoride tungsten. There is essentially no change in DBTT with thermal treatment. This trend is not unexpected since the fluoride portion of the material was very structurally stable.

Table VIII

Bend Ductile-Brittle Transition Temperatures for Welded Duplex CVD Tungsten

<u>Heat Treat Condition</u>	<u>DBTT (°C)</u>	
	<u>Longitudinal</u>	<u>Transverse</u>
As welded	315	430
Outgassed 50 hours at 1800°C	315	455
Outgassed + aged 5000 Hours at 1540°C	<280	315
Outgassed + aged 5000 hours at 1700°C	280	330

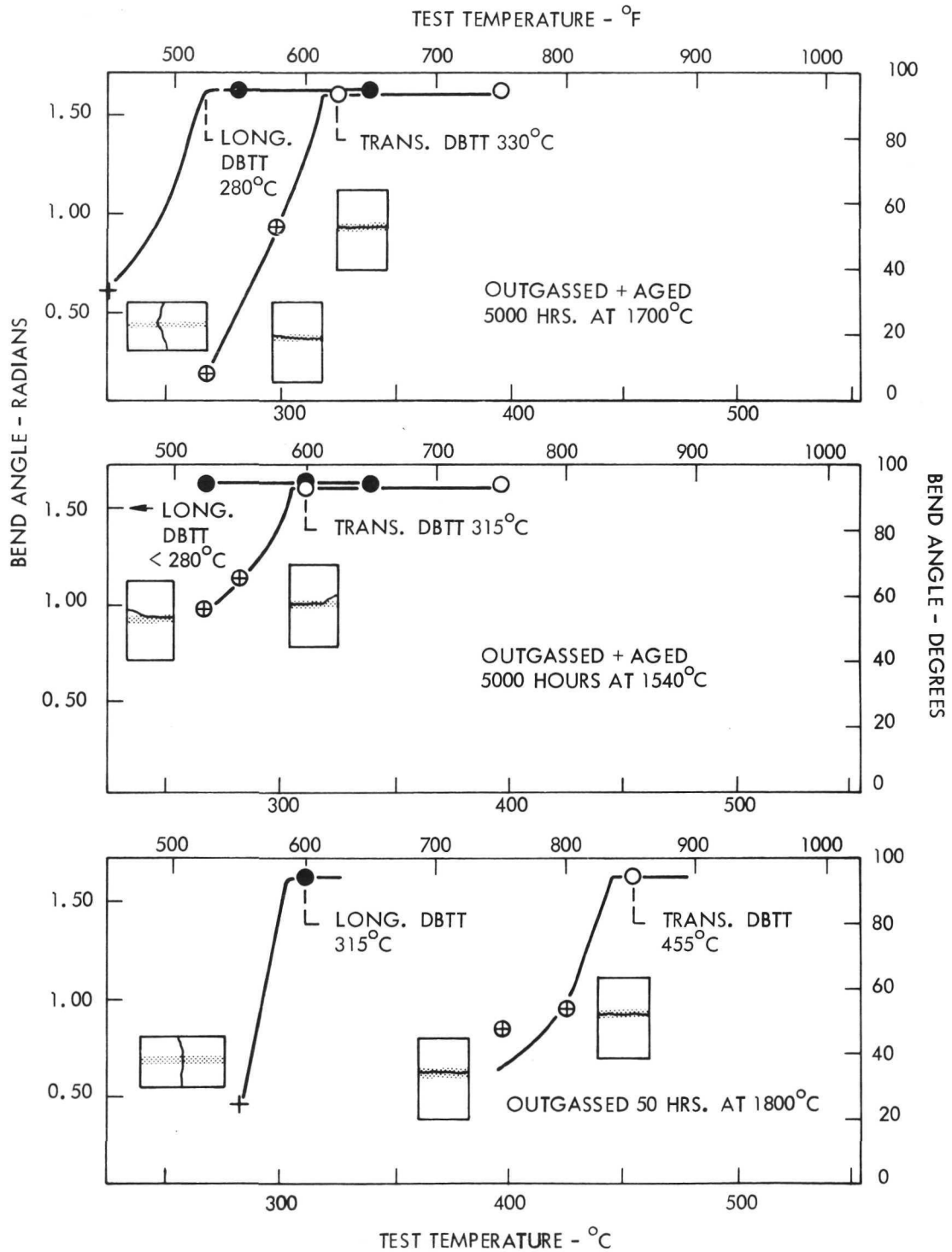


Figure 22. DBTT Data for Welded Duplex CVD Tungsten

5.2 BEND AND TENSILE PROPERTIES

Several thermal treatments, which simulate conditions during thermionic diode startup, were evaluated as to their effect on the ductile-brittle behavior of the three CVD tungsten materials in the unwelded condition. This summary information is given in Table IX which was compiled from the data of Figures 23 through 25.

Table IX. DBTT of CVD Tungsten for Various Thermal Treatments

Thermal Treatment	Fluoride		Chloride		Duplex	
	°C	°F	°C	°F	°C	°F
Stress Relieved (1 hr at 1200°C)	205	400	510	950	290	550
SR+Outgassed (50 hrs at 1800°C)	260	500	455	850	290	550
SR+O+thermally cycled to 1540°C ten times within 500 hours	250	475	455	850	275	525
SR+O+thermally cycled to 1700°C ten times within 500 hours	250	475	455	850	305	575

For the two parent materials, essentially opposite behavior of DBTT with thermal treatment was found. Fluoride produced tungsten was more brittle (increased DBTT) following outgassing. Further high temperature exposure had essentially no effect. This trend is in agreement with that found previously for longitudinally welded material (Table VI). However, as would be expected, the DBTT for the unwelded material is lower for any heat treatment.

In chloride produced tungsten the DBTT was lowered by the outgassing treatment but was unaffected by further thermal treatment. A meaningful comparison between these data and those determined from the longitudinally welded material is not possible, since data for the outgassed welded material were not available and, as previously explained, the welded material occasionally contained weld defects. A tentative explanation

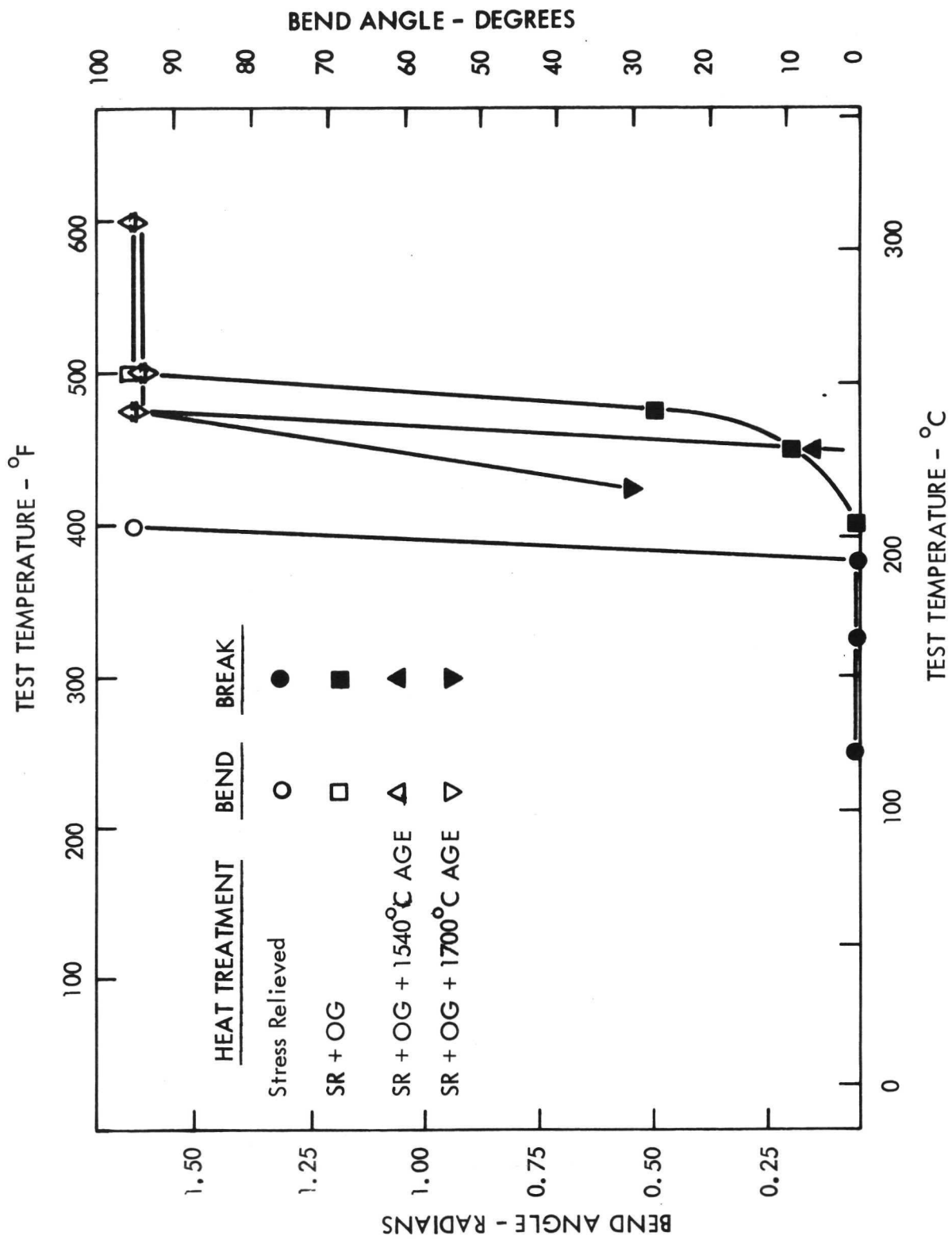


Figure 23. Bend Data for Unwelded Fluoride CVD Tungsten

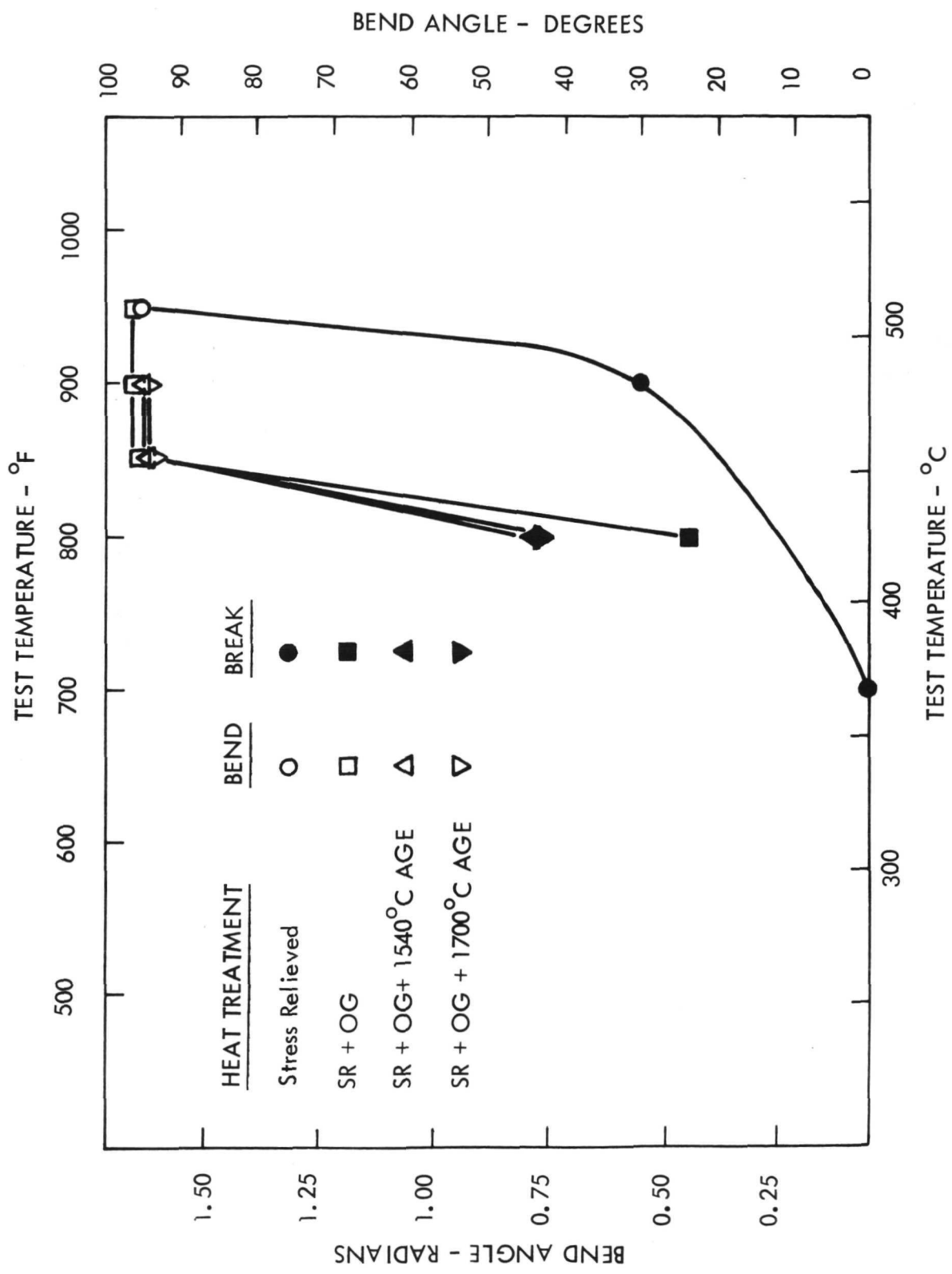


Figure 24. Bend Data for Unwelded Chloride CVD Tungsten

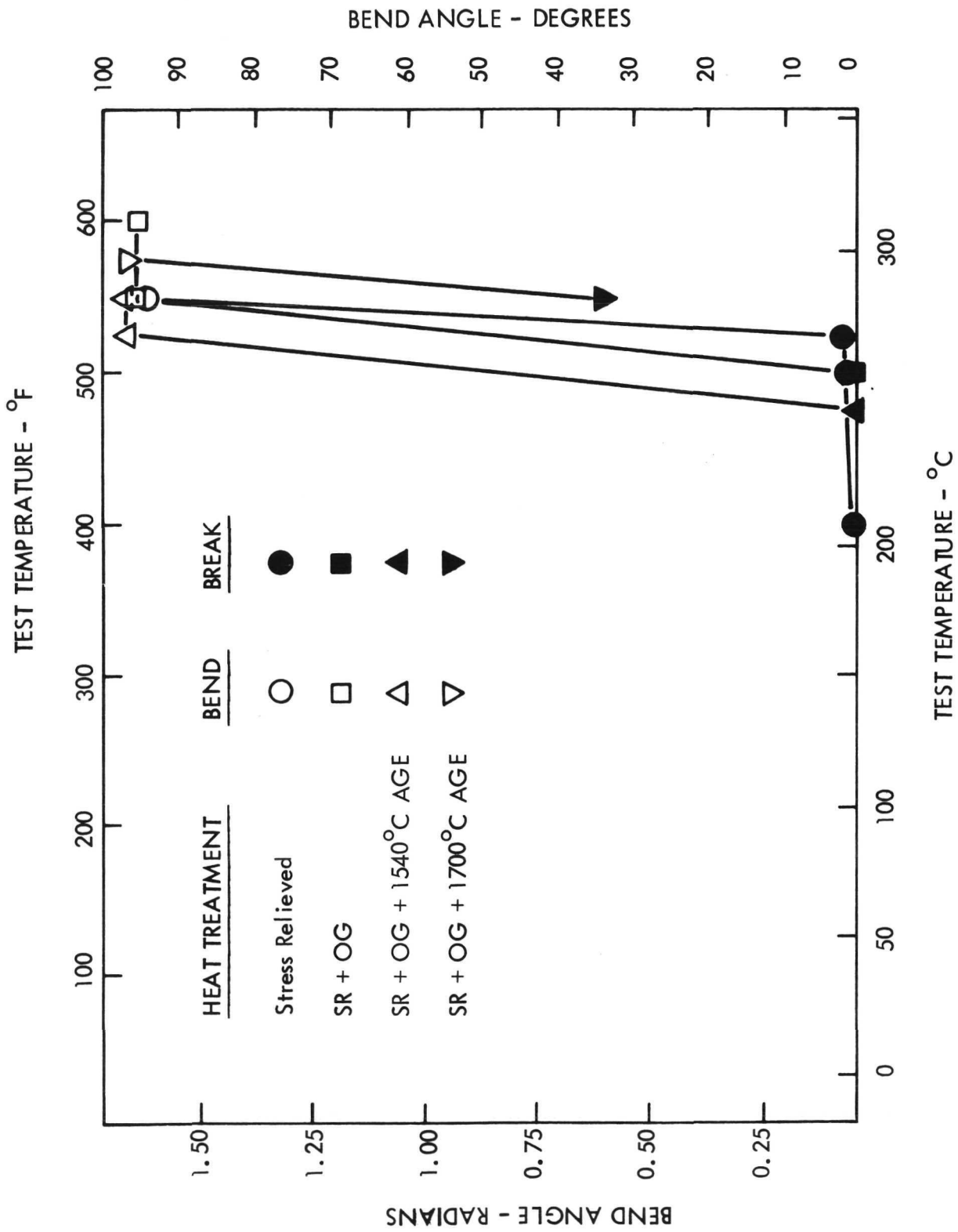


Figure 25. Bend Data for Unwelded Duplex CVD Tungsten

for the observed behavior of the unwelded chloride tungsten is that the expected embrittlement accompanying the extensive grain growth (to be discussed subsequently) was more than offset by the elimination of residual stress which had apparently not been relieved by the stress relief treatment.

The behavior of duplex tungsten as regards its DBTT is essentially unaffected by the series of thermal treatments. In effect the behavior of this material is a compromise between that of its two constituents. This is not totally different from the results observed on the longitudinally welded duplex tungsten (Table VIII).

Elevated temperature tensile tests were run on the materials given the following separate heat treatments.

- o Stress relieved (1 hour at 1200°C) and outgassed (50 hours at 1800°C)
- o Stress relieved, outgassed and aged (5000 hours at 1540°C)
- o Stress relieved, outgassed and aged (5000 hours at 1700°C)

The results are presented in Figures 26 through 37. In each case for the ultimate tensile strength data, essentially brittle fracture (as determined by visual examination of the fractured surface) is denoted by the solid data points while ductile fracture is represented by the open data points. In the majority of cases the yield strength is that determined at 0.2% offset. However where upper and lower yield points occurred the latter were used in the data plots and are so indicated by solid data points to distinguish them from the 0.2% offset values (open data points). Upper yield points are indicated as such.

As mentioned, over the temperature range studied, both brittle and ductile behavior were noted. To better represent the two fracture modes and to correct the ultimate engineering tensile strength for changes in specimen cross-sectional area, true maximum strength values were calculated from the relation:

$$\text{true stress} = \frac{P_{\max} (e + 1)}{A_0}$$

where P_{\max} = maximum load

A_0 = original cross-sectional area

e = engineering strain at $P_{\max} = \frac{L - L_0}{L_0}$

where L = gage length at P_{\max}

L_0 = original gage length (Figure 5)

The yield strength of the fluoride CVD tungsten is seen to decrease slightly with increased severity of thermal treatment as expected (Figures 26, 27, and 28) due possibly in part to the slight coarsening of the grain structure. The initial precipitous drop in yield strength with increasing temperature occurs in the homologous temperature range 0.15 to 0.25 T/T_m (about 350 to 750°C).

Ultimate tensile strengths are essentially unchanged by long exposure to elevated temperature. This is to be expected since grain coarsening effects would have their greatest effect during the early part of deformation.

The ductility of fluoride tungsten as represented by percent tensile elongation as a function of temperature is shown in Figure 29. The minimum at about 1500°C which accompanies the two least severe heat treatments is not an anomalous effect but is the result of microstructural changes occurring during tensile testing. These changes and their causes are described in the Discussion section of this report.

As seen by a comparison of Figures 30, 31 and 32, the elevated temperature tensile strength and yield strength of chloride tungsten is practically unchanged by either of the long time aging treatments.

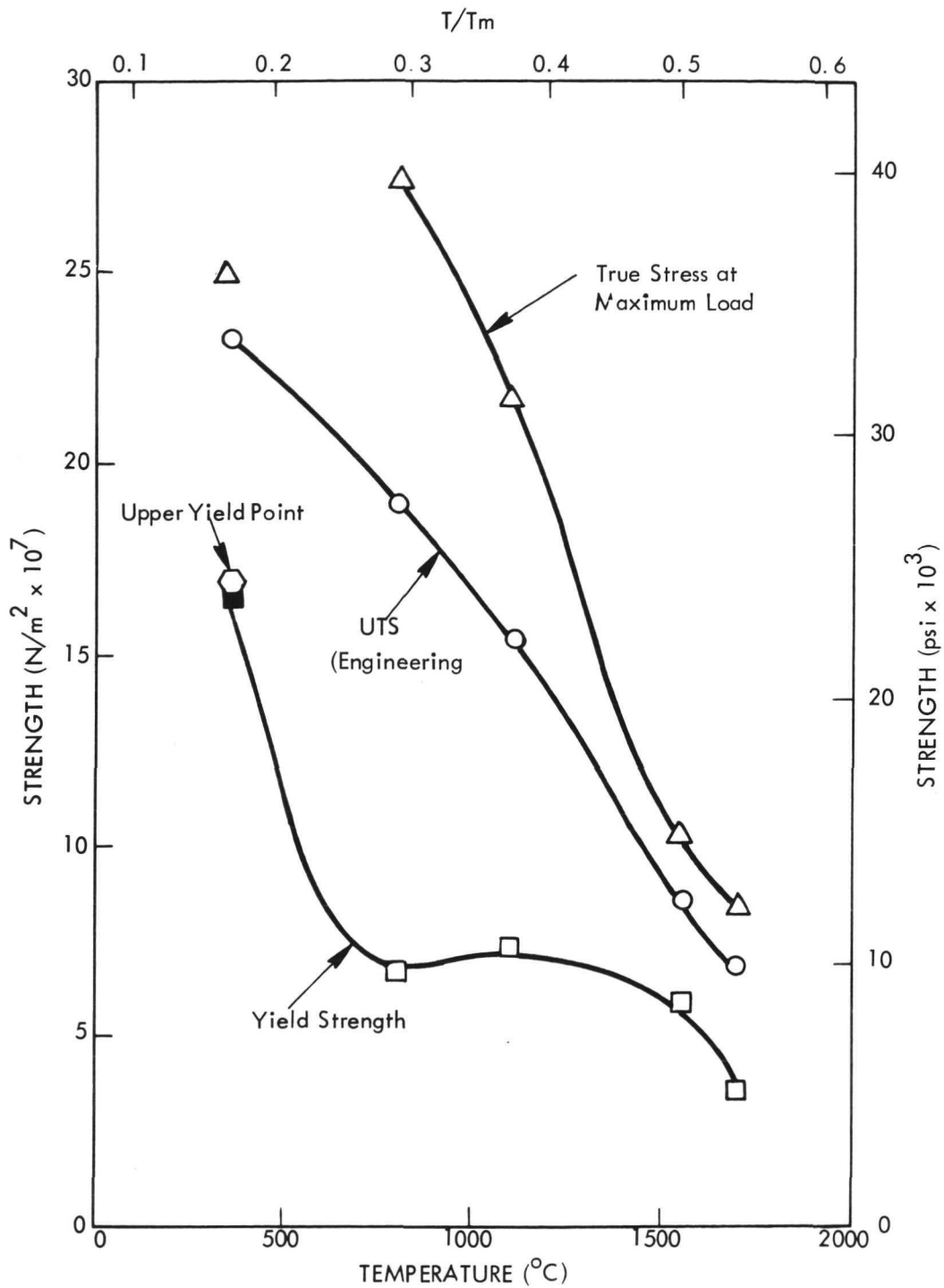


Figure 26. Elevated Temperature Tensile Properties of Fluoride CVD Tungsten Stress Relieved (1 hour at 1200°C) and Outgassed (50 hours at 1800°C).

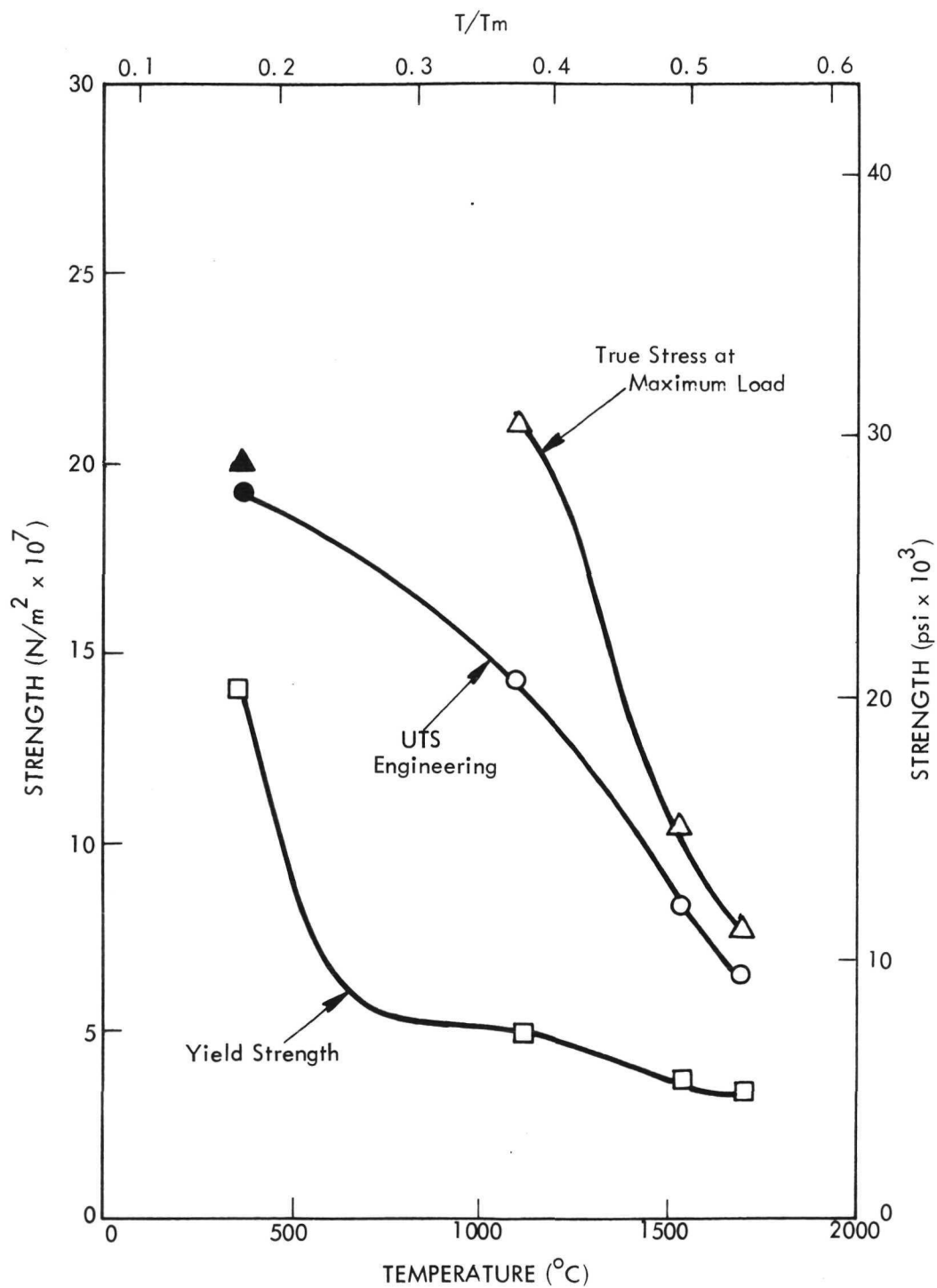


Figure 27. Elevated Temperature Tensile Properties of Fluoride CVD Tungsten Stress Relieved, Outgassed and Aged (5000 hours at 1540°C).

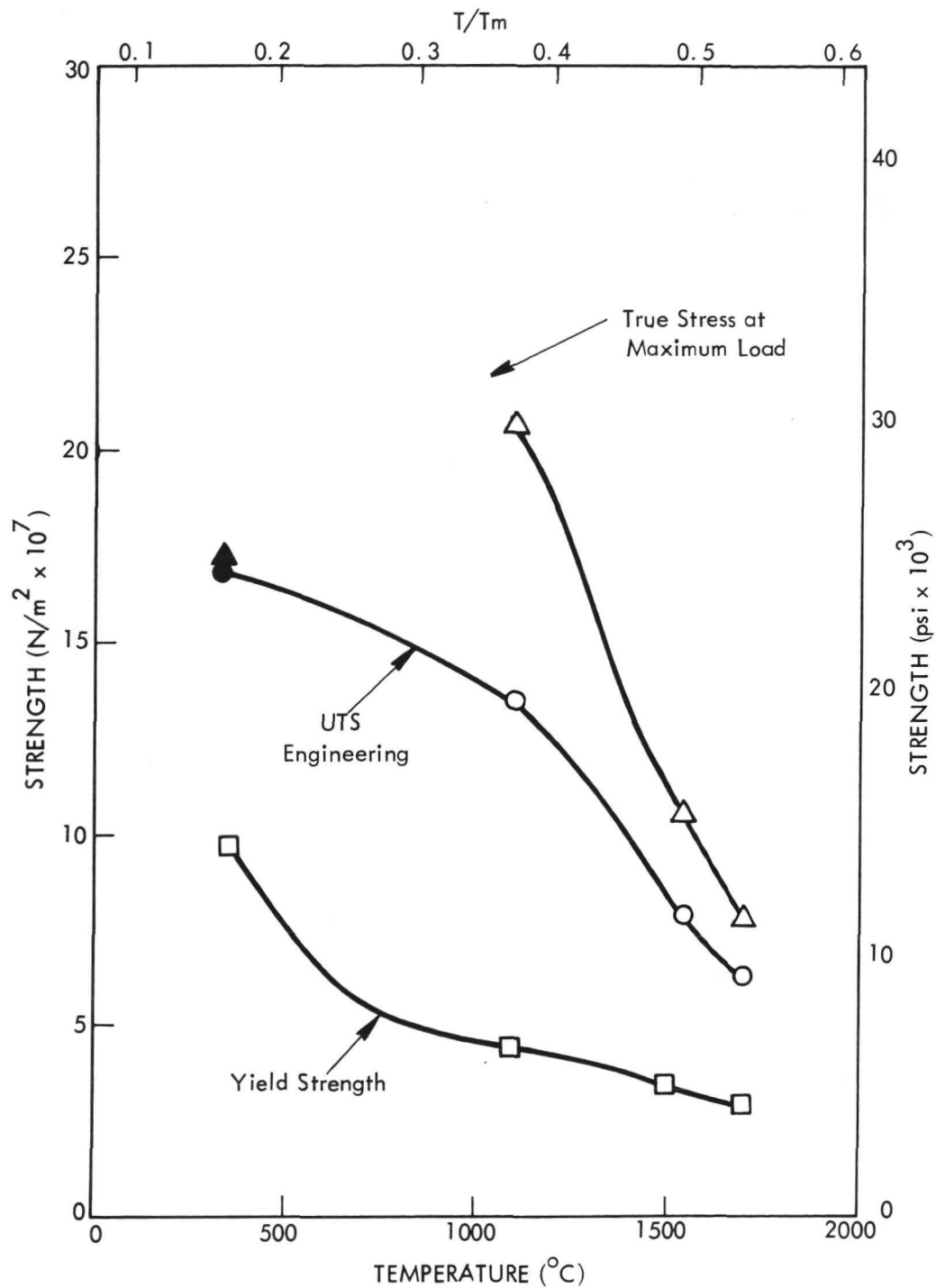


Figure 28. Elevated Temperature Tensile Properties of Fluoride CVD Tungsten Stress Relieved, Outgassed and Aged (5000 hours at 1700°C).

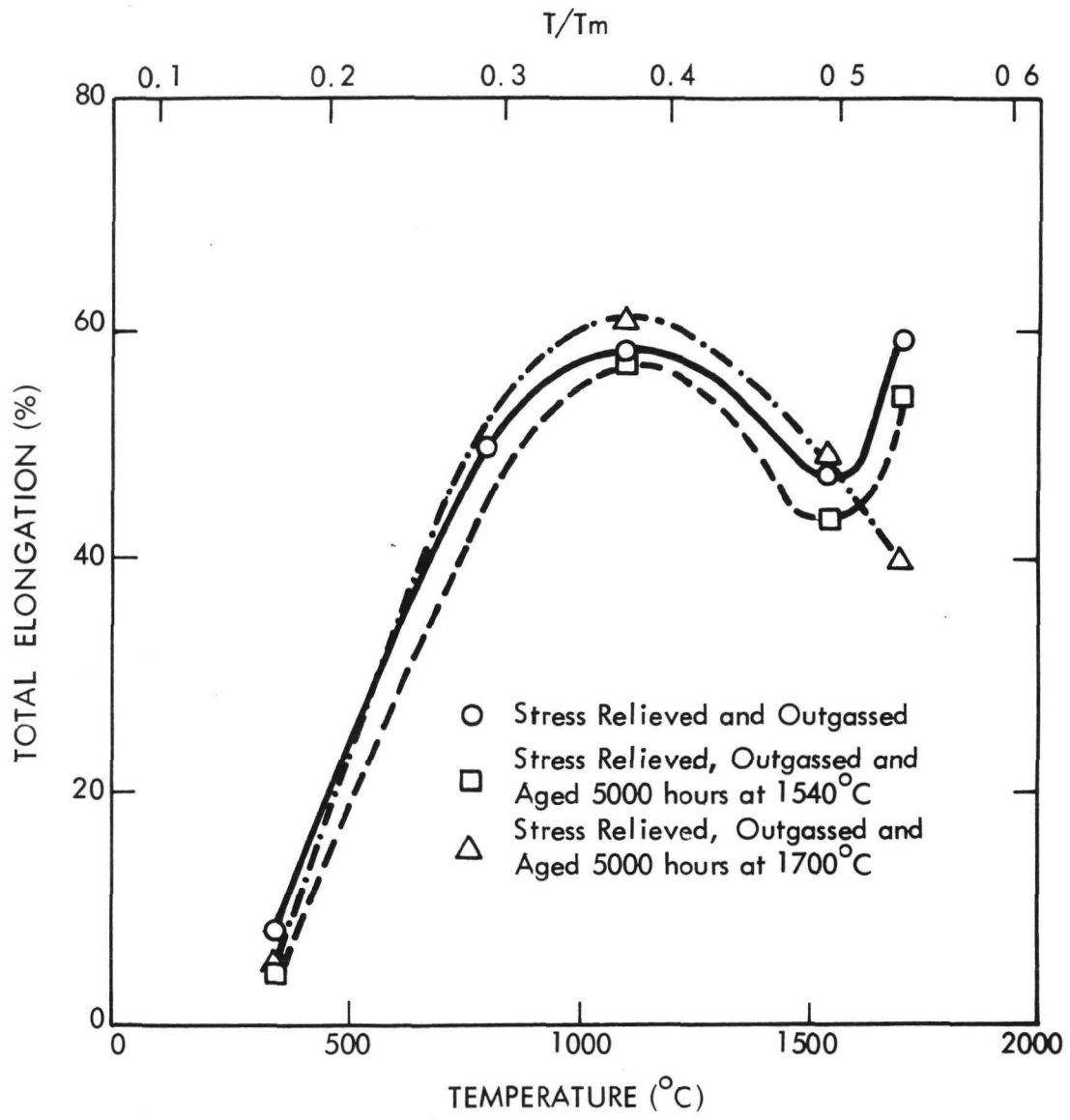


Figure 29. Elevated Temperature Total Elongation of Fluoride CVD Tungsten.

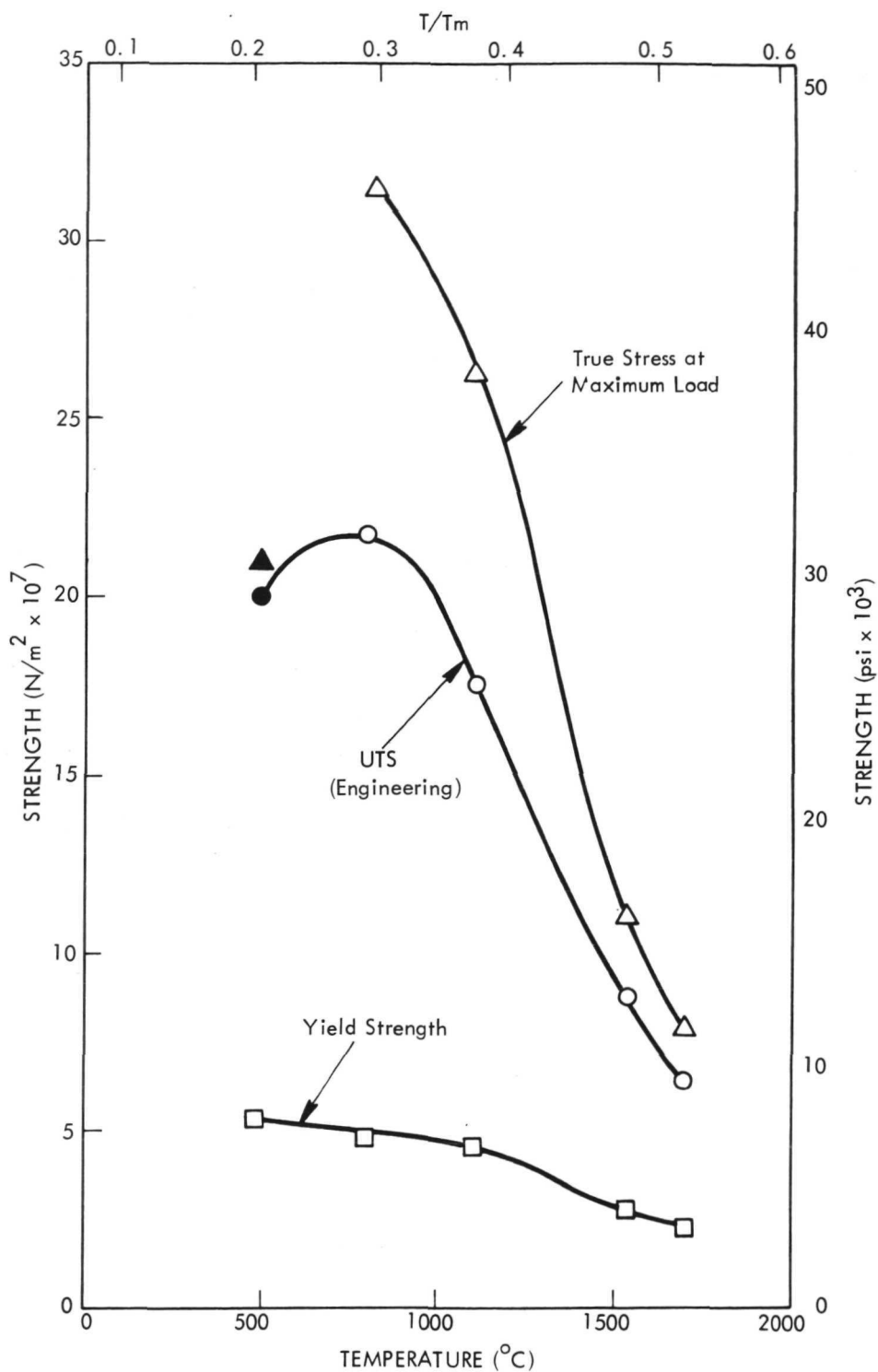


Figure 30. Elevated Temperature Tensile Properties of Chloride CVD Tungsten Stress Relieved (1 hour at 1200°C) and Outgassed (50 hours at 1800°C).

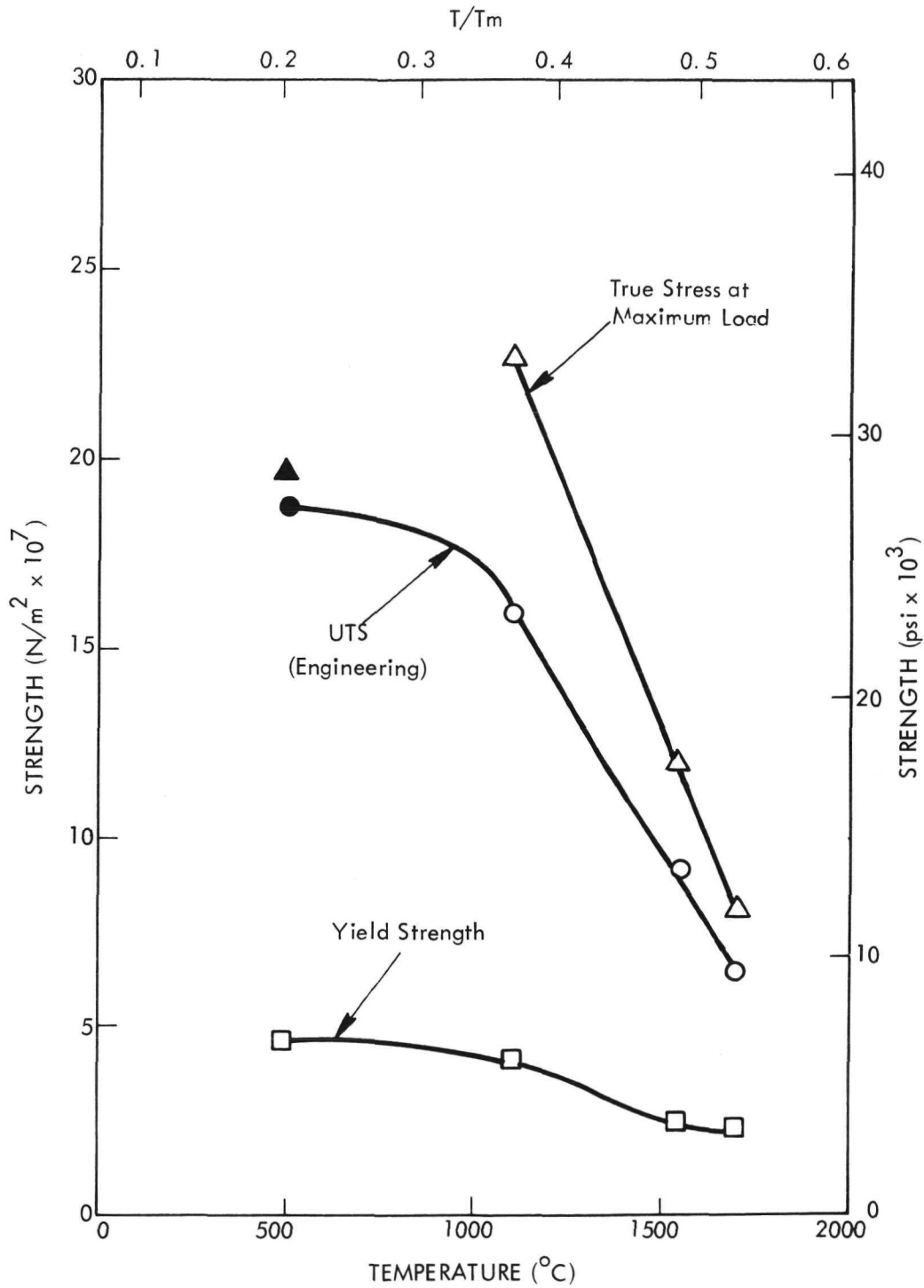


Figure 31. Elevated Temperature Tensile Properties of Chloride CVD Tungsten Stress Relieved, Outgassed and Aged (5000 hours at 1540°C).

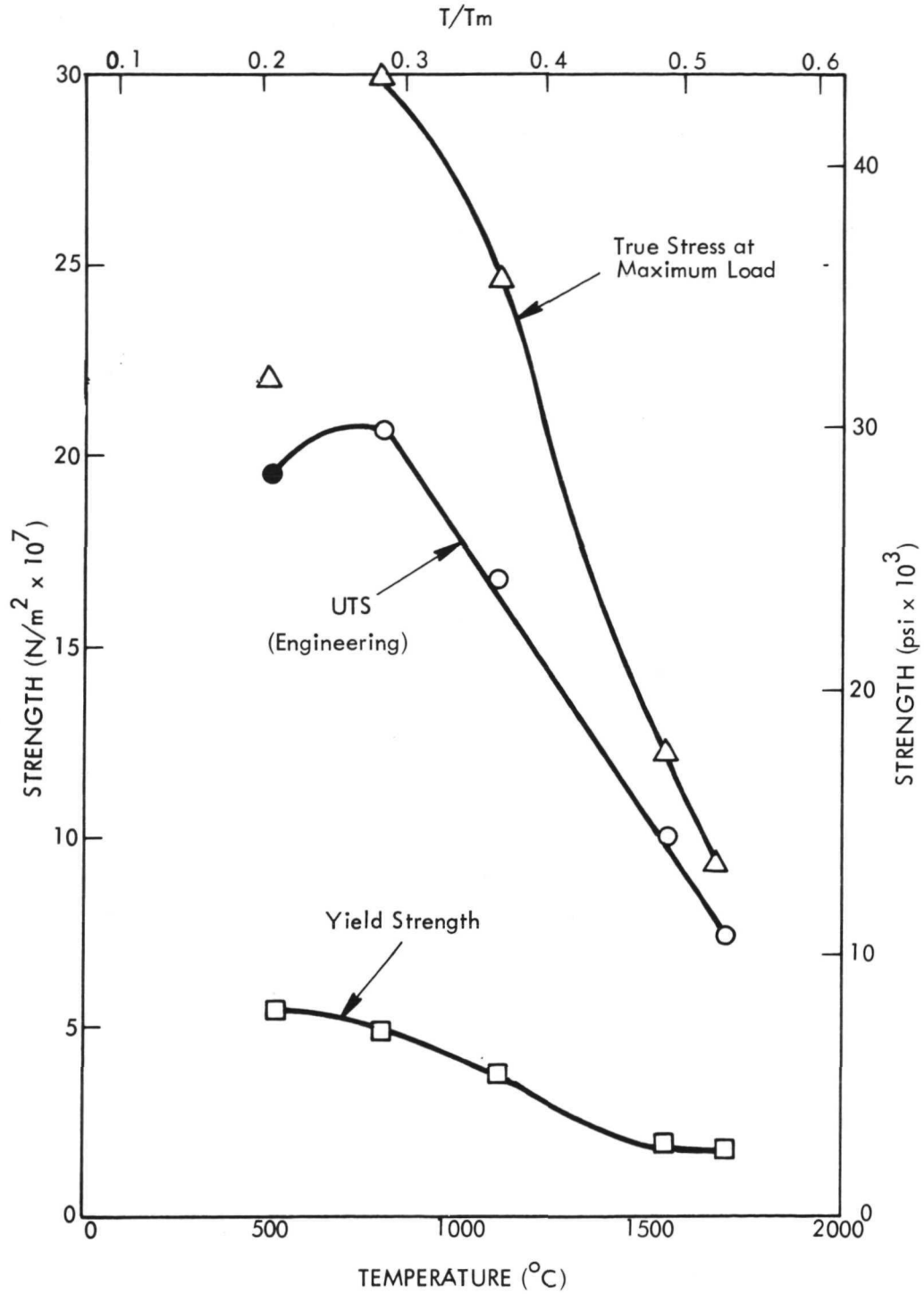


Figure 32. Elevated Temperature Tensile Properties of Chloride CVD Tungsten Stress Relieved, Outgassed and Aged (5000 hours at 1700°C).

With decreasing test temperature the yield strength does not increase appreciably at about 800°C as it does for fluoride tungsten. This would indicate that extensive slip occurs in the chloride material at temperatures at least as low as 0.2 T/T_m.

This increased ease of slip at low temperature is reasonable in view of the coarser grain size possessed by the chloride tungsten.

The ductility of chloride tungsten (Figure 33) as a function of test temperature follows the same general pattern as does the fluoride tungsten. However, the maximum ductility for the former is associated with a lower temperature, possibly related to the very large grain size possessed by this material.

The strength behavior of duplex tungsten (Figures 34 through 36) as compared to that of its separate constituents is roughly an average of the two. The yield strength of duplex tungsten as a function of temperature is similar to that of fluoride tungsten except following extended exposure at 1700°C (Figure 36) when it behaves more nearly like that of chloride material.

Figure 37 shows ductility data for duplex tungsten. Its behavior is more similar to that of chloride than it is to fluoride tungsten in that maximum ductility is found at about 800-900°C rather than near 1100°C.

Strength and elongation data for the three types of CVD tungsten are summarized in Table X.

5.3 MICROSTRUCTURAL STABILITY

A thorough study of the effect of high temperature exposure on grain size was not possible owing to the variable nature of the starting material (in the stress relieved condition) in this respect. However, as shown subsequently, the average behavior of each type of tungsten could be studied and compared with changes in hardness.

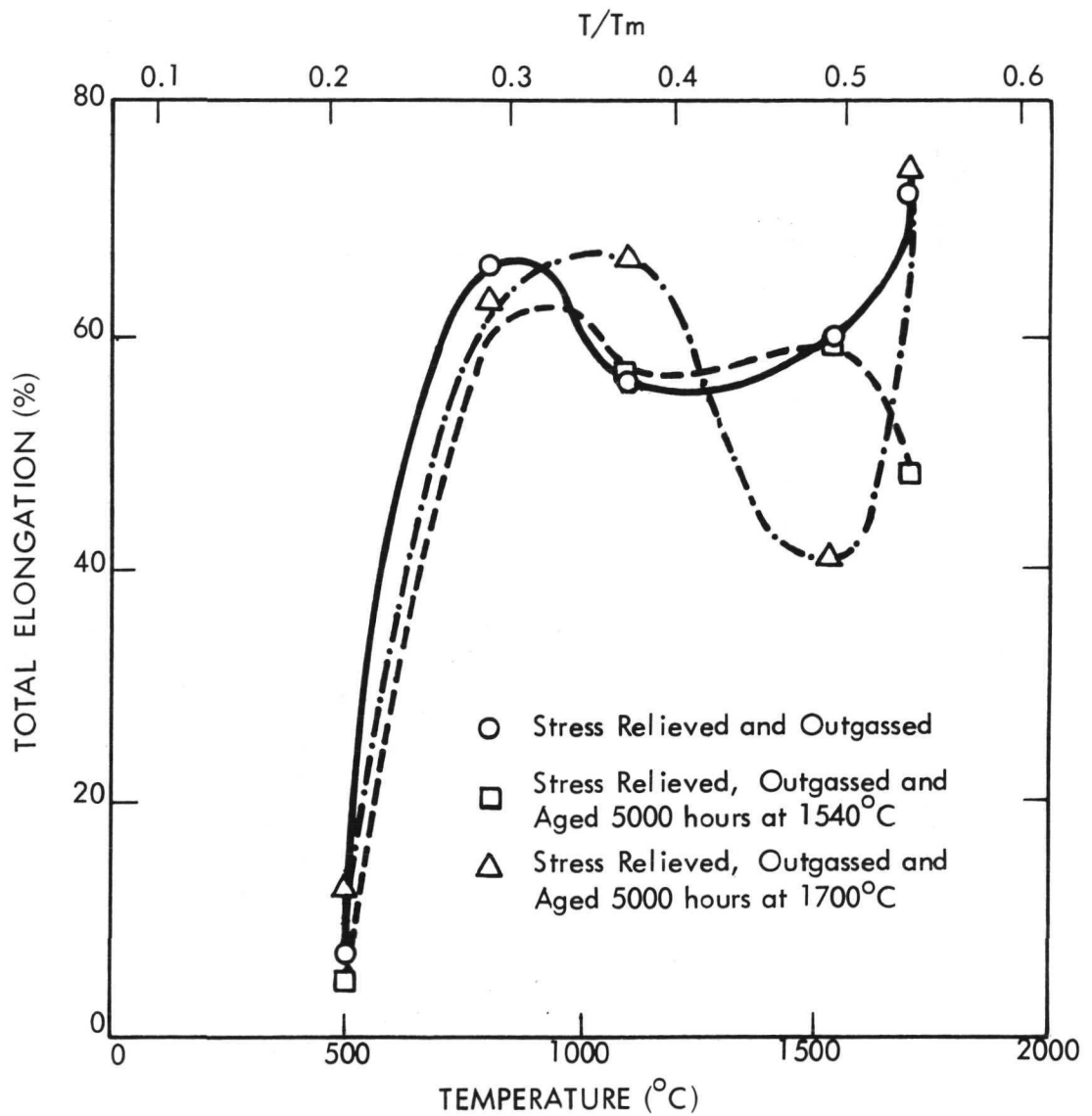


Figure 33. Elevated Temperature Total Elongation of Chloride CVD Tungsten.

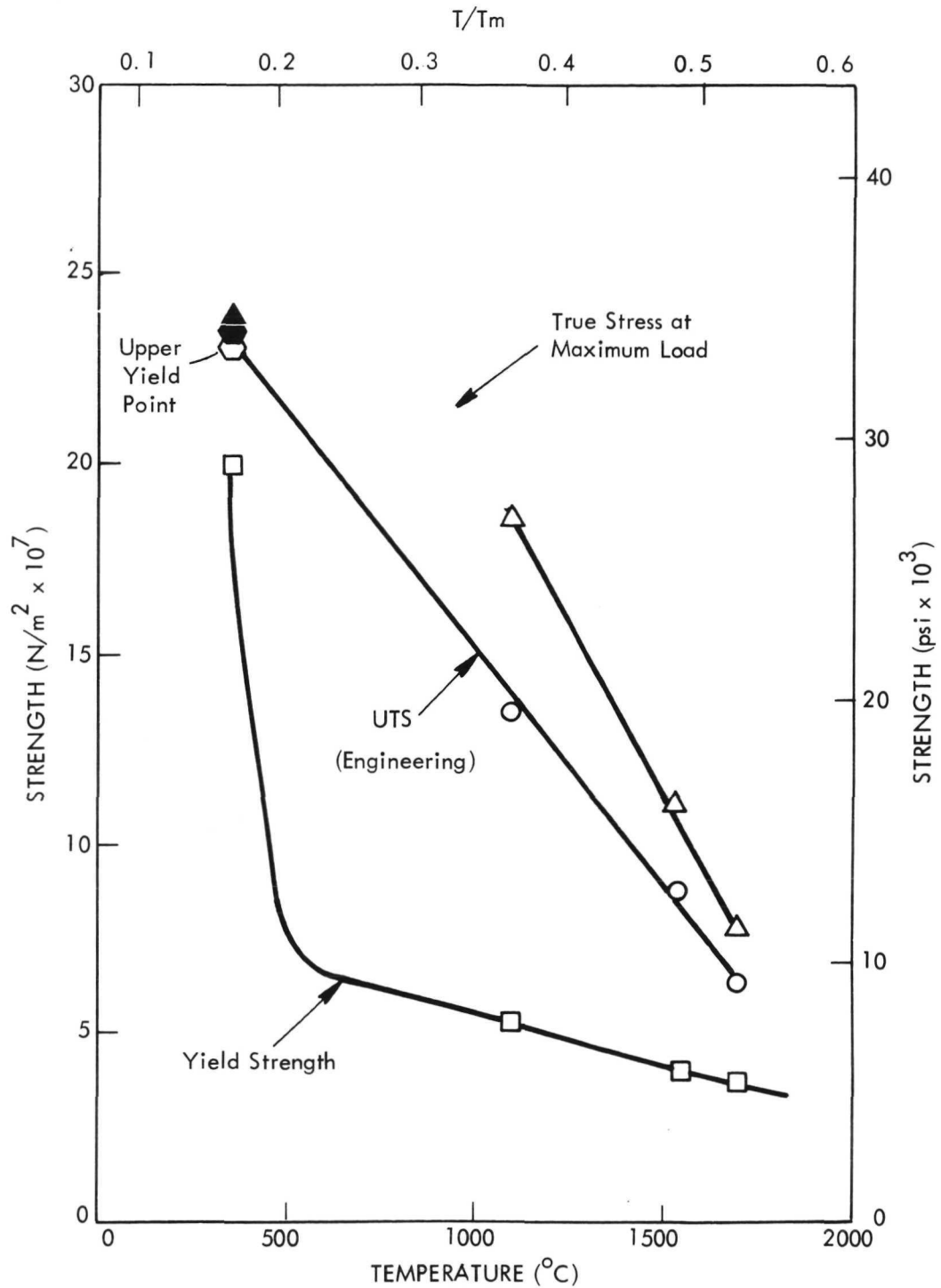


Figure 34. Elevated Temperature Tensile Properties of Duplex CVD Tungsten Stress Relieved (1 hour at 1200°C) and Outgassed (50 hours at 1800°C).

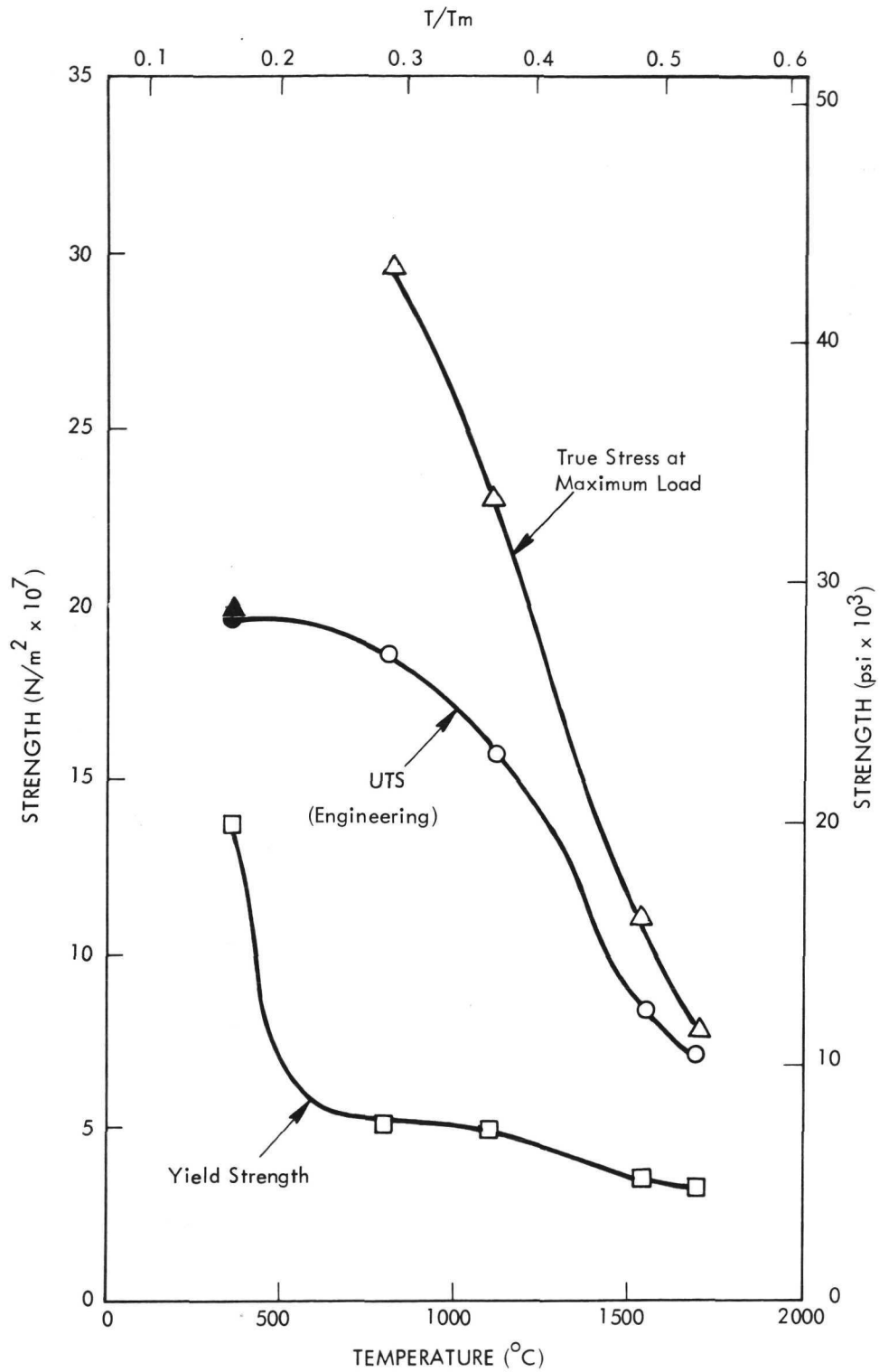


Figure 35. Elevated Temperature Tensile Properties of Duplex CVD Tungsten Stress Relieved, Outgassed and Aged (5000 hours at 1540°C).

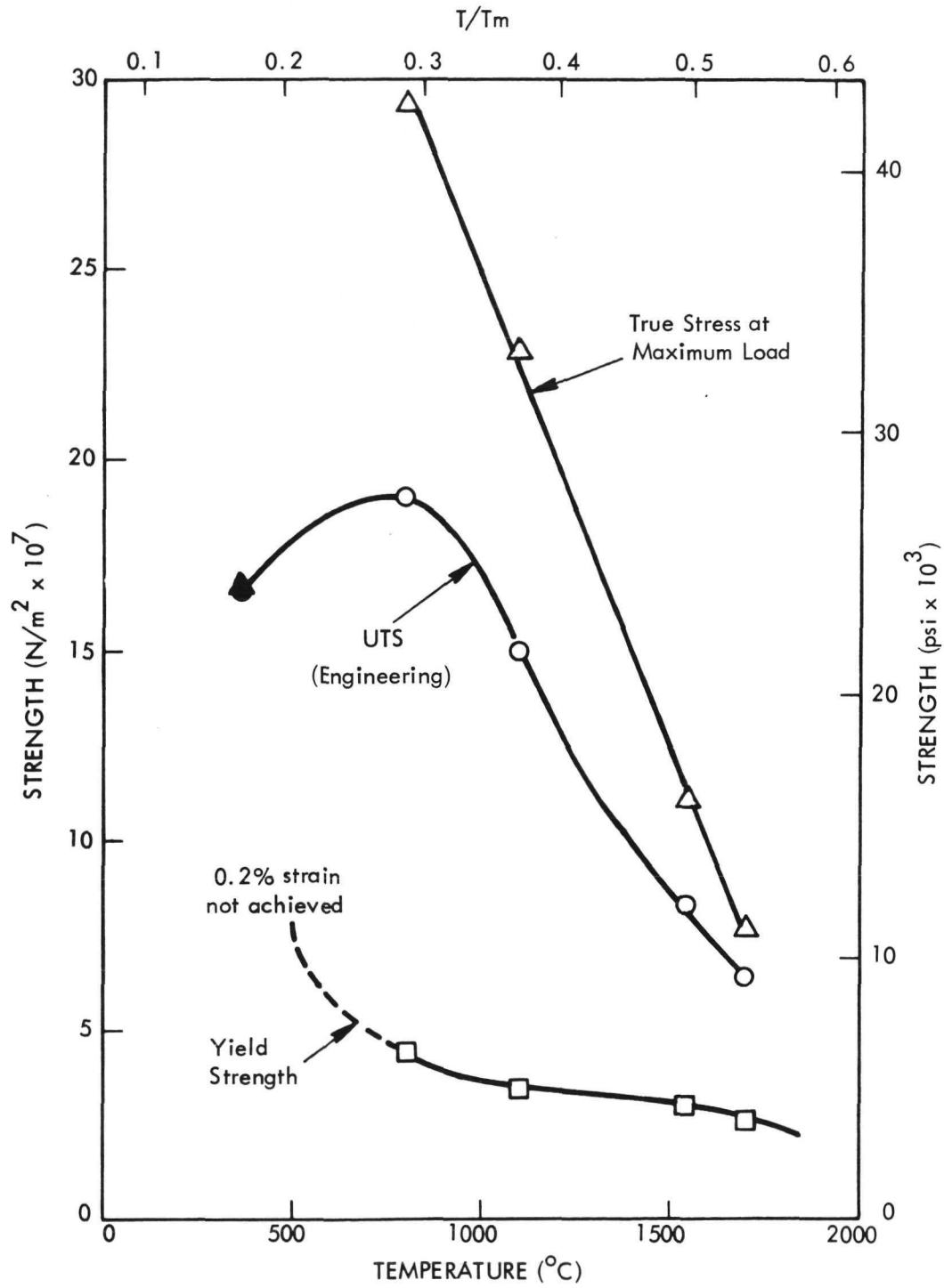


Figure 36. Elevated Temperature Tensile Properties of Duplex CVD Tungsten Stress Relieved, Outgassed and Aged (5000 hours at 1700°C).

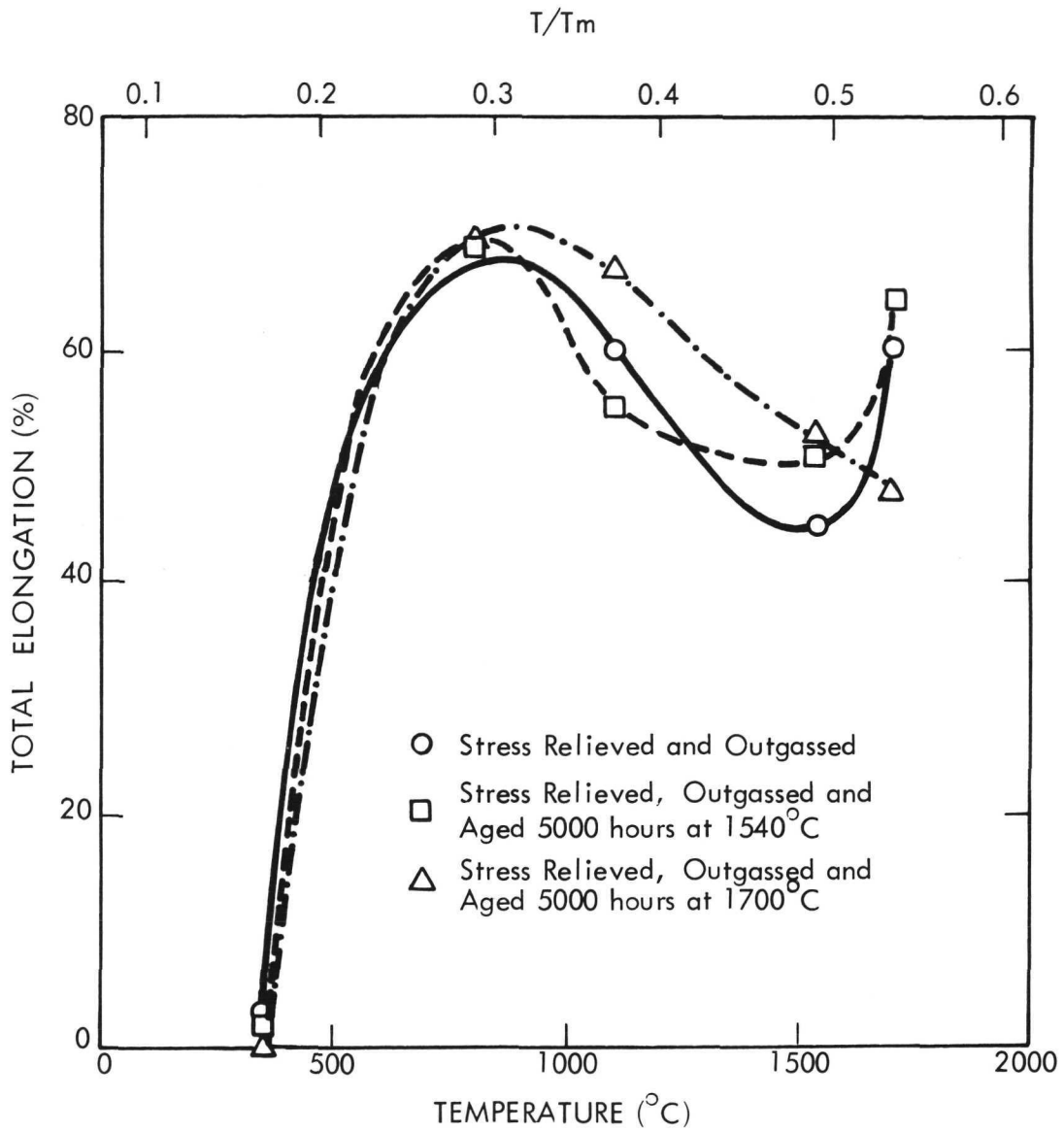


Figure 37. Elevated Temperature Total Elongation of Duplex CVD Tungsten.

Table X. Strength and Elongation Data for CVD Tungsten

Material	Heat Treat Condition	Test Temp. (°C)	0.2% Yield Strength (N/m ² x 10 ⁷)	UTS (N/m ² x 10 ⁷)	Uniform Strain (%)	Fracture Strain (%)
Fluoride	Stress Relieved (1 hour at 1200°C) and Outgassed (50 hours at 1800°C)	350*	16.8	23.2	8.8	8.8
		800	6.7	19.0	42.9	52.2
		1100	7.4	15.3	42.6	59.6
		1540	5.9	8.6	19.1	49.2
	1700	3.5	6.9	20.9	62.5	
	Stress Relieved, Outgassed, and Aged (5000 hours at 1540°C)	350	13.9	19.2	2.3	2.3
		800	--	--	--	--
		1100	4.9	14.2	48.2	60.9
		1540	3.8	8.3	24.7	47.3
	1700	3.3	6.5	19.6	55.0	
	Stress Relieved, Outgassed, and Aged (5000 hours at 1700°C)	350	9.6	16.8	2.9	2.9
		800	--	--	--	--
1100		4.5	13.6	54.0	64.9	
1540		3.2	8.0	32.7	51.4	
1700	3.0	6.4	22.7	42.7		
Chloride	Stress Relieved (1 hour at 1200°C) and Outgassed (50 hours at 1800°C)	500	5.2	20.0	5.2	5.2
		800	4.9	21.8	48.5	69.7
		1100	4.6	17.6	42.2	62.3
		1540	2.9	8.8	25.9	64.5
	1700	2.1	6.3	29.4	74.8	
	Stress Relieved, Outgassed, and Aged (5000 hours at 1540°C)	500	4.7	18.8	4.3	4.3
		800	--	--	--	--
		1100	4.1	16.0	42.6	62.3
		1540	2.5	9.2	29.8	62.2
	1700	2.4	6.6	23.6	42.6	
	Stress Relieved, Outgassed, and Aged (5000 hours at 1700°C)	500	5.6	19.5	12.1	12.1
		800	4.9	20.6	45.8	67.0
1100		3.8	16.8	46.5	73.0	
1540		2.0	9.1	33.0	43.5	
1700	1.9	7.3	25.9	77.9		
Duplex	Stress Relieved (1 hour at 1200°C) and Outgassed (50 hours at 1800°C)	350**	20.1	23.5	2.6	2.6
		800	--	--	--	--
		1100	5.2	13.5	20.8	77.7
		1540	4.0	8.8	25.6	48.4
	1700	3.7	6.4	19.3	64.3	
	Stress Relieved, Outgassed, and Aged (5000 hours at 1540°C)	350	13.8	19.5	1.1	1.1
		800	5.1	18.7	59.0	71.4
		1100	5.0	15.8	46.5	58.0
		1540	3.6	8.5	30.8	54.2
	1700	3.3	7.1	24.2	64.6	
	Stress Relieved, Outgassed, and Aged (5000 hours at 1700°C)	350	Not Attained	16.5	0.1	0.1
		800	4.3	19.0	54.7	72.9
1100		3.3	15.1	51.6	69.7	
1540		3.0	8.4	32.3	50.2	
1700	2.4	6.3	23.9	51.1		

* Upper/lower yield points - 16.8/16.4 x 10⁷ N/m²
 ** Upper/lower yield points - 23.5/19.9 x 10⁷ N/m²

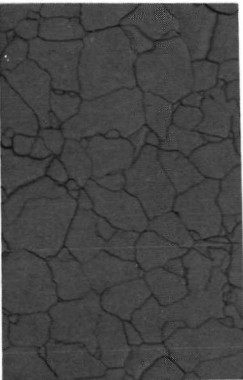
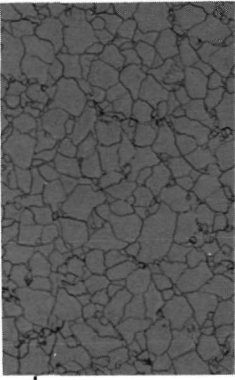
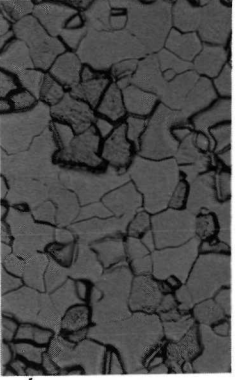
The microstructures and grain sizes of the starting materials are presented in Table XI. For the fluoride material grain size varied considerably both within a single lot and between the two separate lots. Uniformity of grain size was found for the chloride material. In the duplex tungsten the fluoride grain size was again variable while the chloride portion of the material was characterized by a wide distribution of grain sizes within a single metallographic specimen (1/4 inch diameter).

The effects on grain size and hardness of each of the heat treatments employed in this program are shown in Table XII. Unless otherwise noted, reported grain sizes are the result of a single determination. Figure 38 shows the microstructure of fluoride tungsten following stress relief, outgassing, and aging for 5000 hours at 1700°C. This stability of grain structure is in contrast with that noted previously by Schaffhauser and Heestand⁽⁵⁾ who found grain growth at temperatures as low as 1400°C for material containing 1 ppm fluorine. The greater stability noted in the present work is probably the result of the oxygen addition made to the fluoride material.

Chloride tungsten was much less stable. Extensive grain growth accompanied the outgassing treatment and was further accentuated by both of the 5000 hour treatments. Figure 39 shows the microstructure following aging for 5000 hours at 1700°C.

Freshly fractured surfaces of duplex tungsten, which had been subjected to various thermal treatments, were examined with a scanning electron microscope. One such surface, representing material in the outgassed condition (stress relieved 1 hour at 1200°C followed by outgassing for 50 hours at 1800°C), is shown in Figure 40a.

Table XI. Microstructure and Grain Size of CVD Tungsten Materials (Stress Relieved)

Material	Sample* Number	Microstructure (100X)** Perpendicular to Growth Direction	Grain Size (microns)	Remarks
Fluoride	1 a		62	
	b		62	
	c		37	
	d		22	
Fluoride	2 a		34	Note presence of many small grains.
	b		44	
	c		44	
	d		24	
Chloride	2		48	
			200μ	
Chloride	3		48	Same microstructure as Chloride No. 2
Chloride	4		53	Same microstructure as Chloride No. 2

*a single 1/4" diameter sample was utilized from each lot of material.

** 30 lactic - 3 HNO₃ - 1 HF etch

Table XI. Microstructure and Grain Size of CVD Tungsten Materials (Stress Relieved) – continued

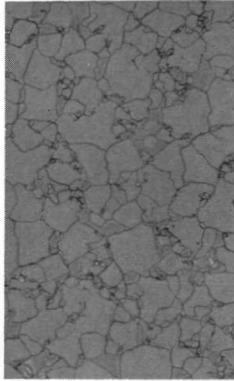
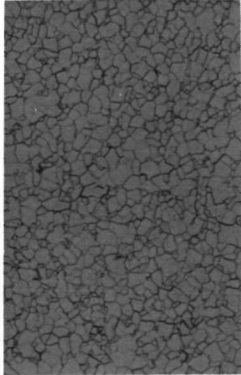
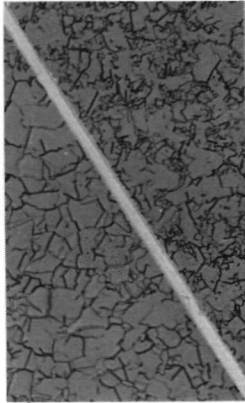
Material	Sample* Number	Microstructure (100X) Perpendicular to Growth Direction	Grain Size (microns)	Remarks
Duplex (Fluoride)	1		38	
Duplex (Fluoride)	2		32	Same microstructure as Duplex (Fluoride) No. 1
Duplex (Fluoride)	4		33	Same microstructure as Duplex (Fluoride) No. 1
Duplex (Fluoride)	5		20	Material produced at later date than other Duplex material.
Duplex (Chloride)	1		--	Essentially two grain structures present; average grain size not determined

Table XI. Microstructure and Grain Size of CVD Tungsten Materials (Stress Relieved) – continued

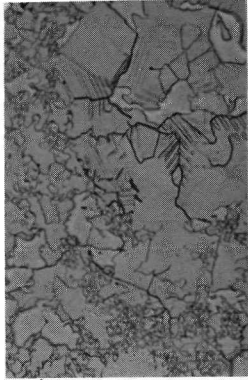
Material	Sample* Number	Microstructure (100X) Perpendicular to Growth Direction	Grain Size (microns)	Remarks
Duplex (Chloride)	2		--	Wide distribution of grain sizes present; average grain size not determined
Duplex (Chloride)	5		38	Uniform grain size; material produced at later date than other duplex material.

Table XII. Effect of Heat Treatment on Hardness and Grain Size of Fluoride- and Chloride-Produced Tungsten

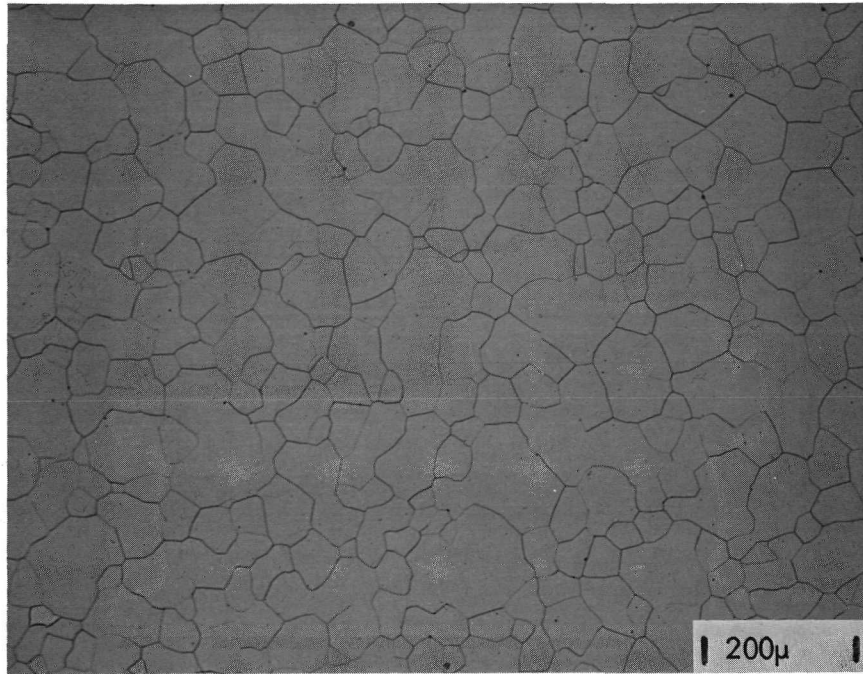
HEAT TREAT CONDITION	FLUORIDE TUNGSTEN		CHLORIDE TUNGSTEN	
	Hardness* (DPH-30kg load)	Grain Size (microns)	Hardness* (DPH-30kg load)	Grain Size (microns)
1. Stress Relieved (1 hr at 1200°C)	369	41**	361	50***
2. SR + Outgassed (50 hrs at 1800°C)	358	41	366	135
3. SR+O+Cycled (500 hrs RT to 1540°C)	361	N. D.	358	N. D.
4. SR+O+Cycled (500 hrs RT to 1700°C)	360	N. D.	360	N. D.
5. SR+O+Aged (5000 hrs at 1540°C)	347	49	333	586
6. SR+O+Aged (5000 hrs at 1700°C)	334	68	337	570

* Average of 3 determinations

** Average of 8 determinations (4 taken randomly from each of 2 lots)

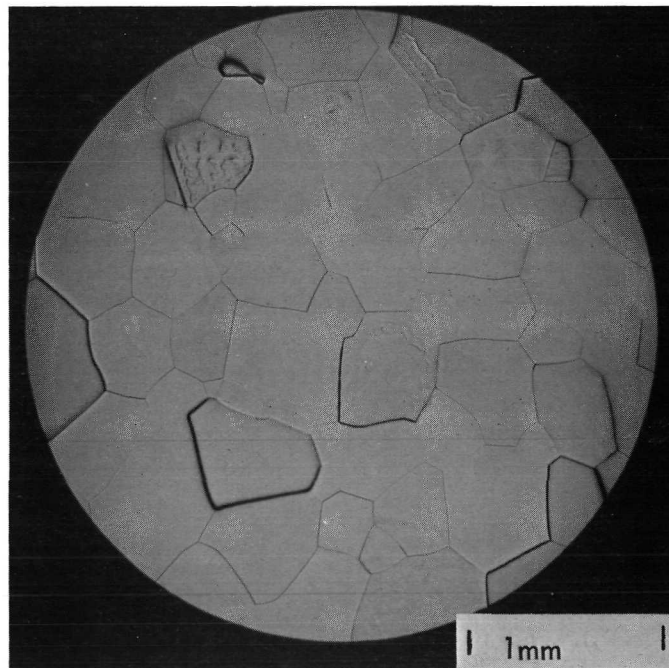
*** Average of 3 determinations (1 taken randomly from each of 3 lots)

N.D. Not Determined



100X

Figure 38. Grain Structure of Fluoride Tungsten Following Stress Relief, Outgassing and Aging for 5000 Hours at 1700°C (30 lactic - 3 HNO₃ - 1 HF etch)



25X

Figure 39. Grain Structure of Chloride Tungsten Following Stress Relief, Outgassing and Aging for 5000 Hours at 1700°C (30 lactic - 3 HNO₃ - 1 HF etch)

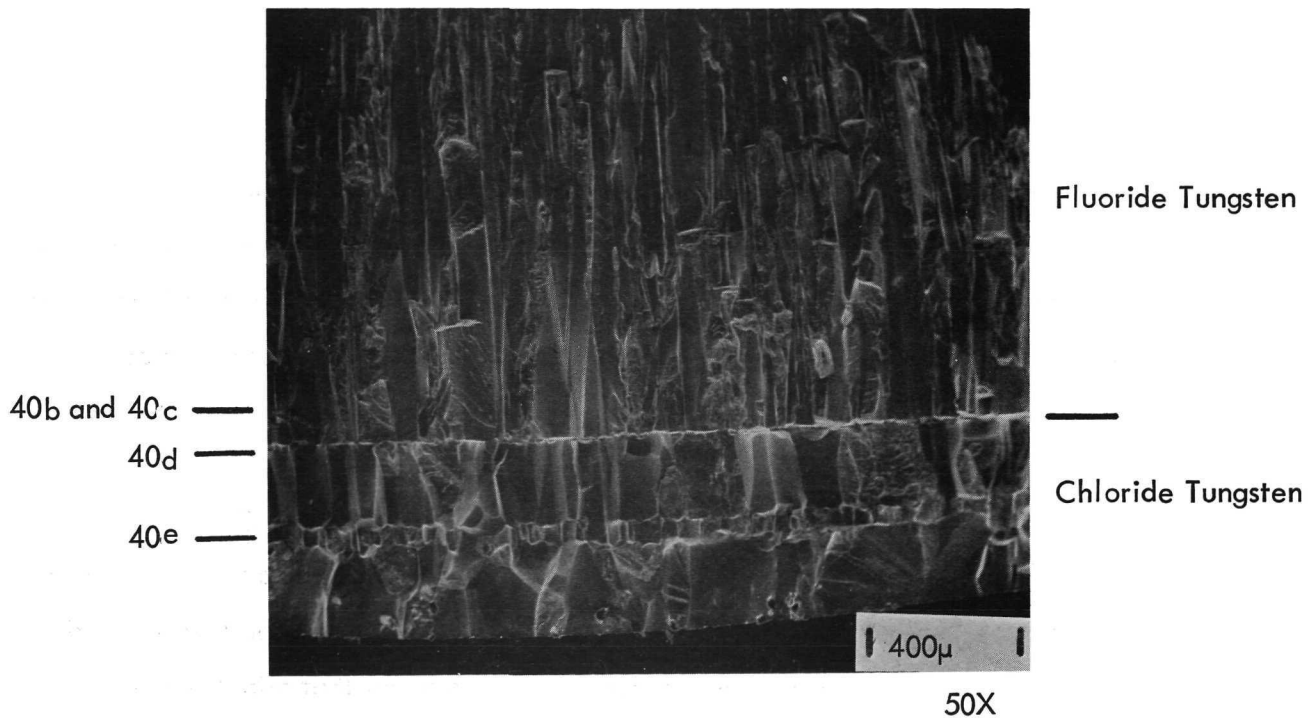


Figure 40a. Scanning Electron Micrograph of Fractured Surface of Stress Relieved and Outgassed Duplex Tungsten

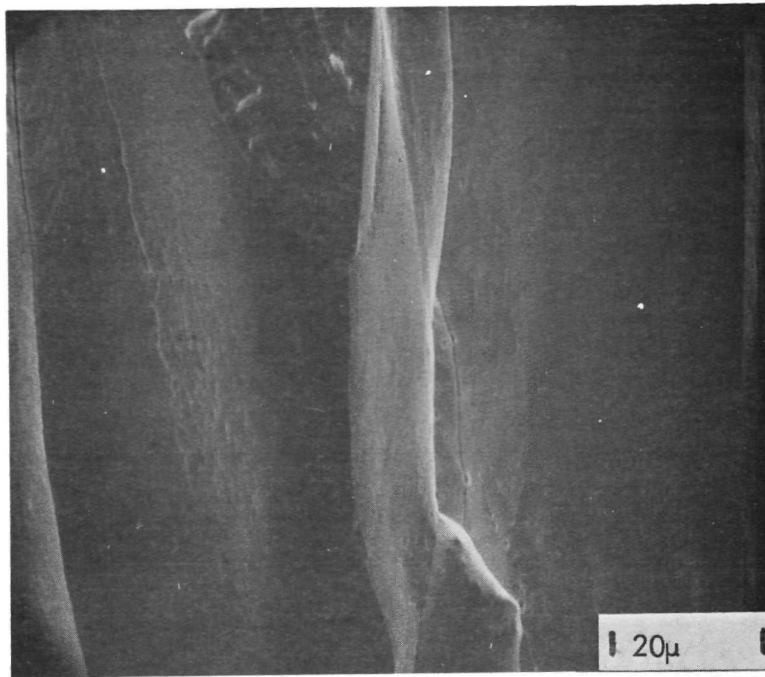
Although some grain boundary surfaces are evident, cleavage surfaces predominate. Within the fluoride tungsten very few bubbles were noted (as typified by Figure 40b) with only a very small fraction of boundaries being heavily populated with them (Figure 40c). The largest bubbles observed were approximately 0.5μ in their longest dimension. Examination of the fluoride-chloride interface at a magnification of 1000 times failed to reveal the presence of bubbles at that location (Figure 40d). The surface locations studied at high magnification are indicated by the supplemental figure number.

Further examination at 1000X of each of the three layers of chloride tungsten showed no bubbles to be present in either the layer comprising the free surface or the one adjacent to the fluoride tungsten. However within the middle chloride layer (shown in its full thickness in Figure 40e) numerous bubbles were noted, the largest of which are 4 to 5μ in size.

The fractured surface of the duplex material given the 5000 hours at 1540°C treatment following stress relief and outgassing is shown in Figure 41a. Again the locations of corresponding supplemental figures are indicated. No bubbles were found in the fluoride material even though examinations up to 1000X were made. Some features that might possibly be taken for bubbles were noted at the fluoride-chloride interface and at one of the chloride-chloride interfaces (Figures 41b and 41c).

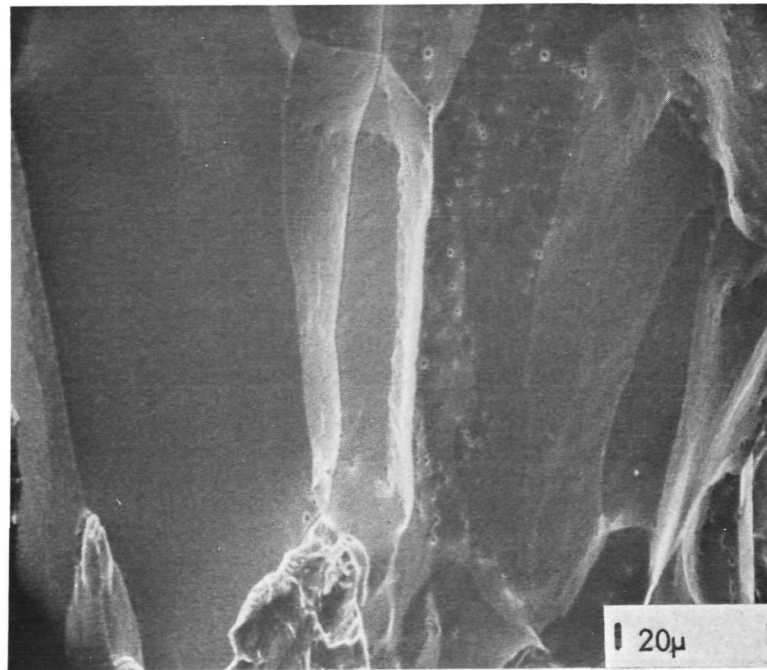
The remaining chloride-chloride interface (Figure 41d) and the bulk chloride material were free of bubbles except for several isolated areas at the interface (Figure 41e) where bubbles as large as $5\text{--}6\mu$ were found.

The fractured surface of duplex material given the 5000 hour, 1700°C aging following stress relief and outgassing is shown in Figure 42a. The instability of the chloride structure produced by this thermal treatment is evident. Numerous bubbles were noted in the fluoride material (Figure 42b) and as usual occurred preferentially along grain boundaries. Essentially no



1000X

Figure 40b. Scanning Electron Micrograph of Fluoride Portion of Stress Relieved and Outgassed Duplex Tungsten Showing Near Absence of Bubbles on Grain Boundary.



1000X

Figure 40c. Scanning Electron Micrograph of Fluoride Portion of Stress Relieved and Outgassed Duplex Tungsten Showing Bubble Formation at Several Grain Boundaries.

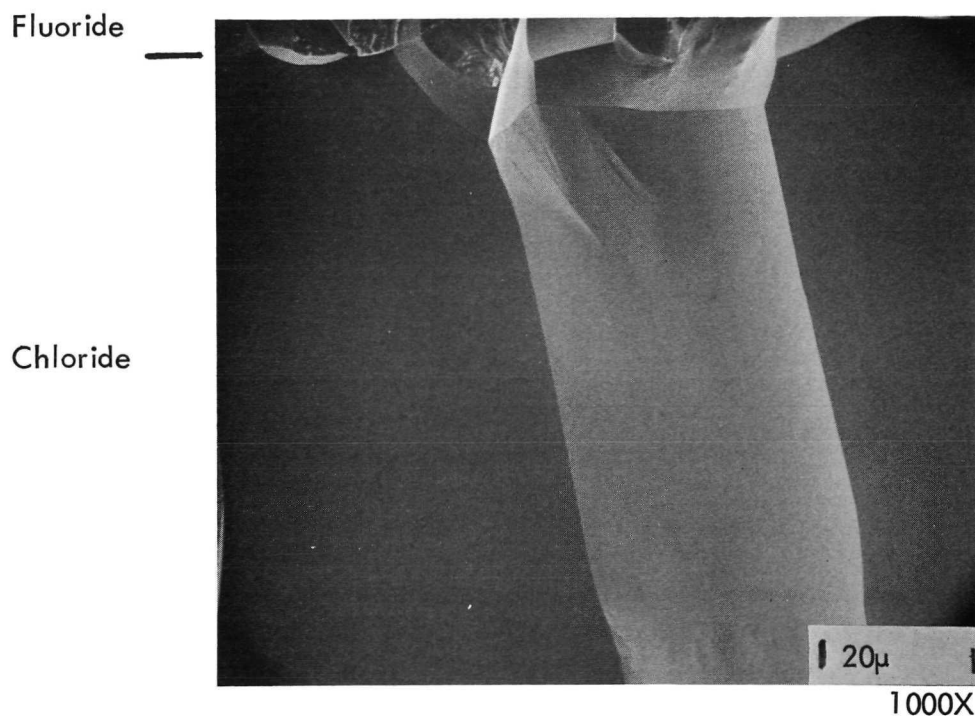


Figure 40d. Scanning Electron Micrograph of Stress Relieved and Outgassed Duplex Tungsten Showing Absence of Bubbles at Fluoride-Chloride Interface.

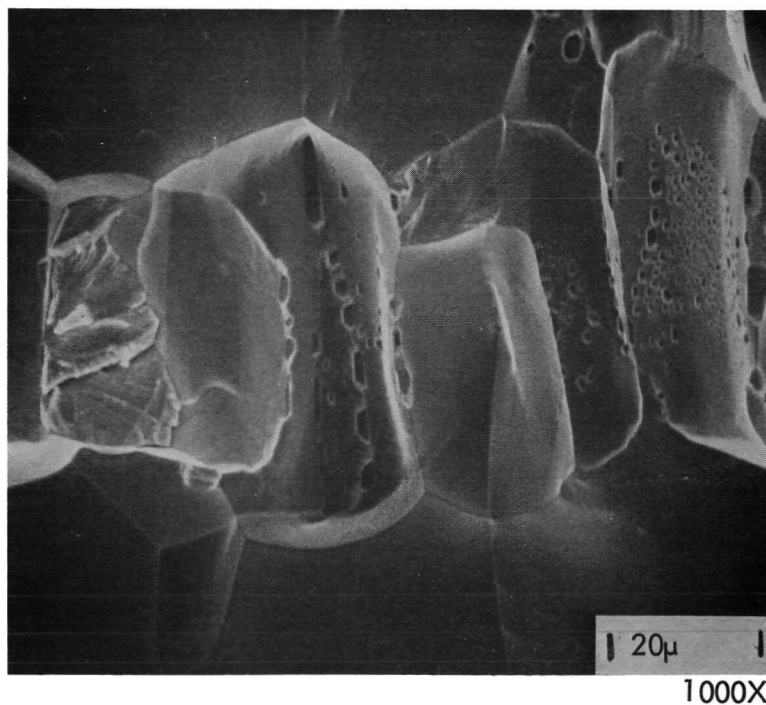


Figure 40e. Scanning Electron Micrograph of Stress Relieved and Outgassed Duplex Tungsten Showing Grain Boundaries in One Chloride Layer that are Heavily Populated with Bubbles.

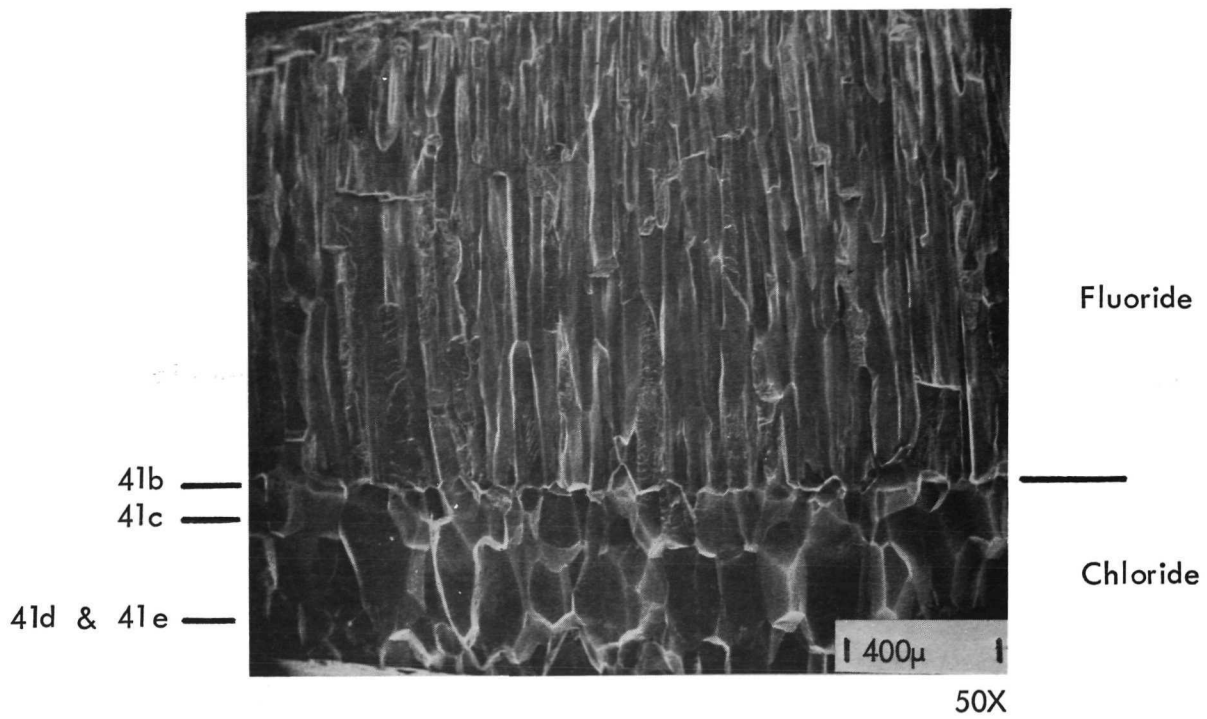
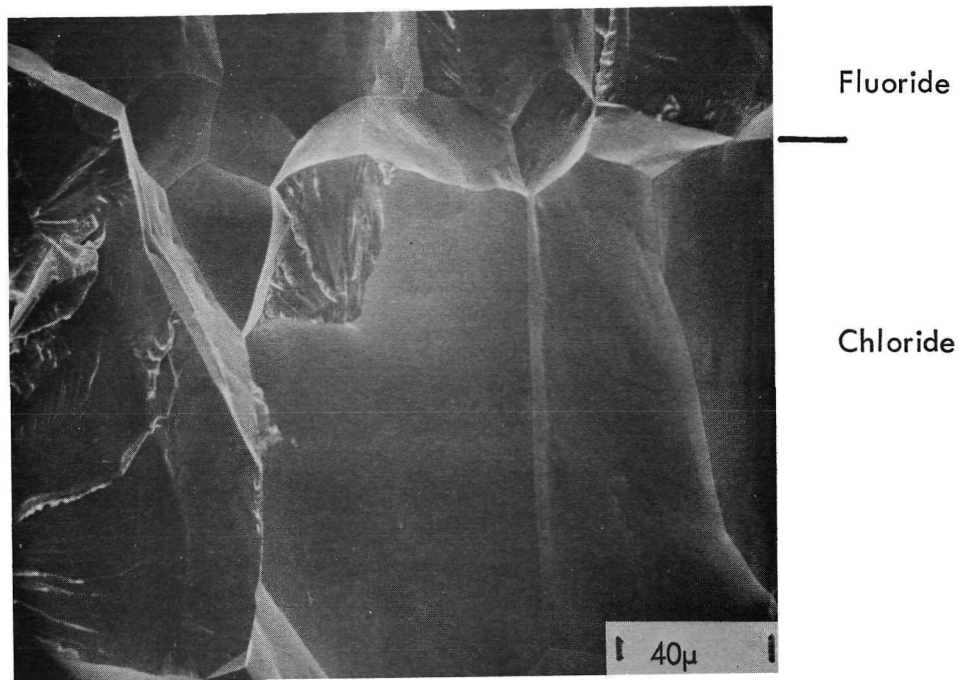
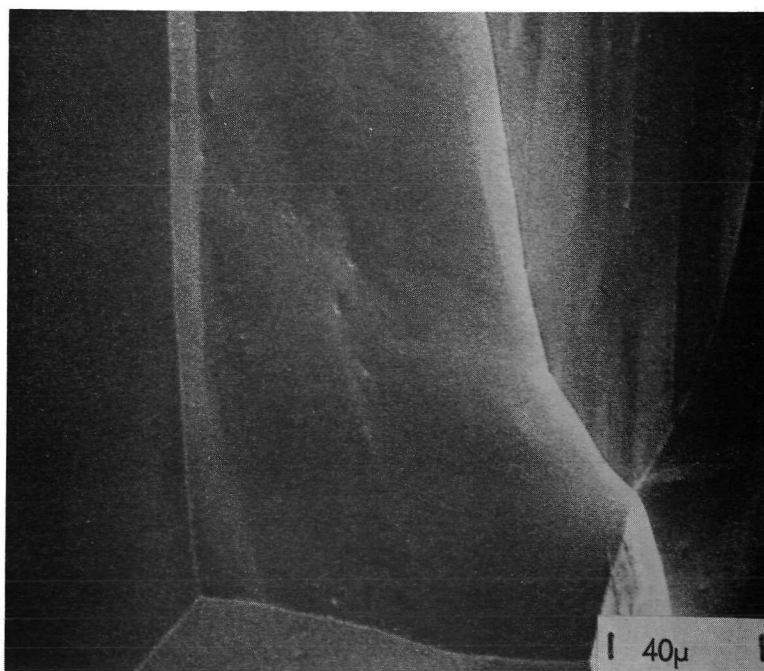


Figure 41a. Scanning Electron Micrograph of Fractured Surface of Duplex Tungsten (Stress Relieved, Outgassed, and Aged 5000 Hours at 1540°C)



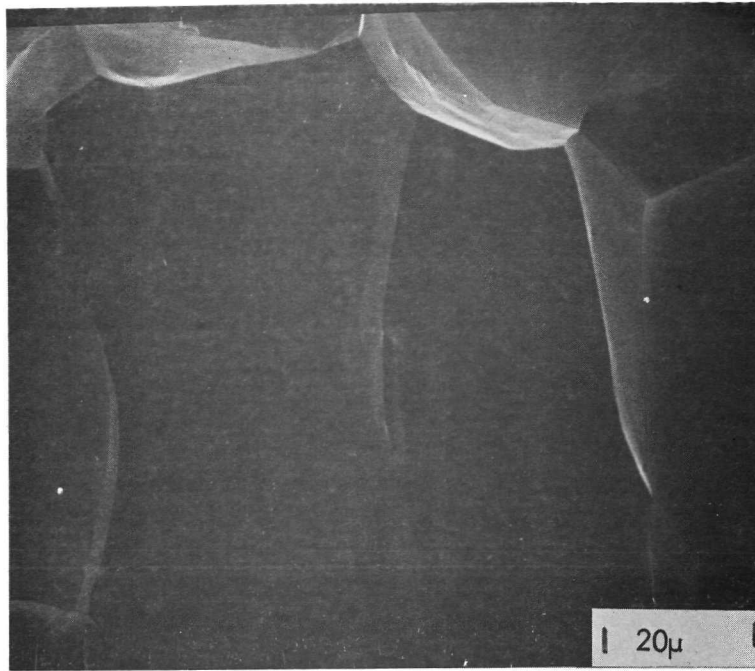
500X

Figure 41b. Fluoride-Chloride Interface of Specimen Shown in Figure 41a



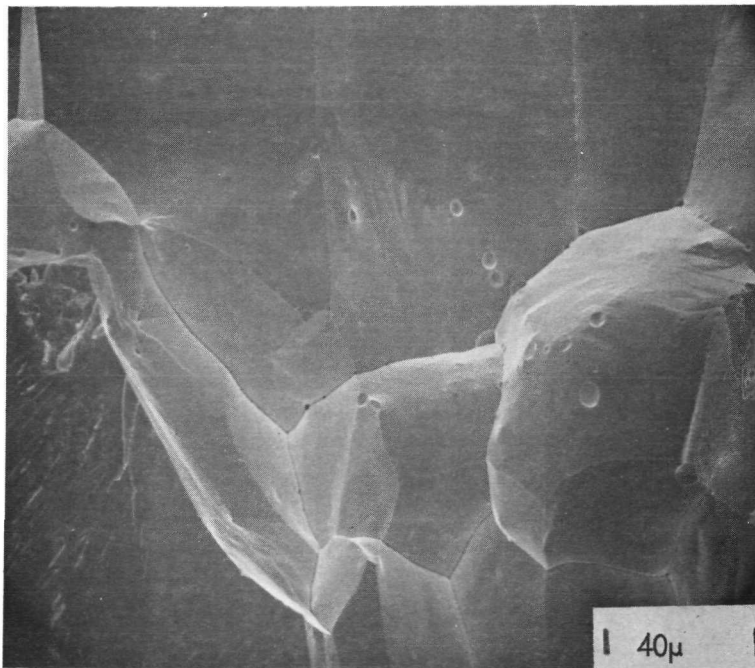
500X

Figure 41c. Chloride-Chloride Interface of Specimen Shown in Figure 41a



1000X

Figure 41d. Chloride-Chloride Interface of Specimen Shown in Figure 41a



500X

Figure 41e. Interface of Figure 41d Showing Isolated Area Containing Bubbles.

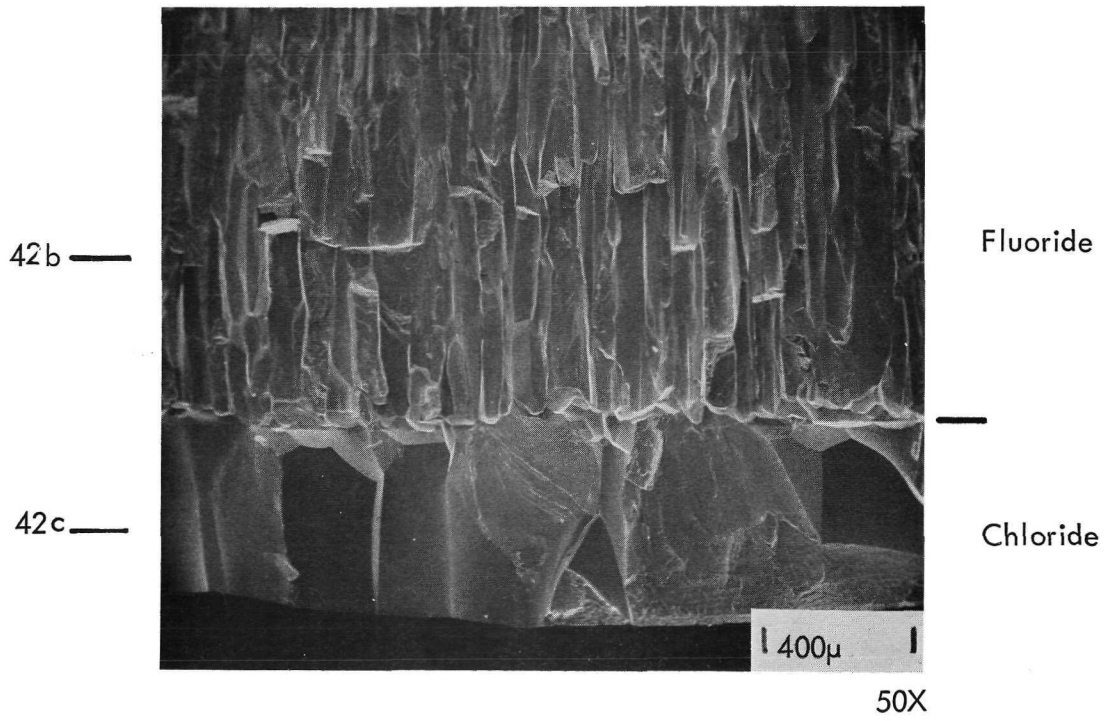
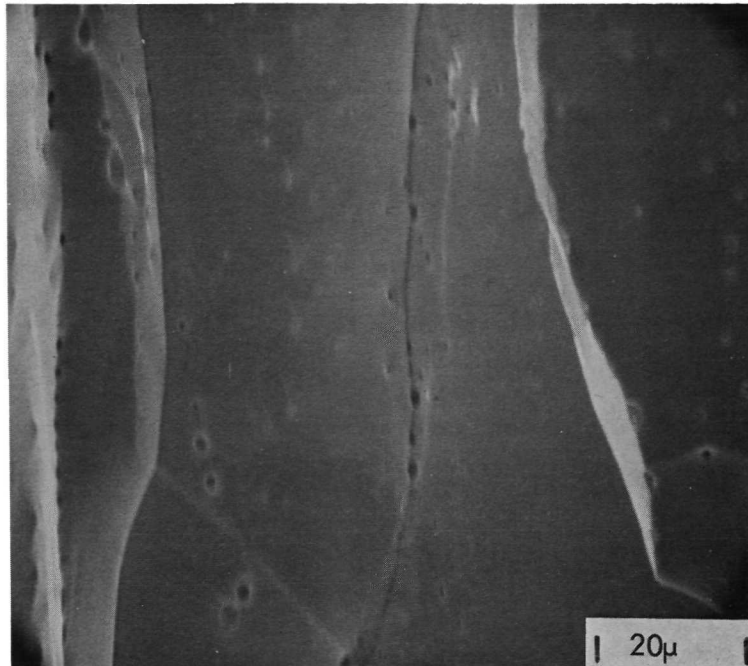
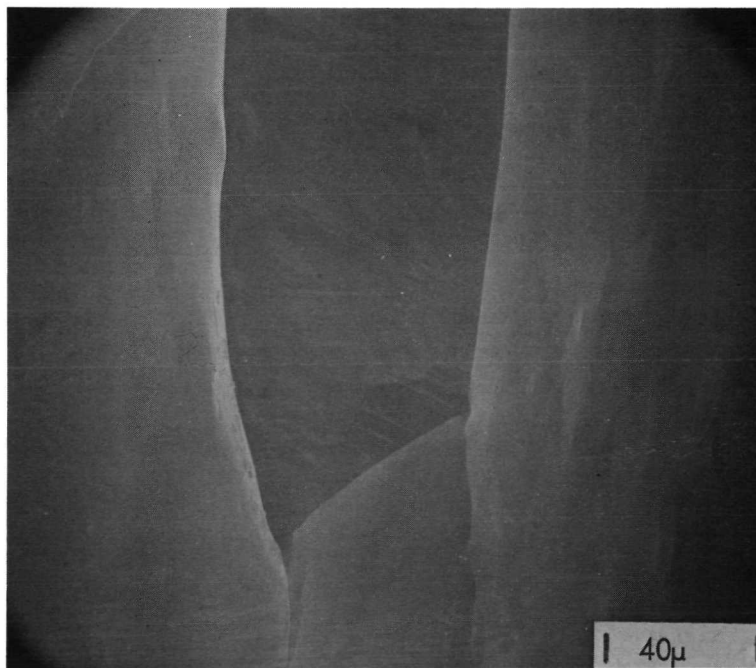


Figure 42a. Scanning Electron Micrograph of Fractured Surface of Duplex Tungsten (Stress Relieved, Outgassed, and Aged 5000 hours at 1700°C)



1000X

Figure 42b. Fluoride Tungsten Portion of Specimen of Figure 42a Showing Presence of Numerous Bubbles.



500X

Figure 42c. Chloride Tungsten Portion of Specimen of Figure 42a Showing Absence of Bubbles.

bubbles were observed at either the interface or within the chloride material (Figure 42c). It is suggested that within the chloride a sufficient time and temperature was provided to permit coalescence of the bubbles that were found following less severe thermal treatments.

6.0 DISCUSSION

6.1 DUCTILE-BRITTLE BEHAVIOR

It is to be expected that the bend ductile-brittle transition temperature of outgassed and outgassed plus aged fluoride tungsten be less than that of chloride tungsten. Fracture occurs by the sequential process of slip dislocation unlocking, the formation of crack nuclei (by one of a number of proposed mechanisms) and finally crack propagation to yield the typically observed transgranular cleavage crack. In the simplest sense a material will fail in a brittle manner if its yield strength is greater than the stress needed to propagate a brittle crack.

It has been shown⁽⁶⁾ that this stress value can be given by

$$\sigma_F = \frac{4\gamma'}{nb(1 + 1/\sqrt{2})} \quad (2)$$

where n is the number of coalesced dislocations of Burgers vector b and γ' is the effective surface energy of the propagating crack. The effective stress operating on the dislocations ($\sigma_F - \sigma_i$, the lattice friction stress) is opposed by a back stress resulting from the dislocation pileup found at the end of the slip band. Since the length of this slip band is determined by the grain diameter, d , these two stresses can be related by

$$\sigma_F - \sigma_i = \frac{4 G nb}{(1-\nu) d} \quad (3)$$

in which G is the shear modulus and ν is Poisson's ratio. Combining equations (2) and (3) and consolidating the constants gives the expression

$$\sigma_F = \frac{4 G \gamma'}{\alpha (\sigma_F - \sigma_i) d} \quad (4)$$

By assuming that fracture occurs at the yield stress and using a Hall-Petch type relation for the yield stress, the fracture stress can finally be expressed

$$\sigma_F = \frac{4 G \gamma'}{\alpha k d^{1/2}} \quad (5)$$

where k is the coefficient in the Hall-Petch relation. Brittle fracture is associated with stresses greater than σ_F .

The shear modulus is essentially identical for the $\{110\}$ and $\{100\}$ preferred orientation (chloride and fluoride tungsten respectively). The cleavage plane surface energies for the two materials also would not be different by a considerable amount since their atomic packing densities are similar in magnitude.

However the grain size for the two materials, once they have been outgassed, differs considerably. Thus chloride tungsten with its larger grain size should, by equation (5), be more susceptible to brittle fracture as demonstrated experimentally.

The even more pronounced difference in brittle fracture behavior of the two materials following stress relief treatment is possibly attributable to the chloride tungsten still retaining a high degree of residual stress. This materials residual stress in the as-deposited condition would be expected to be greater than that of fluoride tungsten since the former's deposition temperature is considerably higher.

The ductile-brittle behavior of duplex material more closely followed that of the fluoride tungsten. This is to be expected since the data were obtained on specimens bent with the fluoride component being in tension.

6.2 STRENGTH AND ELONGATION

In general the chloride tungsten was found to have lower yield strength but higher ultimate strength (for the lower temperatures studied) than fluoride tungsten given identical thermal treatments. These observations are based on the plots of Figures 43 through 45 which summarize the previously presented strength data. The difference in yield strengths is the result of the chloride material's larger grain size for the thermal treatments evaluated. It is a generally observed phenomenon that grain size effects are the most influential during the early stages of deformation.

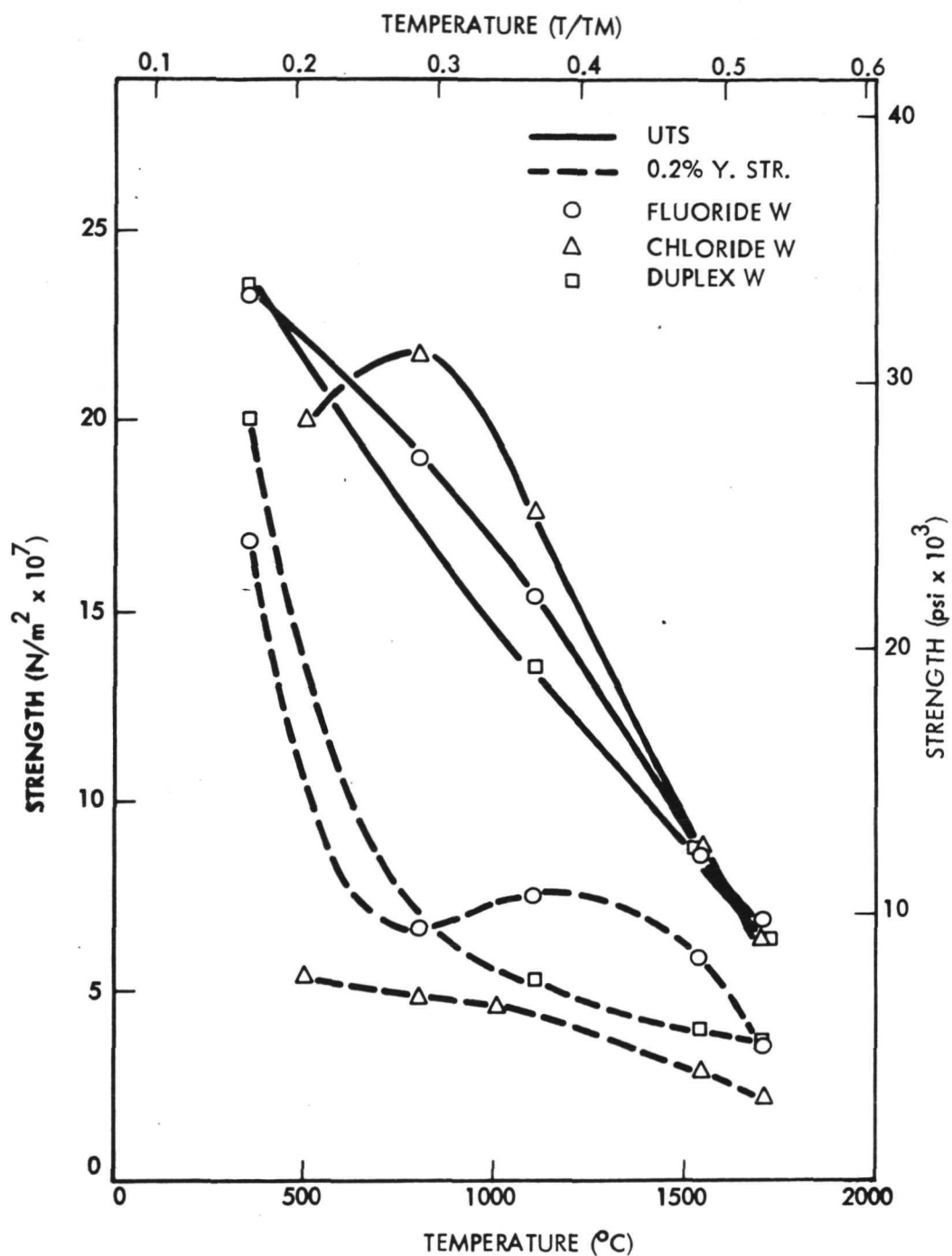


Figure 43. Comparison of UTS and 0.2% Yield Strength for CVD Tungsten Materials Following Stress Relief (1 hour at 1200°C) and Outgassing (50 hours at 1800°C)

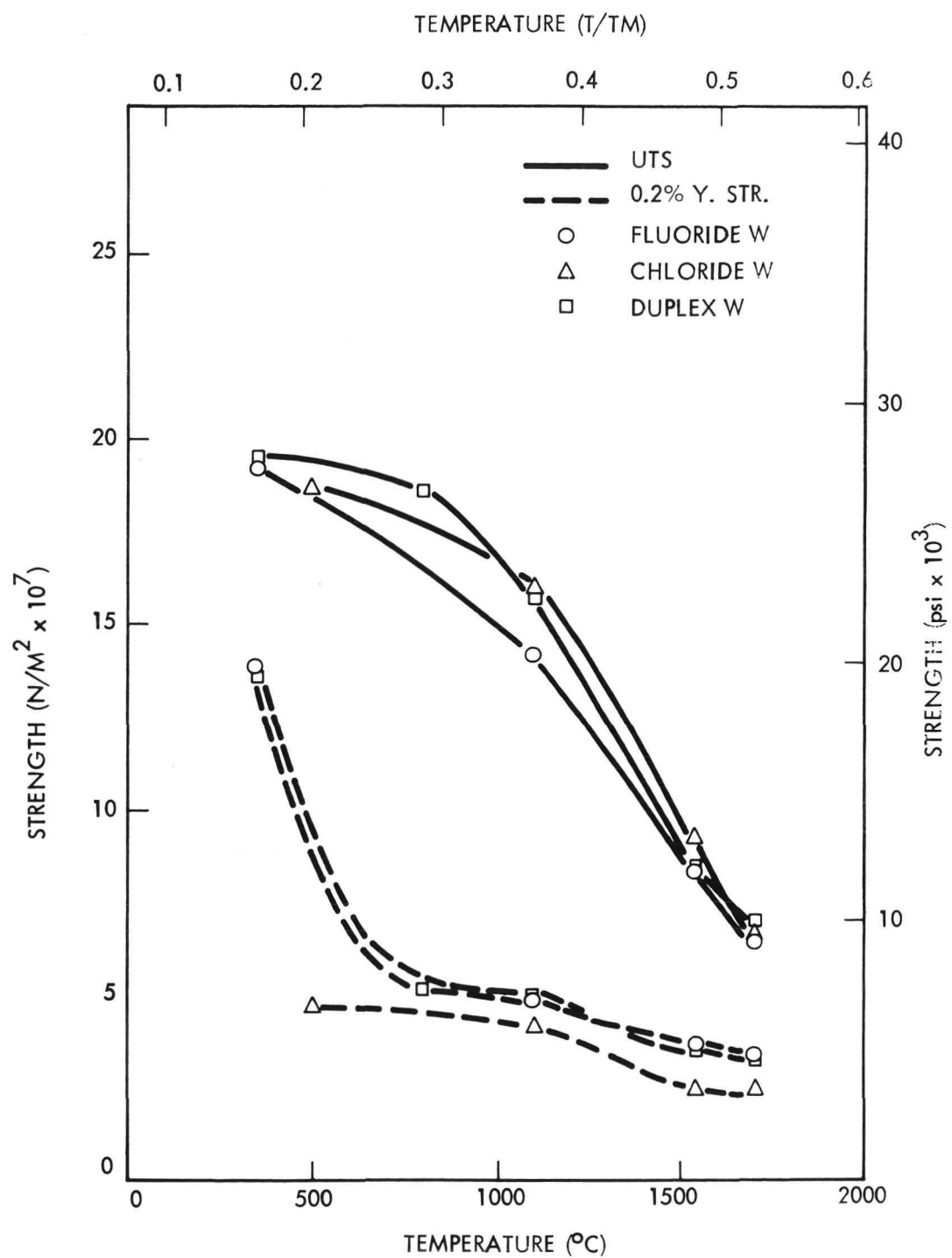


Figure 44. Comparison of UTS and 0.2% Yield Strength for CVD Tungsten Materials Following Stress Relief, Outgassing, and Aging (5000 hours at 1540°C)

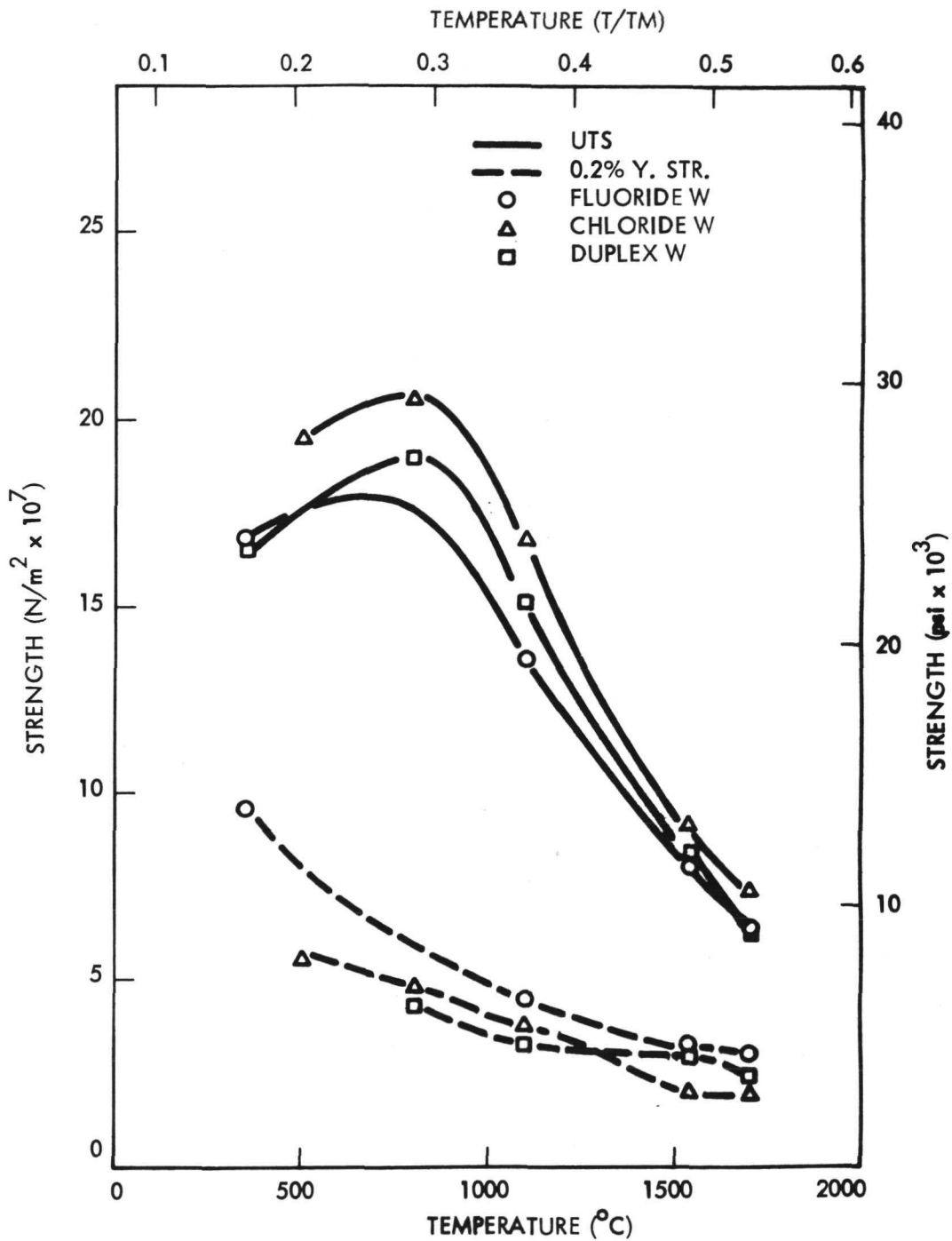


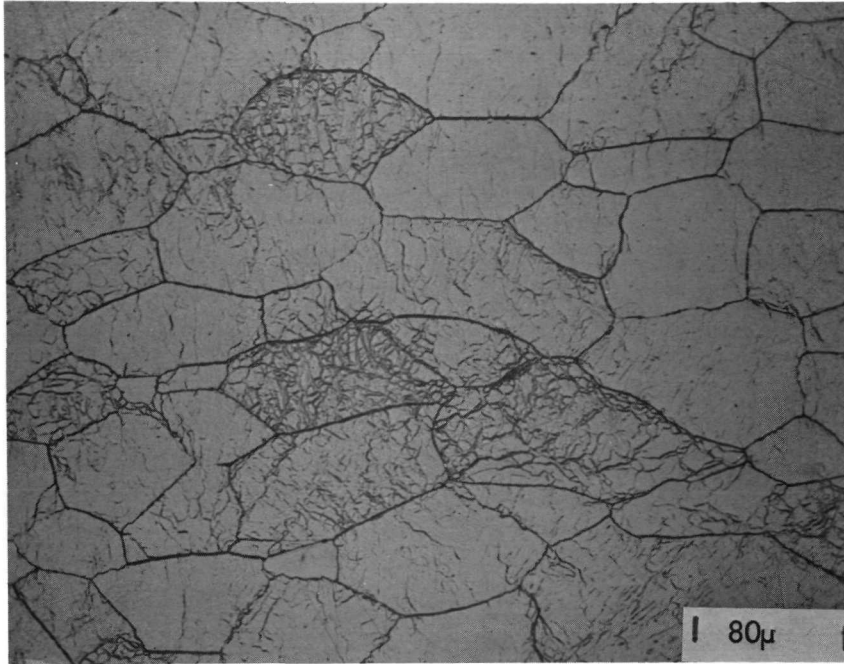
Figure 45. Comparison of UTS and 0.2% Yield Strength for CVD Tungsten Materials Following Stress Relief, Outgassing, and Aging (5000 hours at 1700°C)

At greater deformations strength is more controlled by dislocation interactions within the grains. For BCC metals glide can occur on a number of planes, provided only that they contain a $\langle 111 \rangle$ direction. Assume that slip takes place only on the $\{110\}$ planes since these are the most densely packed planes. The more preferentially oriented fluoride tungsten would appear approximately as a collection of single crystals each oriented such that the tensile axis lies along a $[001] - [101]$ type symmetry boundary. In this orientation the maximum number of $\{110\}$ planes are in the most favored position for shear stresses. Were a FCC structure being considered, increased strength would be associated with this arrangement since it favors work hardening by multiple slip. However in BCC, slip bands are formed and preserved (owing to the actual possibility of slip in any of the $\langle 111 \rangle$ directions) and thereby hinder slip on other intersecting planes. For this reason work hardening is very weak and results in the lower ultimate tensile strength of the fluoride tungsten (at the lower temperatures studied) as compared to the more randomly oriented chloride tungsten for which the fraction of grains possessing the orientation of easiest slip is less.

At the high temperatures investigated (1540°C and 1700°C) the ultimate strengths of the two basic types of CVD tungsten are equivalent. At these temperatures cross slip is favorable.

The elongation behavior of fluoride tungsten was studied to determine the causes for the generally observed occurrence of minima in elongation as a function of tensile test temperature (Figures 29, 33 and 37). In Figure 29 it is noted that for stress relieved and outgassed material the elongation follows "normal" behavior up to approximately $T/T_m = 0.4$. At this and lower temperature deformation occurs principally by slip within individual grains since grain boundaries serve as effective barriers to their movement. This is illustrated by Figure 46 which shows that for a test temperature of 1100°C the grains have been severely deformed in the direction of applied stress. At this temperature most of the grain boundaries are essentially undistorted.

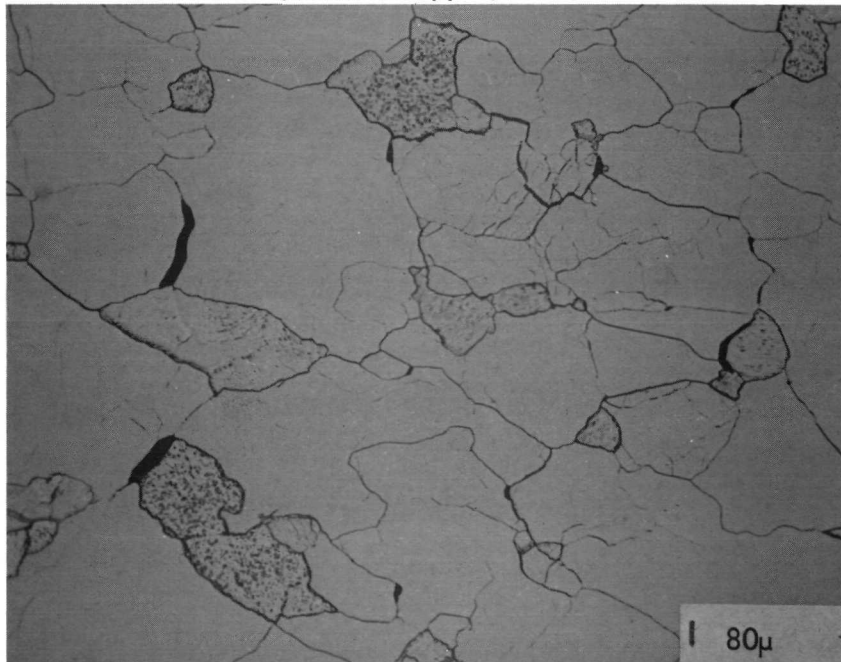
← Direction of Applied Stress →



250X

Figure 46. Fluoride Tungsten (Stress Relieved and Outgassed) Following Tensile Testing at 1100°C. (30 lactic - 3 HNO₃ - 1 HF etch)

← Direction of Applied Stress →



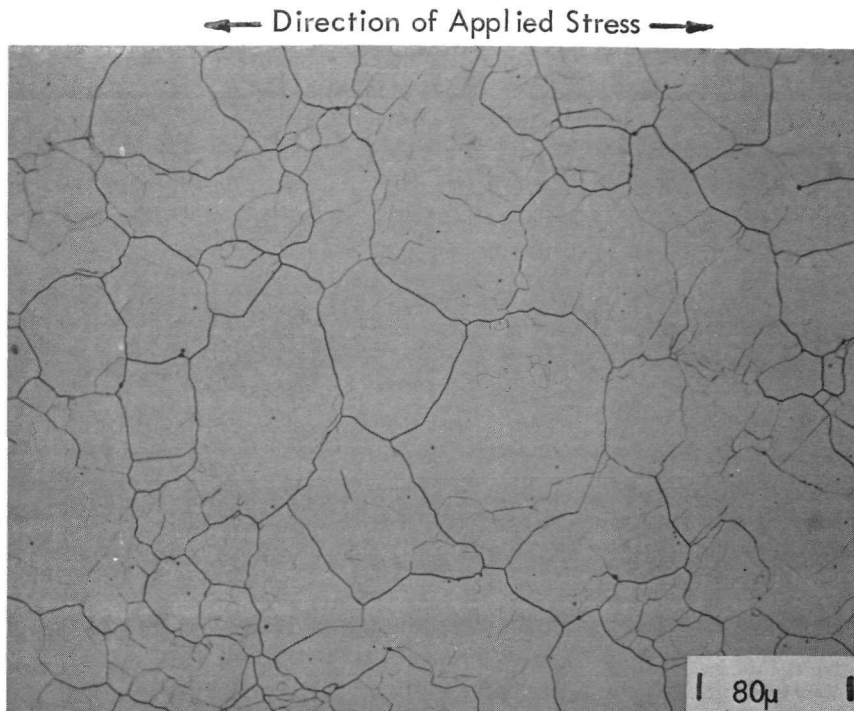
250X

Figure 47. Fluoride Tungsten (Stress Relieved and Outgassed) Following Tensile Testing at 1540°C. (30 lactic - 3 HNO₃ - 1 HF etch)

At higher temperature (typified by the data at 1540°C and corresponding to T/T_m of 0.49) dislocation motion within grains occurs much more readily since climb is now possible and cross slip permits the avoidance of dislocation pileups and tangles. Accompanying the increased dislocation mobility is the formation of a substructure by polygonization which serves to relieve the level of stresses within the grains. Meanwhile, (as suggested by McLean⁽⁷⁾) cavities form at grain boundaries, possibly as the result of ledges being opened into holes from the action of grain boundary sliding. The applied tensile stress results in a preferential growth of those cavities which occur at grain boundaries situated transverse to the direction of applied stress since the diffusion of vacancies to those cavities is thereby enhanced. This cavity formation is clearly indicated in Figure 47 which shows the microstructure of fluoride tungsten tested at 1540°C ($T/T_m = 0.49$).

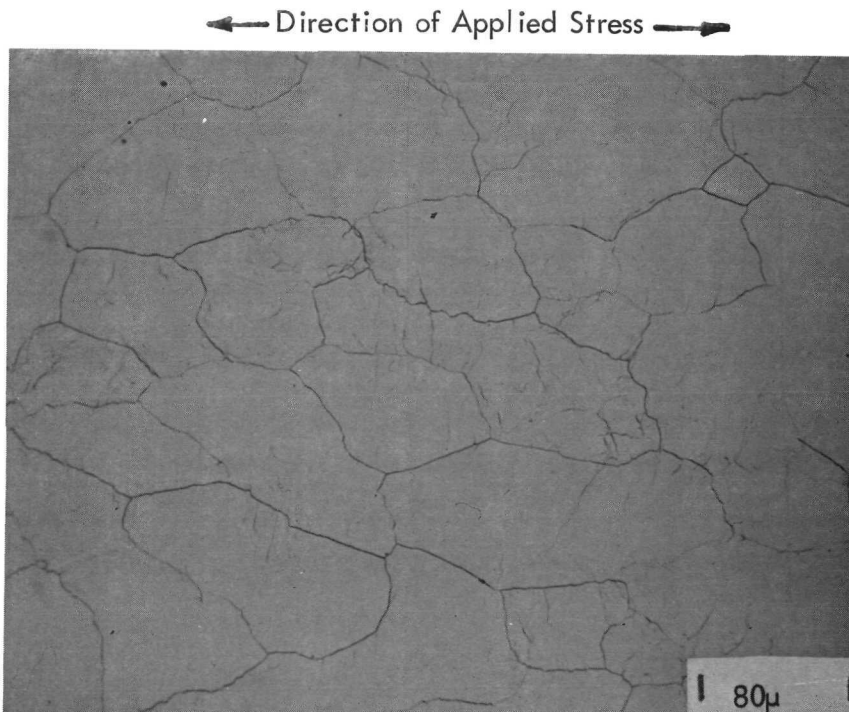
At still higher temperature (represented by the test temperature of 1700°C) the elongated grain structure has been replaced by a more equi-axed structure (Figure 48). The resultant boundary movement has eliminated grain boundary cracking with a consequent return to greater ductility.

Up to the temperature limit studied (1700°C) fluoride material which had been given the 5000 hour, 1700°C aging treatment following stress relief and outgassing did not experience behavior identical to that just described for the non-aged material. These elongation data are compared in Figure 29. From the series of photomicrographs taken from tensile specimens tested at 1100, 1540, and 1700°C (Figures 49 through 51), it is apparent that the same sequence of events that occurred for the non-aged material has taken place but with the onset of grain boundary cracking and considerable polygonization being delayed to higher temperature (1700°C) and with recrystallization having been retarded. This behavior is related to the presence of a considerable number of bubbles in the 1700°C aged material (as demonstrated previously) compared to a virtual absence of same in the non-aged material. It is hypothesized



250X

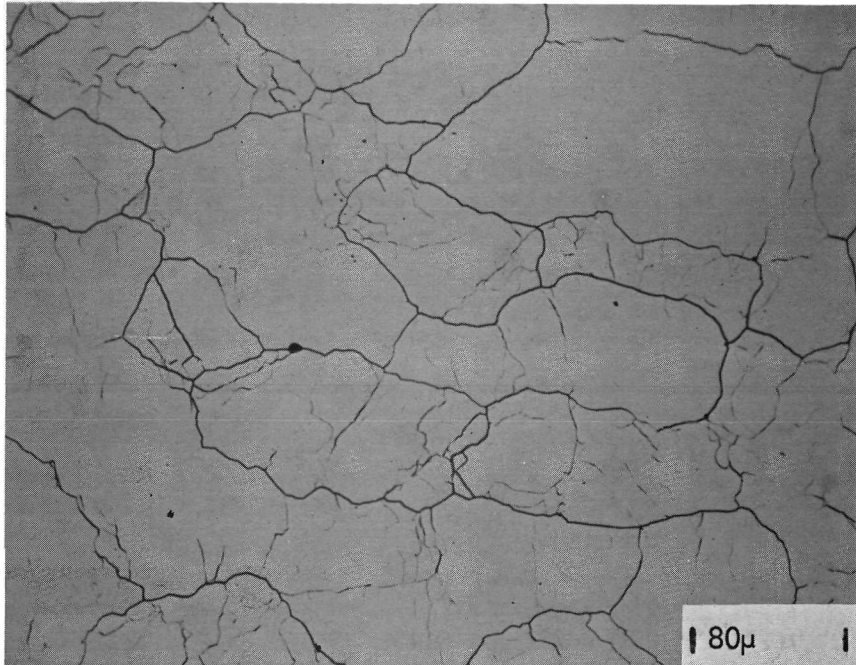
Figure 48. Fluoride Tungsten (Stress Relieved and Outgassed) Following Tensile Testing at 1700°C. (30 lactic - 3 HNO₃ - 1 HF etch)



250X

Figure 49. Fluoride Tungsten (Stress Relieved, Outgassed and Aged 5000 Hours at 1700°C) Following Tensile Testing at 1100°C. (30 lactic - 3 HNO₃ - 1 HF etch)

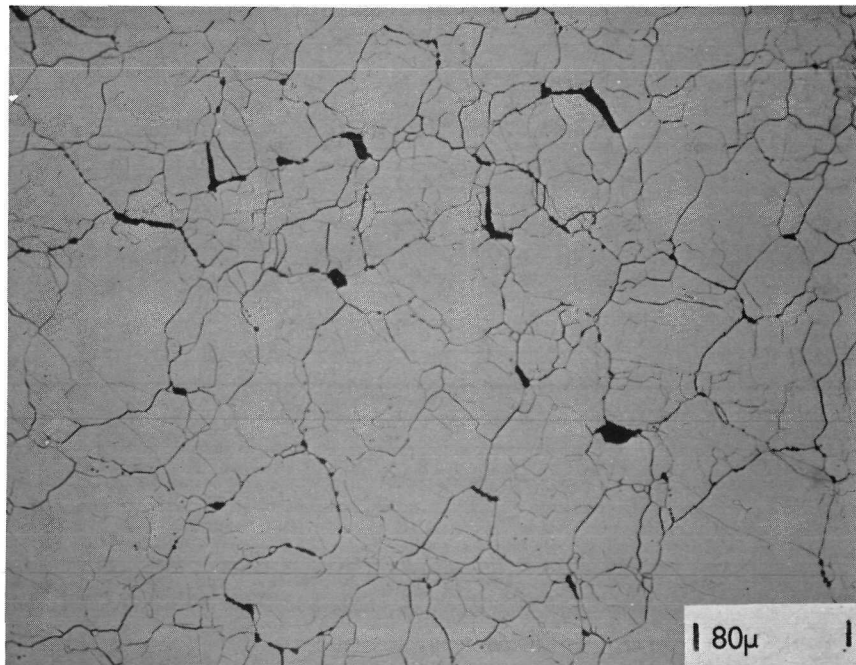
← Direction of Applied Stress →



250X

Figure 50. Fluoride Tungsten (Stress Relieved, Outgassed and Aged 5000 Hours at 1700°C Following Tensile Testing at 1540°C. (30 lactic - 3 HNO₃ - 1 HF etch)

← Direction of Applied Stress →



250X

Figure 51. Fluoride Tungsten (Stress Relieved, Outgassed and Aged 5000 Hours at 1700°C Following Tensile Testing at 1700°C. (30 lactic - 3 HNO₃ - 1 HF etch)

that the excess vacancies, which would otherwise diffuse to the grain boundary cavity nuclei, have already been effectively "removed" from the material by their combination to form bubbles. In addition, these bubbles, by lowering the interfacial energy of the grain boundaries upon which they are situated, serve to hinder the motion of the recrystallized grains' boundaries. This action delayed significant boundary motion to some temperature in excess of 1700°C and thus permitted crack formation which would otherwise not occur at this high a temperature.

Some support for the preceding argument is supplied by the elongation behavior of the fluoride tungsten aged for 5000 hours at 1540°C following stress relief and outgassing (Figure 29). This material followed the behavior of the non-aged material and, like it, did not contain bubbles.

Although the tensile specimens for the chloride and duplex materials were not examined metallographically it is expected that the same general behavior as found for the elongation of fluoride tungsten is operable.

7.0 CONCLUSIONS

Based on the results of this program and their evaluation, the following conclusions are made:

1. All three types of CVD tungsten are weldable by electron beam. These results are especially encouraging when compared to previous results on non-CVD tungsten sheet.
2. Using grain growth as the criterion, the fluoride material (< 2 ppm F) was found to be exceptionally stable to 5000 hour exposure temperatures as high as 1700°C . In contrast, the chloride material had poor grain growth resistance even though on occasion, an individual layer within the total thickness of chloride tungsten exhibited only slight grain growth following high temperature treatment.
3. The strength properties of the three CVD tungsten materials indicate that they possess essentially equivalent high temperature stability.
4. The high temperature strength properties of these materials are comparable to those possessed by tungsten produced by other means (power metallurgy, arc cast, and electron beam melted).
5. The materials studied were variable in nature as evidenced by their microstructure prior to thermal treatment. This variability was especially pronounced for the chloride-produced material.
6. The role of fluorine content as to its influence on weldability and structural stability was not discernible.

8.0 RECOMMENDATIONS

On the basis of the conclusions, it is recommended that:

- The CVD process be investigated to define critical deposition parameters and parameter control necessary to reproducibly deposit material of specified purity and microstructure.
- The grain growth behavior and thermal stability of CVD tungsten be more explicitly characterized, particularly the role of fluorine on grain growth kinetics.

These accomplishments will be required before the strength weldability and thermal stability of CVD tungsten can be completely characterized.

9.0 REFERENCES

1. Holzl, R. A., U. S. Patent 3,565,676, (1971).
2. Glaski, F. A., "Controlling Grain Orientation in CVD Tungsten", Chemical Vapor Deposition - Second International Conference, Electrochemical Society, 1970.
3. Lessman, G. G., and R. E. Gold, "The Weldability of Tungsten Base Alloys," paper presented at AWS 50th Annual Meeting, Philadelphia, 1969.
4. Rostoken, W., and J. R. Dvorak, "Interpretation of Metallographic Microstructures," p. 202, Academic Press, New York, 1965.
5. Schaffhauser, A. C., and R. L. Heestand, "Effect of Fluorine on the Grain Stability of Thermochemically Deposited Tungsten," paper presented at Thermionic Conversion Specialist Conference, Houston, 1966.
6. Honeycombe, R. W. K., "The Plastic Deformation of Metals," p. 439, Edward Arnold, London, 1968.
7. McLean, D., "Mechanical Properties of Metals", p. 329, Wiley, New York, 1962.

DISTRIBUTION LIST

National Aeronautics and Space Administration
400 Maryland, SW
Washington, D. C. 20546

Attention: J. J. Lynch, Code NS-1
C. Johnson, Code NS-1
R. E. Anderson, Code NS-1
P. R. Miller, Code NS-1
J. J. Gangler, Code RWM
F. Schulman, Code NS-2
S. V. Manson, Code NS-1
W. H. Woodward, Code RP
A. M. Smith, Code RNP
G. C. Deutsch, Code RW

National Aeronautics and Space Administration
Lewis Research Center
21000 Brookpark Road
Cleveland, Ohio 44135

Attention: Report Control, MS 5-5
Technology Util. Office, MS 3-19
Library, MS 60-3
E. J. Kolman, MS 500-313
G. M. Ault, MS 3-13
S. S. Manson, MS 49-1
R. W. Hall, MS 105-1
N. T. Saunders, MS 105-1
R. L. Davies, MS 106-1
R. Britwieser, MS 302-1
J. Ward, MS 302-1
R&QA, MS 500-111
V. Hlavin, MS 3-15
N. T. Musial, MS 500-311
E. E. Kempke, MS 500-201
R. W. Vernon, MS 500-202
J. W. Creagh, MS 49-2
H. H. Hinckley, MS 500-309
S. J. Kaufman, MS 49-2
P. L. Donoughe, MS 49-2
G. M. Kaplan, MS 500-202
R. A. Lindberg, MS 106-1 (3 copies)
H. A. Shumaker, MS 54-1

National Aeronautics and Space Administration
Ames Research Center
Moffett Field, Calif. 94035
Attention: Librarian

National Aeronautics and Space Administration
Manned Spacecraft Center
Houston, Texas 77058
Attention: Technical Infor. Program Div.
B. J. Bragg
W. E. Rice

National Aeronautics and Space Administration
Marshall Space Flight Center
Huntsville, Alabama 35812
Attention: Library/R. Aden

National Aeronautics and Space Administration
Jet Propulsion Laboratory
4800 Oak Grove Drive
Pasadena, Calif. 91103
Attention: Librarian

Jet Propulsion Laboratory
California Institute of Technology
4800 Oak Grove Drive
Pasadena, Calif. 91103
Attention: P. Rouklove
J. Mondt
V. Truscello

National Aeronautics and Space Administration
Scientific and Technical Infor. Facility
P. O. Box 33
College Park, Md. 20740
Attention: NASA Representative (2 copies)

National Aeronautics and Space Administration
Goddard Space Flight Center
Greenbelt, Md. 20771
Attention: Library
J. Epstein

National Aeronautics and Space Administration
Langley Research Center
Langley Field, Virginia 23365
Attention: Library

Los Alamos Scientific Laboratory
University of California
Los Alamos, N. M. 87544
Attention: Librarian
W. A. Ranken

National Bureau of Standards
Washington, D. C.
Attention: Librarian

Bureau of Mines
Albany, Oregon
Attention: Librarian

Bureau of Ships
Dept. of the Navy
Washington, D. C. 20360
Attention: Librarian

Bureau of Weapons
Research and Engineering
Materials Division
Washington, D. C. 20360
Attention: Librarian

U. S. Atomic Energy Commission
Technical Information Service Extension
P. O. Box 62
Oak Ridge, Tenn. 37831

U. S. Atomic Energy Commission
Technical Reports Library
Washington, D. C. 20545
Attention: J. M. O'Leary (2 copies)

U. S. Atomic Energy Commission
Space Nuclear Systems Division, F309
Reactor Power Systems Branch
Washington, D. C. 20545
Attention: D. S. Beard

U. S. Atomic Energy Commission
Germantown, Md. 20545
Attention: Librarian

Brookhaven National Laboratory
Upton, Long Island, N. Y. 11973
Attention: Librarian

Oak Ridge National Laboratory
Oak Ridge, Tennessee 37831
Attention: Librarian

Oak Ridge National Laboratory
Oak Ridge, Tennessee 37831
Attention: Library/A. C. Schaffhauser

DISTRIBUTION LIST (Cont'd.)

Air Force Cambridge Research Laboratories
L. G. Hanscom Field
Bedford, Mass. 01731
Attention: CRZAP

Air Force Weapons Laboratory
Kirtland AFB
New Mexico 87117
Attention: Library

U. S. Army Electronics Command
225 South 18th
Philadelphia, Pa. 19103
Attention: Librarian

U. S. Army Erdl
Fort Monmouth, N. J. 07703
Attention: E. Kittl

Amy Ordnance Frankford Arsenal
Pridesburg Station
Philadelphia, Pa. 19103
Attention: Librarian

U. S. Naval Research Laboratory
Washington, D. C. 20390
Attention: Librarian

Office of Naval Research
Power Division
Washington, D. C. 20360
Attention: Librarian

Office of Naval Research
Power Branch
Dept. of the Navy
Washington, D. C. 20325
Attention: Cmdr. O. J. Loper

Naval Ship Systems Command
Dept. of the Navy
Washington, D. C. 20360
Attention: E. P. Lewis, Code 08

Advanced Technology Laboratories
Div. of American Standard
360 Whisman Rd.
Mountain View, Calif.
Attention: Librarian

Aerospace Corporation
P. O. Box 95085
Los Angeles, Calif. 90045
Attention: Library

Aerojet General Corporation
P. O. Box 296
Azusa, Calif. 91703
Attention: Librarian

AiResearch Manufacturing Co.
9851-9951 Sepulveda Blvd.
Los Angeles, Calif. 90009
Attention: Librarian

AiResearch Manufacturing Co.
402 South 36th St.
Phoenix, Arizona 85034
Attention: Librarian

American Society of Metals
Novelty, Ohio 44073
Attention: Librarian

Applied Technology Div.
AVCO Corp.
Lowell Mass. 01851
Attention: R. J. Hill

Astro Met Associates, Inc.
95 Barron Dr.
Cincinnati, Ohio 45315
Attention: J. W. Graham/Librarian

AVCO
Research and Advanced Development
201 Lowell St.
Wilmington, Mass. 01887
Attention: Library

Babcock and Wilcox Company
Research Center
Alliance, Ohio
Attention: Librarian

Babcock and Wilcox Company
1201 Kemper St.
Lynchburg, Virginia 24501
Attention: Library

Bell Telephone Laboratories
Mountain Ave.
Murry Hill, N. J. 07971
Attention: Library

Battelle Memorial Institute
505 King Ave.
Columbus, Ohio 43201
Attention: Library
D. Kizer
D. Keller

The Boeing Company
P. O. Box 3707
Seattle, Wash. 98101
Attention: Library

Convair Astronautics Div.
General Dynamics
5001 Leamy Villa Rd.
San Diego, Calif. 92112
Attention: Library

Douglas Aircraft Co., Inc.
Missile and Space Systems Div.
3000 Ocean Park Blvd.
Santa Monica, Calif. 90406
Attention: Librarian

Electro-Optical Systems, Inc.
300 North Halstead St.
Pasadena, Calif. 91107
Attention: Library
A. Jensen

E. I. duPont de Nemours and Co., Inc.
1007 Market St.
Wilmington, Delaware 19898
Attention: Library

Eimac Div. of Varian
301 Industrial Way
San Carlos, Calif. 94070
Attention: Library
M. Parkman

Ford Motor Company
Aeroutronic Div.
Newport Beach, Calif. 92663
Attention: Library

Gulf Oil Corporation
P. O. Box 608
San Diego, Calif. 92112
Attention: L. Yang

General Electric Company
Electronic Components Div.
One River Rd.
Schenectady, N. Y. 12345
Attention: D. A. Wilbur, Manager,
Tube Research

DISTRIBUTION LIST (Cont'd.)

General Electric Company
Knolls Atomic Power Laboratory
P. O. Box 1072
Schenectady, N. Y. 12301
Attention: R. Ehrlich

General Electric Power Tube Dept.
General Electric Company
One River Rd.
Schenectady, N. Y. 12345
Attention: Library

General Dynamics
P. O. Box 748
Fort Worth, Texas
Attention: Library

General Motors Corp.
Defense Research Laboratories
6767 Hollister St.
Santa Barbara, Calif. 93105
Attention: Library

General Motors Corp.
Research Laboratories
12 Mile and Mound Rds.
Warren, Mich. 48092
Attention: F. E. Jamerson

General Technologies Corp.
1821 Michael Faraday Dr.
Reston, Virginia 22070
Attention: R. G. Shaver

High Voltage Engineering Corp.
Burlington, Mass.
Attention: Librarian

Hughes Aircraft Co.
Engineering Div.
Culver City, Calif. 90232
Attention: Library

IIT
10 West 35th St.
Chicago, Ill. 60616
Attention: Library

I. L. C. Laboratories, Inc.
164 Commercial St.
Sunnyvale, Calif. 94086
Attention: L. Reed, Director

Institute for Defense Analysis
400 Army Navy Dr.
Arlington, Virginia 48092
Attention: R. C. Hamilton

International Telephone and Telegraph
Federal Laboratories
500 Washington Ave.
Nutley, N. J. 07110
Attention: Library

Lawrence Radiation Laboratory
P. O. Box 808
Livermore, Calif. 94550
Attention: Library

Lear-Siegler, Inc.
Power Equipment Div.
P. O. Box 6719
Cleveland, O. 44101

Long-Tempo-Vought, Inc.
P. O. Box 5003
Dallas, Texas 75222
Attention: Library

Litton Industries, Inc.
336 North Foothill Rd.
Beverly Hills, Calif. 94703
Attention: Library

Lockheed Missiles and Space Co.
P. O. Box 504
Sunnyvale, Calif. 94088
Attention: Library

Lockheed Missile and Space Division
Lockheed Aircraft Corp.
Sunnyvale, Calif. 94086
Attention: H. H. Greenfield

Marquardt Corporation
Astro Division
16555 Saticoy St.
Van Nuys, Calif. 91406
Attention: A. N. Thomas

The Martin-Marietta Corp.
P. O. Box 179
Denver, Colorado 80201
Attention: Librarian

McDonnell Aircraft
P. O. Box 516
St. Louis, Mo. 63166
Attention: Library

McDonnell-Douglas Corp.
Missile and Space Engineering
Nuclear Research (A2-260)
3000 Ocean Park Blvd.
Santa Monica, Calif. 90405
Attention: Library

Melpar, Inc.
7700 Arlington Blvd.
Falls Church, Virginia 22046
Attention: Librarian

Minneapolis-Honeywell
2747 Fourth Ave., S
Minneapolis, Minn. 55408
Attention: Library

3M Company
Electrical Products Laboratory
2501 Hudson Rd.
St. Paul, Minn. 55119
Attention: Librarian

North American Rockwell Corp.
Los Angeles Div.
Los Angeles, Calif.
Attention: Library

North American Rockwell Corp.
Atomics International
P. O. Box 309
Canoga Park, Calif. 91304
Attention: Librarian
R. C. Allen
C. E. Smith

North American Rockwell Corp.
S&ID Div.
12214 Lakewood Blvd.
Downey, Calif. 90241
Attention: C. L. Gould

Pratt and Whitney Aircraft
400 Main St.
East Hartford, Conn. 06108
Attention: Library

DISTRIBUTION LIST (Cont'd.)

Radiation Effects Information Center
 Battelle Memorial Institute
 505 King Ave.
 Columbus, Ohio 43201
 Attention: R. E. Bowman

Radio Corporation of America
 David Samoff Research Center
 Princeton, N. J. 08640
 Attention: P. Rappaport

Radio Corporation of America
 Front and Cooper Streets
 Camden, N. J. 08103
 Attention: Librarian

The Rand Corporation
 1700 Main St.
 Santa Monica, Calif. 90401
 Attention: B. Pinkel

Raytheon Company
 Research Division Library
 28 Seyon St.
 Waltham, Mass. 02154

Rocketdyne
 6633 Canoga Ave.
 Canoga Park, Calif. 91303
 Attention: Library

Solar Division
 International Harvester Company
 2200 Pacific Highway
 San Diego, Calif. 92112
 Attention: Library

Space Systems Division (SSTRE)
 AF Unit Post Office
 Los Angeles, Calif. 90045
 Attention: Major W. Iller

Stanford Research Institute
 Menlo Park, Calif.
 Attention: Library

Sylvania Electric Products, Inc.
 Chemical and Metallurgical
 Towanda, Pa.
 Attention: Library

Texas Instruments, Inc.
 Apparatus Division
 P. O. Box 5936
 Dallas, Texas 75222
 Attention: Library

Thermo Electron Corporation
 85 First Ave.
 Waltham, Mass. 02154
 Attention: R. Howard

TRW, Inc.
 TRW Systems Group
 One Space Park
 Redondo Beach, Calif. 90278
 Attention: Library

TRW, Inc.
 23555 Euclid Ave.
 Cleveland, O. 44117
 Attention: Library

Union Carbide Nuclear Company
 P. O. Box X
 Oak Ridge, Tennessee 37831
 Attention: X-10 Laboratory Records

Union Carbide Metals
 Niagara Falls, N. Y.
 Attention: Library

United Aircraft Corp.
 Pratt and Whitney Aircraft Div.
 East Hartford, Conn. 06108
 Attention: Library

Varian Associates
 611 Hansen Way
 Palo Alto, Calif. 94304
 Attention: I. Weismann

Western Electric Manufacturing Assoc.
 3600 Wilshire Blvd.
 Los Angeles, Calif. 90005
 Attention: Library

Western Electric Company
 222 Broadway
 New York, N. Y. 10038
 Attention: Library

Westinghouse Electric Corporation
 Research and Development Center
 Pittsburgh, Pa. 15235
 Attention: Library